

## INFORMATION TO USERS

This manuscript has been reproduced from the microfilm master. UMI films the text directly from the original or copy submitted. Thus, some thesis and dissertation copies are in typewriter face, while others may be from any type of computer printer.

**The quality of this reproduction is dependent upon the quality of the copy submitted.** Broken or indistinct print, colored or poor quality illustrations and photographs, print bleedthrough, substandard margins, and improper alignment can adversely affect reproduction.

In the unlikely event that the author did not send UMI a complete manuscript and there are missing pages, these will be noted. Also, if unauthorized copyright material had to be removed, a note will indicate the deletion.

Oversize materials (e.g., maps, drawings, charts) are reproduced by sectioning the original, beginning at the upper left-hand corner and continuing from left to right in equal sections with small overlaps. Each original is also photographed in one exposure and is included in reduced form at the back of the book.

Photographs included in the original manuscript have been reproduced xerographically in this copy. Higher quality 6" x 9" black and white photographic prints are available for any photographs or illustrations appearing in this copy for an additional charge. Contact UMI directly to order.

**UMI<sup>®</sup>**

Bell & Howell Information and Learning  
300 North Zeeb Road, Ann Arbor, MI 48106-1346 USA  
800-521-0600



**University of Alberta**

**Mechanism of FinOP Fertility Inhibition of F-like Plasmids**

by

Lori Jean Jerome



A thesis submitted to the Faculty of Graduate Studies and Research in  
partial fulfillment of the requirements for the degree of Doctor of  
Philosophy

Department of Biological Sciences

Edmonton, Alberta

Spring 1999



National Library  
of Canada

Acquisitions and  
Bibliographic Services

395 Wellington Street  
Ottawa ON K1A 0N4  
Canada

Bibliothèque nationale  
du Canada

Acquisitions et  
services bibliographiques

395, rue Wellington  
Ottawa ON K1A 0N4  
Canada

*Your file* *Votre référence*

*Our file* *Notre référence*

The author has granted a non-exclusive licence allowing the National Library of Canada to reproduce, loan, distribute or sell copies of this thesis in microform, paper or electronic formats.

The author retains ownership of the copyright in this thesis. Neither the thesis nor substantial extracts from it may be printed or otherwise reproduced without the author's permission.

L'auteur a accordé une licence non exclusive permettant à la Bibliothèque nationale du Canada de reproduire, prêter, distribuer ou vendre des copies de cette thèse sous la forme de microfiche/film, de reproduction sur papier ou sur format électronique.

L'auteur conserve la propriété du droit d'auteur qui protège cette thèse. Ni la thèse ni des extraits substantiels de celle-ci ne doivent être imprimés ou autrement reproduits sans son autorisation.

0-612-39545-6

Canada

**University of Alberta**

**Library Release Form**

**Name of Author:** Lori Jean Jerome

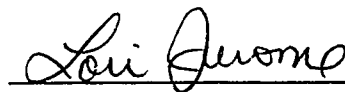
**Title of Thesis:** Mechanism of FinOP Fertility Inhibition of F-like Plasmids

**Degree:** Doctor of Philosophy

**Year this Degree Granted:** 1999

Permission is hereby granted to the University of Alberta Library to reproduce single copies of this thesis and to lend or sell such copies for private, scholarly, or scientific research purposes only.

The author reserves all other publication and other rights in association with the copyright in the thesis, and except as hereinbefore provided, neither the thesis nor any substantial portion thereof may be printed or otherwise reproduced in any material form whatever without the author's prior written permission.



---

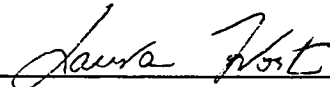
#603 - 3470 Durocher Street  
Montreal, Quebec  
H2X 2E1

**DATED:** Dec. 10, 1998

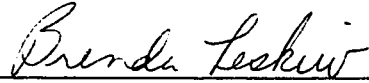
**University of Alberta**

**Faculty of Graduate Studies and Research**

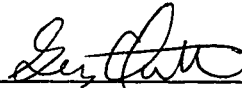
The undersigned certify that they have read, and recommend to the Faculty of Graduate Studies and Research for acceptance, a thesis entitled **Mechanism of FinOP Fertility Inhibition of F-like plasmids** submitted by **Lori Jean Jerome** in partial fulfillment of the requirements for the degree of **Doctor of Philosophy**.



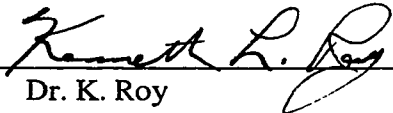
Dr. L.S. Frost  
(Supervisor)



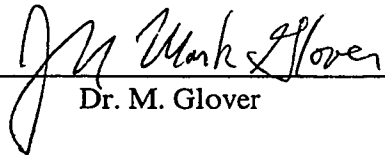
Dr. B.K. Leskiw



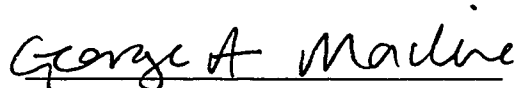
Dr. G. Owtrim



Dr. K. Roy



Dr. M. Glover



Dr. G.A. Mackie  
(External Examiner)

DATED: Dec. 4, 1998

To my parents, Glenn & Rita,  
my siblings, Melanie, Ronnie, Terry, Tami, Cheryl & Diane,  
and my soul-mate, Pieter

## Abstract

The transfer potential of F-like plasmids is determined by the levels of *finP* and *traJ* gene products. TraJ is a 27 kDa protein which acts as a positive regulator of the transfer operon. FinP is a 79 base antisense RNA which forms two stem-loops and is complementary to part of the 5' untranslated leader of *traJ* mRNA. The intracellular levels of FinP are dependent on co-expression of the FinO protein, which binds to FinP and prevents its decay. The *traJ* mRNA leader, which is also bound by FinO, forms a duplex with FinP *in vitro* that is thought to prevent *traJ* mRNA translation through occlusion of its ribosome binding site, leading to repression of plasmid transfer.

FinP decay was characterized in a series of ribonuclease-deficient strains by Northern blot analysis. The results indicate that, in the absence of FinO, FinP degradation is initiated by the endonuclease, RNase E. The major site of cleavage was mapped to the spacer between stem-loops I and II of FinP synthesized *in vitro* using purified RNase E. The FinP half-life was prolonged *in vivo* by co-expression of FinO or mutation of the spacer sequence. A GST-FinO fusion protein reduced RNase E cleavage of the FinP spacer *in vitro*, suggesting that FinO stabilizes FinP by protecting it from RNase E. Characterization of a FinP mutant with a single base change in stem I showed that reduced levels of FinP, due in part to increased RNase E cleavage in a region not protected by FinO, leads to loss of *traJ* repression and increased transfer.

In the absence of FinO, two FinP/*traJ* mRNA duplexes were detected in a strain lacking the double-strand-specific endonuclease, RNase III. The larger duplex resulted



from extension of the FinP transcript at its 3' end, suggesting read-through at the terminator that corresponds to FinP stem-loop II.

Mutational analysis of FinP and truncated *traJ* mRNAs showed that FinO recognizes RNA in a structure-dependent, sequence-independent manner. An updated model for FinP repression of TraJ expression is proposed based on temporal regulation of FinP antisense RNA levels by competing host- (RNase E) and plasmid-encoded (FinO) proteins.

## Acknowledgements

First, deepest appreciation is extended to my supervisor, Laura Frost, for introducing me to the "RNA World". It was an exciting four years working on antisense RNA control of bacterial conjugation. Laura's unending enthusiasm and commitment to science provided me with a sound foundation for research. Her continuous support and patience taught me to persist even when the task at hand seemed insurmountable. Our common passion for hiking permitted me to explore the majestic Canadian Rocky Mountains and I even thought about FinOP once in a while during these excursions!

I really enjoyed working in the Frost lab and am grateful to my colleagues (Jan Manchak, Bill Klimke, Richard Fekette, Jim Sandercock, Mike Gubbins and Karen Anthony) for technical and moral support. I was especially fortunate to have had the opportunity to learn from the expert hand of Karen Anthony. Karen was instrumental in helping me to establish my molecular biology skills in the early days and made me feel truly welcome in the lab.

I spent lunch hours and many evenings conversing with my colleagues in chemistry (Darren, Sue & Karl). Talking with chemists about molecular biology certainly gave me a different perspective on my research and at the same time, I seem to have picked up a few tidbits about electronics and chemistry!

I thank my family and many close friends (especially Sam Salama) for their support in my endeavor to obtain my PhD. Finally, I am deeply indebted to my husband, Pieter, who provided twenty four hour support and encouragement during my years as a student. I could not have completed this journey without you!

# Table of Contents

<b>Chapter 1.</b>	<b>General Introduction</b>	<b>Page</b>
1.1	Early studies on bacterial conjugation .....	2
1.2	The conjugative cycle .....	4
1.3	F plasmid transfer ( <i>tra</i> ) genes .....	8
1.4	FinOP Fertility Inhibition .....	11
1.4.1	The role of TraJ in regulating transcription from the pY promoter .....	12
1.4.2	FinP antisense RNA .....	16
1.4.3	The RNA-binding protein, FinO .....	22
1.5	Regulation by other antisense RNA systems .....	25
1.5.1	Regulation of ColE1 plasmid replication by antisense RNA.	26
1.5.2	Antisense RNA control of IS10 transposition .....	33
1.6	mRNA degradation in <i>Escherichia coli</i> .....	38
1.6.1	<i>E. coli</i> exonucleases .....	38
1.6.2	<i>E. coli</i> endonucleases .....	41
1.6.3	The role of polyadenylation in mRNA degradation .....	42
1.6.4	Mechanism of mRNA degradation in <i>E. coli</i> .....	43
1.6.5	Degradation of ColE1 RNA I .....	47
1.6.6	The unusual stability of IS10 antisense RNA, RNA-OUT ..	50
1.7	RNA-binding proteins .....	52
1.7.1	Rom/Rop protein of plasmid ColE1 .....	53
1.7.2	Rev protein of HIV-1 .....	57
1.7.3	Histone mRNA stem-loop binding protein (SLBP) .....	61

1.8	Summary and research objectives .....	65
<b>Chapter 2.</b>	<b>Materials and Methods</b>	
2.1	Bacterial strains, growth media and plasmids .....	69
2.2	DNA sequencing .....	74
2.3	Site-directed mutagenesis of <i>finP</i> .....	74
2.4	$\beta$ -galactosidase assay .....	75
2.5	Isolation of total cellular RNA .....	76
2.6	Northern analysis and chemical half-life determination .....	77
2.7	Generation of DNA templates for <i>in vitro</i> transcription .....	78
2.8	<i>In vitro</i> transcription of RNA .....	80
2.9	Purification of GST and GST-FinO proteins .....	82
2.10	<i>In vitro</i> RNase E cleavage of FinP-G <sub>4</sub> AUC and <i>finP305</i> -G <sub>4</sub> AUC ..	83
2.11	Assay for FinO protection of RNA cleavage by RNase E .....	84
2.12	Gel-shift analysis of RNA-protein interactions .....	85
<b>Chapter 3.</b>	<b>Characterization of FinP antisense RNA degradation <i>in vivo</i></b>	
3.1	Introduction .....	88
3.2	Results	
3.2.1	Full-length FinP antisense RNA accumulates in RNase E-deficient strains .....	89
3.2.2	RNase II, PNPase and PAP I are not involved in the degradation of full-length FinP .....	98
3.2.3	FinP is degraded by RNase III when duplexed with <i>traJ</i> mRNA .....	103
3.2.4	FinO does not affect transcription from the <i>finP</i> promoter ..	109
3.3	Discussion .....	114

## **Chapter 4. *In vitro* analysis of FinP cleavage by RNase E**

4.1	Introduction .....	120
4.2	Results	
4.2.1	FinP RNA is cleaved <i>in vitro</i> by RNase E .....	123
4.2.2	Mutation of the single-stranded spacer stabilizes FinP <i>in vivo</i> .....	127
4.2.3	GST-FinO protects FinP from RNase E cleavage <i>in vitro</i> ..	130
4.2.4	GST-FinO and RNase E compete for binding to FinP <i>in vitro</i> .....	135
4.3	Discussion .....	143

## **Chapter 5. Characterization of the *finP305* mutation in FinP antisense RNA**

5.1	Introduction .....	148
5.2	Results	
5.2.1	<i>finP305</i> RNA has a shorter half-life than FinP and accumulates in an RNase E-deficient strain .....	152
5.2.2	<i>In vitro</i> cleavage of <i>finP305</i> RNA by RNase E .....	157
5.2.3	GST-FinO does not protect <i>finP305</i> RNA from RNase E cleavage .....	161
5.3	Discussion .....	166

## **Chapter 6. Characterization of the RNA features recognized by the FinO protein *in vitro***

6.1	Introduction .....	171
-----	--------------------	-----

6.2	Results	
6.2.1	Mutations in stem II have minor effects on GST-FinO binding .....	177
6.2.2	GST-FinO binding is enhanced by single-stranded regions on either side of SLII .....	187
6.2.3	The <u>length</u> , but not sequence, of the FinP 3' tail is important for GST-FinO binding .....	196
6.2.4	GST-FinO recognizes the same structural features in <i>traJ</i> mRNA .....	196
6.3	Discussion .....	202
<b>Chapter 7.</b>	<b>Discussion &amp; Conclusions</b>	
7.1	Degradation of FinP antisense RNA in the absence of FinO .....	208
7.2	The role of FinO in stabilizing FinP .....	213
7.3	Recognition of RNA by FinO .....	216
7.4	A refined model for Fertility Inhibition .....	218
7.5	Future experiments .....	222
<b>Chapter 8.</b>	<b>References .....</b>	<b>225</b>

## List of Tables

	Page
<b>Chapter 1</b>	
1.1 <i>E. coli</i> RNases implicated in mRNA degradation .....	39
<b>Chapter 2</b>	
2.1 <i>E. coli</i> strains used in this study .....	70
2.2 Plasmids used in this study .....	71
2.3 PCR primers used in this study .....	73
2.4 RNAs derived by <i>in vitro</i> transcription from PCR-generated templates ....	79
<b>Chapter 3</b>	
3.1 FinP RNA half-life in wild-type and mutant strains .....	95
3.2 Effect of FinO on <i>finP</i> -driven $\beta$ -galactosidase activity in DH5 $\alpha$ .....	113
<b>Chapter 6</b>	
6.1 GST-FinO binding to FinP RNA variants .....	180
6.2 Effect of ionic strength on GST-FinO binding to wild-type FinP .....	186
6.3 The tail <u>length</u> , but not sequence, is critical for FinP recognition .....	188

## List of Figures

<b>Chapter 1</b>	<b>Page</b>
1.1 The conjugative cycle of F-like plasmids .....	6
1.2 Conjugative transfer genes of the F plasmid .....	9
1.3 FinOP regulation of F plasmid transfer .....	13
1.4 Secondary structures of FinP antisense RNA and the first 117 bases of <i>traJ</i> mRNA .....	17
1.5a Antisense RNA control of plasmid ColE1 primer maturation .....	28
1.5b Pathway for duplex formation between ColE1 antisense RNA and the replication preprimer, RNA II .....	31
1.6a Regulation of <i>IS10</i> transposition by antisense RNA .....	34
1.6b Pathway for duplex formation between <i>IS10</i> RNA-IN and RNA-OUT ....	34
1.7 Model for mRNA degradation in <i>E. coli</i> .....	44
1.8a Secondary structure of pBR322 RNA I antisense RNA .....	48
1.8b RNA-OUT secondary structure .....	48
1.9a Model for RNA I/RNA II “kissing complex” and its interaction with the Rom dimer .....	54
1.9b Ribbon diagram of the Rom dimer .....	54
1.10 Secondary structure of the RRE .....	58
1.11 Consensus structure of the histone mRNA 3' end .....	62
 <b>Chapter 3</b>	
3.1 Map of the origin of transfer ( <i>oriT</i> ) region of F .....	90
3.2 FinP decay is dependent on RNase E and is stabilized by FinO .....	93
3.3 The half-life of FinP is also extended in an <i>rne-3071</i> mutant .....	96
3.4 FinP decay is not dependent on 3' exonucleases .....	99



3.5	Mutation of the gene encoding PAP I does not affect the half-life of FinP .	101
3.6	FinP is destabilized when co-expressed with <i>traJ</i> mRNA .....	104
3.7	Two FinP/ <i>traJ</i> duplexes (d1 and d2) are stabilized in the absence of RNase III .....	106
3.8	FinP is not degraded by RNase III in the absence of <i>traJ</i> mRNA .....	110

#### Chapter 4

4.1	Secondary structure of FinP antisense RNA and sites of RNase E cleavage <i>in vitro</i> .....	121
4.2	RNase E cleavage of <i>in vitro</i> synthesized 5'-labelled FinP-G <sub>4</sub> AUC .....	124
4.3	Mutation of the spacer from GACA to GCCC stabilizes FinP .....	128
4.4a	GST-FinO protects FinP from RNase E cleavage <i>in vitro</i> .....	131
4.4b	Graphic representation of GST-FinO protection of FinP .....	133
4.5	RNA mobility shift analysis of GST-FinO binding to FinP .....	137
4.6	RNA mobility shift analysis of RNase E binding to FinP .....	139
4.7	RNase E and GST-FinO compete for binding to FinP .....	141

#### Chapter 5

5.1	The <i>finP305</i> mutation of FinP antisense RNA .....	150
5.2	Northern analysis of <i>finP305</i> RNA decay .....	153
5.3	Graphic representation of <i>finP305</i> RNA decay .....	155
5.4	RNase E cleavage of <i>in vitro</i> synthesized <i>finP305</i> -G <sub>4</sub> AUC RNA .....	158
5.5a	RNase E cleavage of <i>in vitro</i> synthesized <i>finP305</i> -G <sub>4</sub> AUC RNA in the presence of GST-FinO .....	162
5.5b	Graphic representation of GST-FinO protection of RNase E cleavage of <i>finP305</i> -G <sub>4</sub> AUC RNA .....	164

## Chapter 6

6.1	Secondary structures of FinP antisense RNA and the <i>traJ</i> mRNA 5' UTR .	173
6.2a	Comparison of the FinP RNA sequences .....	175
6.2b	Comparison between FinO Type I (F and ColB2) and Type II (R6-5 and R100) alleles .....	175
6.3	Comparison of GST-FinO binding to FinP, SLI and SLII .....	178
6.4	GST does not bind to FinP, SLI or SLII .....	182
6.5	The spacer and 3' tail contribute to high affinity SLII binding by GST-FinO .....	189
6.6	Competition of GST-FinO binding to FinP with tRNA and poly(U) .....	192
6.7	The spacer and 3' tail improve SLI binding by GST-FinO .....	194
6.8	The length of the SLII 3' tail is important for RNA recognition .....	197
6.9	GST-FinO recognizes the same structural features in <i>traJ</i> mRNA .....	200

## Chapter 7

7.1	Refined model for FinOP Fertility Inhibition of F-like plasmids .....	219
-----	---	-----

## List of Abbreviations

aa	amino acid
ADP	adenosine diphosphate
AMP	adenosine monophosphate
Ap	ampicillin
ARM	arginine-rich motif
bp	base pair
BSA	bovine serum albumin
cAMP	cyclic adenosine monophosphate
C <sub>f</sub>	final concentration
Cm	chloramphenicol
CRP	cAMP receptor protein
Δ	deletion
DEPC	diethyl-pyrocarbonate
DNA	deoxyribonucleic acid
DNase	deoxyribonuclease
dNTP(s)	deoxyribonucleoside triphosphate(s)
dsRNA	double-stranded RNA
DTT	dithiothreitol
EDTA	ethylenediaminetetraacetic acid
EIF	exonuclease impeding factor
EtBr	ethidium bromide
F	fertility sex factor
<i>fbi</i>	fold-back inhibition
Fin	fertility inhibition
GST	glutathione S-transferase
h	hour
Hfr	high frequency recombination
IHF	integration host factor
Inc	incompatibility
IPTG	isopropyl β-D-thiogalactopyranoside
IRP	iron regulatory protein
IS	insertion sequence

$K_a$	equilibrium association constant
$k_{app}$	apparent rate constant
kb	kilobase
kDa	kiloDaltons
Km	kanamycin
LB	Luria Bertani
min	minute(s)
mRNA	messenger RNA
NS	nucleoside
ONPG	<i>o</i> -nitrophenyl $\beta$ -D-galactopyranoside
ORF	open reading frame
<i>oriT</i>	origin of transfer
PABP	poly(A) binding protein
PAP	poly(A)-polymerase
PNPase	polynucleotide phosphorylase
PPK	polyphosphate kinase
R	resistance factor
RBD	RNA binding domain
RBS	ribosome binding site
RNA	ribonucleic acid
RNase	ribonuclease
RNP	ribonucleoprotein
rNTP(s)	ribonucleoside triphosphate(s)
rRNA	ribosomal RNA
sec	second(s)
SL	stem-loop
Tc	tetracycline
<i>tra</i>	transfer
tRNA	transfer RNA
TSB	trypticase soy broth
UTR	untranslated region

**Chapter 1**  
**General Introduction**

## 1.1 Early studies on bacterial conjugation

Horizontal transfer of genetic information among microorganisms is a major driving force for the outstanding adaptability of microbial communities to environmental changes. The three most common forms of horizontal gene transfer are transformation, transduction and conjugation. Transformation was the earliest mechanism of bacterial gene transfer to be identified (Griffith, 1928). A gene is said to be successfully exchanged through transformation if it is taken up as free DNA and brings about genetic change in the recipient cell. In transduction, bacteriophages acquire genetic material from one bacterial cell and deposit it in another. Conjugation, the transfer of DNA from a donor to a recipient cell in a process requiring physical contact, was the first mechanism of bacterial gene transfer to be studied extensively and is the subject of this thesis.

The history of conjugation is intriguing because of its strong contribution to the evolution of bacterial genetics. Bacterial conjugation was discovered by Lederberg and Tatum (1946) who noticed that if they mixed two cultures of *Escherichia coli* K-12 with different nutritional requirements, they obtained recombinant bacteria with altered biochemical requirements and phage sensitivities. Attempts to induce transformation of the cultures by the use of sterile filtrates were unsuccessful and purified deoxyribonuclease (DNase) had no effect on the number of recombinants obtained. This ruled out the presence of “transforming factors” in the growth medium capable of inducing the gene mutations. Instead, Lederberg and Tatum suggested that in order for the genes to recombine, a cell fusion was required, implying the occurrence of a conventional sexual process in bacteria. Subsequently, Davis (1950) showed that recombinants could not be obtained when the two mating strains were inoculated on

either side of a bacteria-impassable fritted glass filter in a U-tube. This established the requirement for cell-cell contact in the mating process. Hayes (1952) went on to demonstrate that during conjugation genes flowed from donors to recipients by a unidirectional and donor-encoded process. Independent work by Hayes (1953) and by the Lederbergs and Cavalli (1952) led to the realization that donor cells harboured an infectious agent, which they named F (for fertility sex factor), that acted as a gene carrier in the transfer of genetic material to recipient cells.

The availability of an Hfr (*high frequency recombination*) strain allowed Jacob and Wollman (1955) to study the physiology of the mating process. Using an interrupted mating technique and genetic analysis of recombinants, they were able to define three stages of conjugation: pairing, transfer and integration of F into the bacterial chromosome. They concluded that there were close analogies between conjugation in bacteria and the process of phage replication and that bacterial mating was not a conventional sexual process. From this and later work they advanced the idea of a circular genetic map for *E. coli*. The first physical evidence of conjugative transfer was obtained using density gradient centrifugation to detect the F factor DNA after it was transferred from *E. coli* to *Serratia marcescens* (Marmur *et al.*, 1961). This study confirmed that genetic exchange could occur between organisms of different genera and that the F factor was in fact DNA. Following the discovery of male-specific bacteriophages, it was shown that the RNA phages attached to a sex pilus on the surface of male (donor) cells, which was necessary for chromosome transfer and made the initial contact between the mating cells (Brinton *et al.*, 1964).

As it turned out, the F sex factor of *E. coli* was only a special case of a very general phenomenon. A new type of transmissible genetic factor, the R (resistance) factor, encoding multiple drug resistance, was discovered in Japan among strains of antibiotic-resistant *Shigella* (Watanabe, 1963) and by 1966, R factors were reported world-wide (Watanabe, 1966). Because of the speed at which bacterial plasmids acquire determinants for toxin production, resistance to heavy metals and antibiotics newly introduced into the environment and because of the possibility of interspecies, intergeneric and interkingdom transfer (Mazodier & Davies, 1991), effective treatment of bacterial infections has become challenging. The inability of streptomycin (Hayes, 1952), tetracycline (Heinemann *et al.*, 1996), rifampicin (Heinemann & Ankenbauer, 1993a) or UV light (Heinemann and Ankenbauer, 1993b) to inhibit conjugation from sensitive donors up to 18 hours after treatment emphasizes the robust survival mechanisms possessed by plasmids. The development of effective therapeutics against bacterial pathogens therefore necessitates a thorough understanding of the environmental conditions, host signals and events of conjugal DNA transfer, which is credited as being the primary route for the dissemination of antibiotic resistance (Silver & Bostian, 1993). Although bacterial conjugation has been studied extensively for more than 50 years, many details of this process are still poorly understood. The current model for bacterial conjugation is outlined in the following section.

## **1.2 The conjugative cycle**

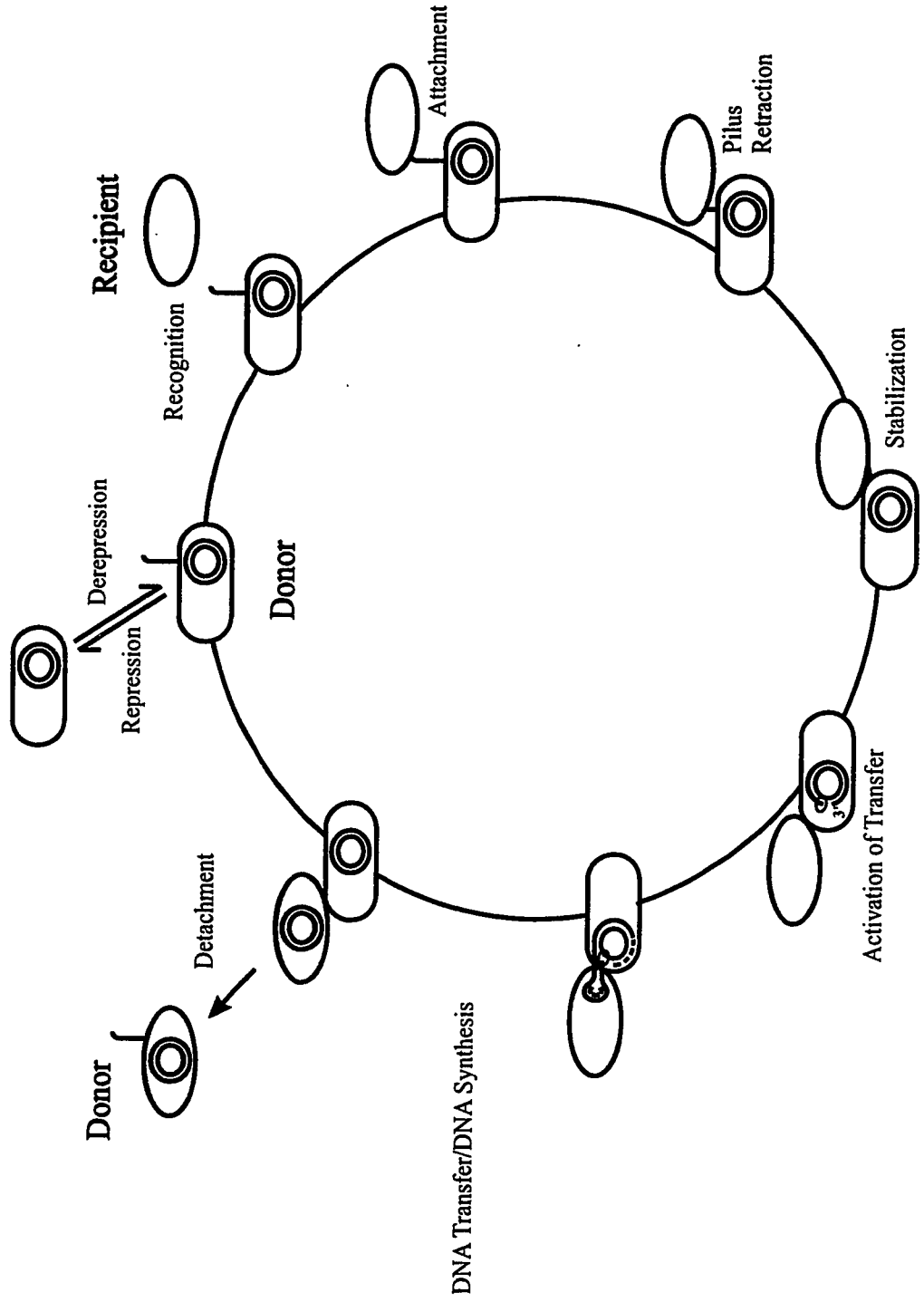
The F conjugative transfer system is the prototype for a large group of plasmids, called F-like, which encode a common transfer mechanism. F-like plasmids were



initially divided into a number of groups based on pilus morphology and serology (Lawn *et al.*, 1967), but have since been reclassified according to plasmid incompatibility (Inc). Two plasmids sharing replication/partition systems are unable to coexist stably in a growing population of bacteria and are said to be incompatible (Datta, 1975; Austin & Nordström, 1990). Plasmids with conjugative systems related to F belong to one of seven IncF subgroups (Ippen-Ihler & Skurray, 1993): IncFI (F, R386), IncFII (ColB2, R1, R6-5, R100), IncFIII (pSU306), IncFIV (R124), IncFV (pED208), IncFVI (pSU212) and IncFVII (pSU233).

The events leading to transfer of F-like plasmids, most recently reviewed by Firth *et al.* (1996), are shown schematically in Figure 1.1. Typically, cells harbouring F-like plasmids are *repressed* for conjugative transfer due to a regulatory system termed “Fertility Inhibition”, detailed in subsequent sections. Occasionally, a cell escapes this control system and becomes *derepressed*, allowing for the expression of a pilus, a long flexible protein appendage on the surface of the donor cell that allows it to recognize and attach to a specific receptor on a suitable recipient cell (Frost *et al.*, 1994). Pilus retraction, mediated by depolymerization of pilus subunits (Novotny & Fives-Taylor, 1974), brings the mating pair into close contact. Interactions between outer-membrane proteins stabilize the donor/recipient contacts, such that association of the mating pair becomes resistant to disruption by shear forces or treatment with detergents (Achtman & Skurray, 1977). An unknown “mating signal” triggers a plasmid-encoded relaxase to nick a single strand of the plasmid DNA at a specific site within a region called the origin of transfer (*oriT*). The relaxase, which becomes covalently attached to the 5' end of the DNA, then promotes the unwinding and transfer of the nicked strand into the recipient

**Figure 1.1** The conjugative cycle of F-like plasmids. Typically, a cell harbouring a conjugative plasmid is repressed for transfer. Occasionally a donor becomes derepressed and upon contact with a suitable plasmidless recipient, an unknown mating signal triggers nicking of the plasmid DNA and transfer of a single strand to the recipient cell. At the completion of complementary strand synthesis in the donor and the recipient, the mating pair detaches and both plasmid-containing cells re-enter the cycle until they have accumulated sufficient levels of inhibitors to repress further transfer events. The F plasmid is naturally derepressed and is therefore competent for unlimited mating cycles.

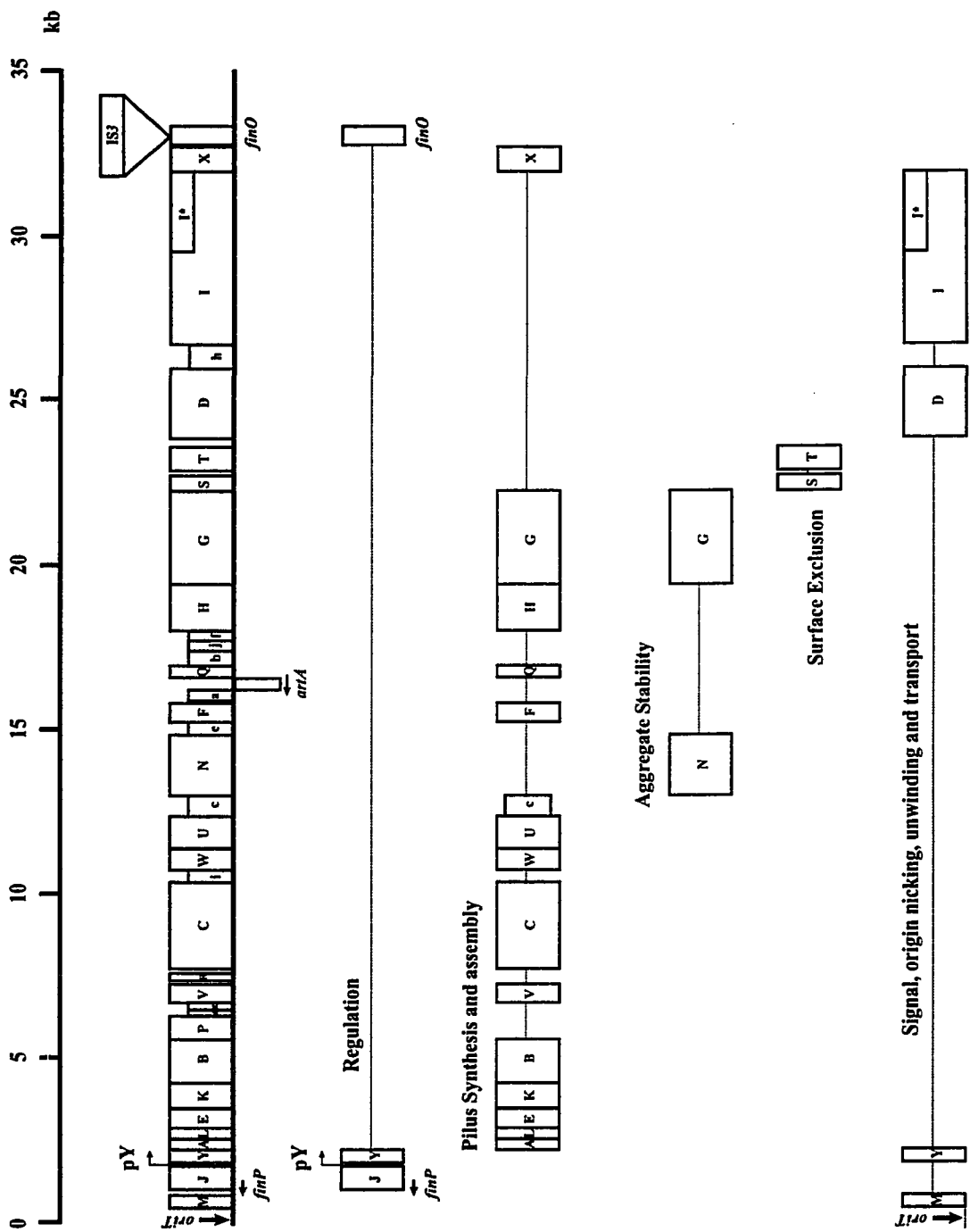


cell in a 5' to 3' direction. Concomitantly, using host-encoded proteins, a replacement for the transferred strand is synthesized in the donor and a complementary strand is generated in the recipient. Transfer is terminated with the completion of DNA synthesis, at which time the mating cells, both competent for subsequent donor activity, detach. Immediately after transfer, expression of plasmid-encoded proteins precludes redundant "homosexual" DNA transfer between donors, but allows for an initial flurry of conjugation events until the fertility inhibition products accumulate to a level which represses transfer. The F plasmid is continuously derepressed due to the loss of expression of a functional FinO regulatory protein. It was this exceptional property of F that allowed the detection of recombinants by Lederberg and Tatum and the subsequent study of bacterial conjugation. One cycle of conjugation for the F plasmid (100 kb) takes approximately 3 minutes at 37°C (Frost *et al.*, 1994).

### 1.3 F plasmid transfer (*tra*) genes

One third (33.3 kb) of the F plasmid sequence is devoted to conjugation and constitutes the transfer (*tra*) region (Figure 1.2). The complete sequence of the *tra* genes and the properties of their products have been compiled recently by Frost *et al.* (1994). These include 36 open reading frames (ORFs) and an untranslated regulatory RNA, FinP. Due to the location of the *oriT* site immediately upstream of the *tra* genes, the sequences encoding transfer functions enter the recipient last. Most of the transfer region is transcribed as a single operon from the pY promoter, located between *traJ* and *traY* (Mullineaux & Willetts, 1985). Three *trans*-acting regulatory genes, *traM*, *traJ*, and *finP*, lie outside of the *tra* operon and are transcribed from their own promoters. A fourth

**Figure 1.2** Conjugative transfer genes of the F plasmid. The length of the transfer region is indicated at the top in kilobases (kb). *tra* and *trb* genes are labelled with capital and lowercase letters, respectively. The origin of transfer (*ori*) and the major transfer operon promoter pY are shown. Note that *finP* and *artA* are transcribed in the direction opposite to the other genes and the presence of an IS3 element within the *finO* gene. The *tra* gene products are grouped according to function. Modified from Frost *et al.* (1994).



regulatory gene, *finO*, is located at the distal end of the *tra* region and may be transcribed from its own promoter. The products of the *tra* region are functionally classified according to the stage in the transfer process (regulation; pilus synthesis and assembly; aggregate stability; surface exclusion; and signalling, origin nicking, unwinding and transfer) in which they participate. This thesis will focus on the regulation of conjugation which occurs at the pY promoter in response to the activities of the *traJ*, *finP* and *finO* gene products in the process termed Fertility Inhibition.

#### 1.4 FinOP Fertility Inhibition

Fertility inhibition (Fin) of IncF plasmids is dependent on the ability of two components, FinO and FinP, to repress the stimulatory effect of the TraJ protein on *tra* operon transcription. TraJ is a positive regulator of the *tra* operon, required for activation of high levels of transcription from the pY promoter (Willetts, 1977). FinP, which is transcribed from the opposite strand and in a direction opposite to *traJ*, is a small antisense RNA molecule complementary to part of the untranslated leader of *traJ* mRNA (Finnegan & Willetts, 1971; Mullineaux & Willetts, 1985). In combination with the FinO protein, FinP negatively regulates *traJ* expression, reducing transcription of the *tra* genes and ultimately leading to repression of conjugation (Willetts, 1977).

The F plasmid is naturally derepressed for transfer due to the insertion of an IS3 transposable element within its *finO* gene (Figure 1.2; Cheah & Skurray, 1986; Yoshioka *et al.*, 1987). This results in constitutive expression of *traJ* and consequently, *tra* functions, which is metabolically expensive and makes the host cell vulnerable to infection by pilus-specific bacteriophages (Hedges *et al.*, 1973). Repressed plasmids

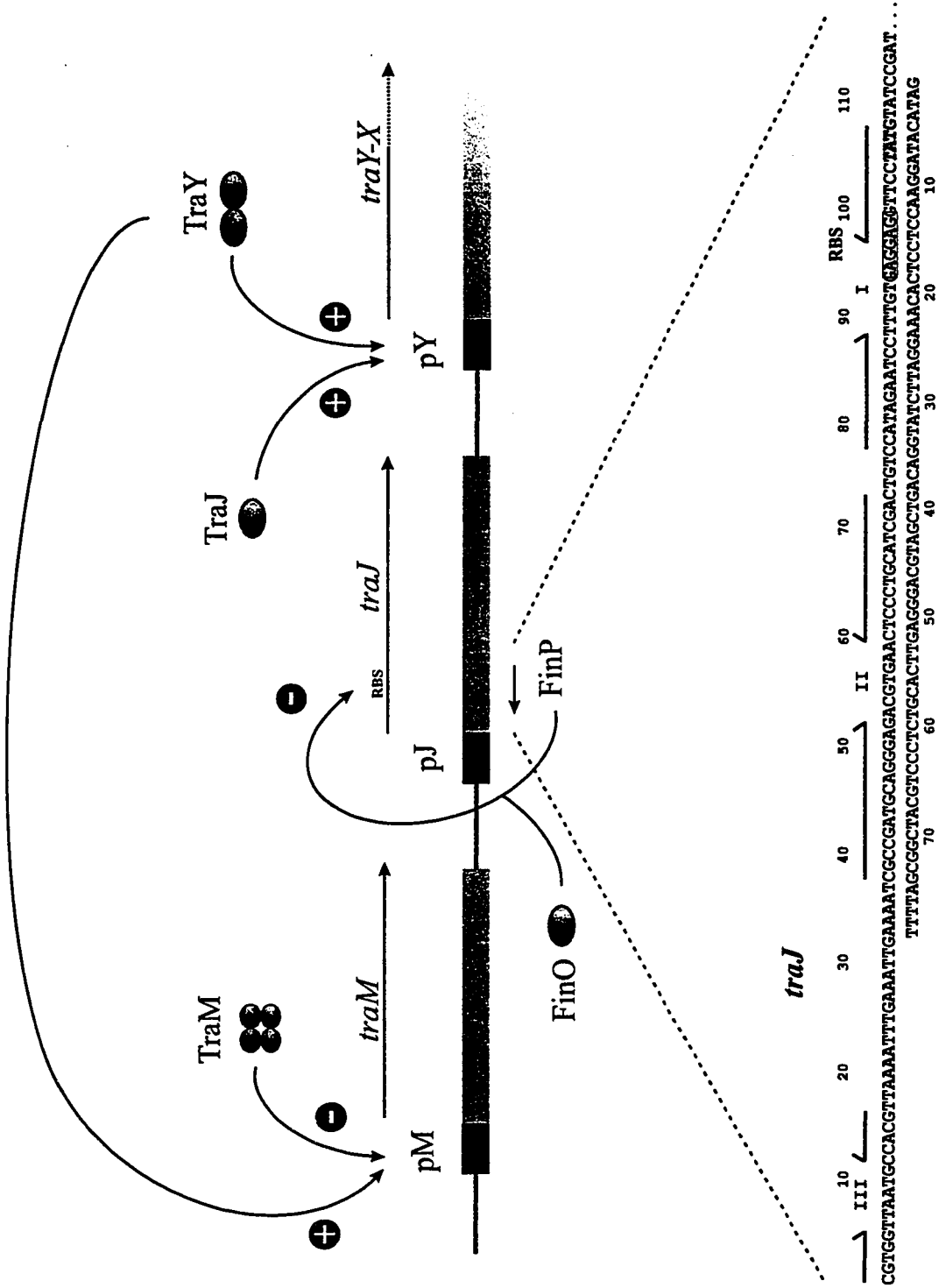
elude these repercussions while maintaining the capacity for horizontal transfer through a phenomenon known as “transient derepression” (Broda, 1975). A recipient cell which has newly acquired a conjugative plasmid exhibits transient derepression (high-frequency transfer) until the *Fin* products accumulate to inhibitory levels (approximately 6 generations; Willetts, 1974), allowing for infectious spread of the plasmid through a recipient population (Simonsen, 1990). F transfer can be repressed *in trans* if the *finO* gene is expressed from a compatible coresident plasmid (Finnegan & Willetts, 1973; van Biesen & Frost, 1992). A description of the components and process of Fertility Inhibition appear in the following sections and are shown schematically in Figure 1.3.

#### **1.4.1 The role of TraJ in regulating transcription from the pY promoter**

Expression of the *tra* operon requires both host- and plasmid-encoded proteins, with TraJ serving as the main activator. TraJ is a 27 kDa plasmid-specific, cytoplasmic protein which has been shown to stimulate transcription from the pY promoter when fused to *lacZ* (Gaffney, *et al.*, 1983) or *galK* (Mullineaux & Willetts, 1985) reporter genes. Five alleles of *traJ* have been reported (Willetts & Maule, 1986; Di Laurenzio *et al.*, 1991; Graus-Goldner *et al.*, 1990) which show very little homology except for the presence of a helix-bend-helix DNA-binding motif at their N-termini (Takeda *et al.*, 1983). DNA-binding by TraJ has not been demonstrated and the mechanism by which TraJ activates transcription from pY is unknown. In addition to TraJ, the chromosomally-encoded ArcA protein is required for maximal transcription from pY (Silverman *et al.*, 1991). ArcA is the response-regulator of a two-component system involved in sensing and adapting to changes in the redox state of a bacterial cell (Lynch &



**Figure 1.3** FinOP regulation of F plasmid transfer. The *finP/traJ* DNA sequence is shown below the diagram. The arrows above the sequence mark inverted repeats which allow FinP and the *traJ* mRNA to fold into the structures shown in Figure 1.4. The *traJ* RBS is outlined with a box and the start codon is shaded in grey. I, II and III indicate stem-loops I, II and III in Figure 1.4. The numbers above and below the DNA sequence indicate the number of bases from the 5' end of *traJ* and FinP, respectively.



*finP*

Lin, 1996). Binding of ArcA to the pY promoter of plasmid R1 has been demonstrated (Strohmaier *et al.*, 1998), however transcriptional activation by ArcA occurs only in the presence of TraJ (Strohmaier *et al.*, 1998; Silverman *et al.*, 1991). Two other proteins, IHF (*integration host factor*; host-encoded) and TraY (plasmid-encoded) also influence *tra* operon transcription. TraY has three DNA binding sites, two within *oriT* and one near the pY promoter (Nelson *et al.*, 1993). *traY* amber mutations reduce pY-driven alkaline phosphatase activity by 75-90% (Silverman & Scholl, 1996), suggesting that TraY regulates its own synthesis as well as other genes under pY control. TraY also activates transcription of the *traM* gene immediately upstream of *traJ* (Penfold *et al.*, 1996; Stockwell & Dempsey, 1997), which encodes an essential transfer protein involved in relaxosome formation at *oriT* (Di Laurenzio *et al.*, 1992; Penfold, 1995). IHF also binds to the *oriT* region of F (Tsai *et al.*, 1990) and its mutation reduces pY promoter activity by about 45% (Silverman *et al.*, 1991). Gaudin & Silverman (1993) propose that TraJ induces transcription in combination with other activator proteins (ArcA, TraY, IHF) by formation of a nucleoprotein complex which increases the superhelical density of the pY promoter, leading to the generation of a stable polymerase-promoter complex.

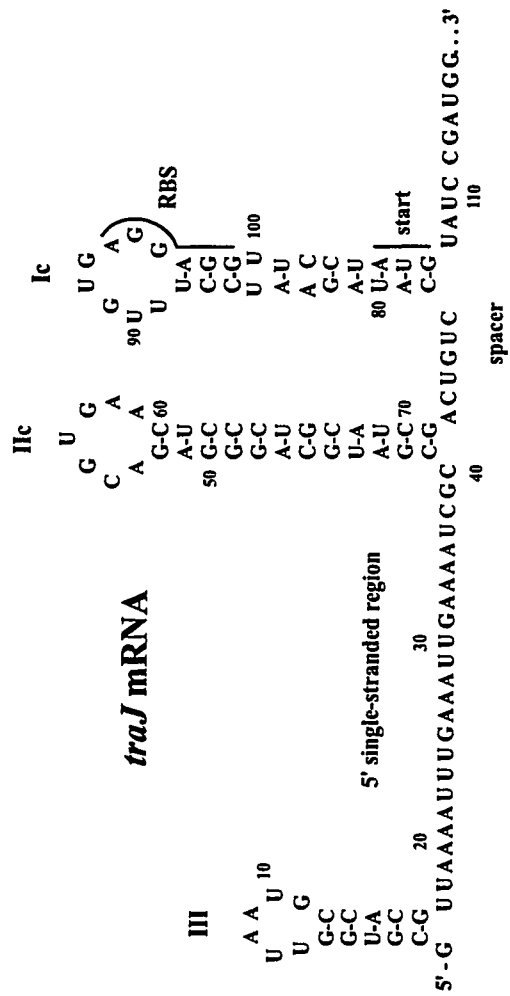
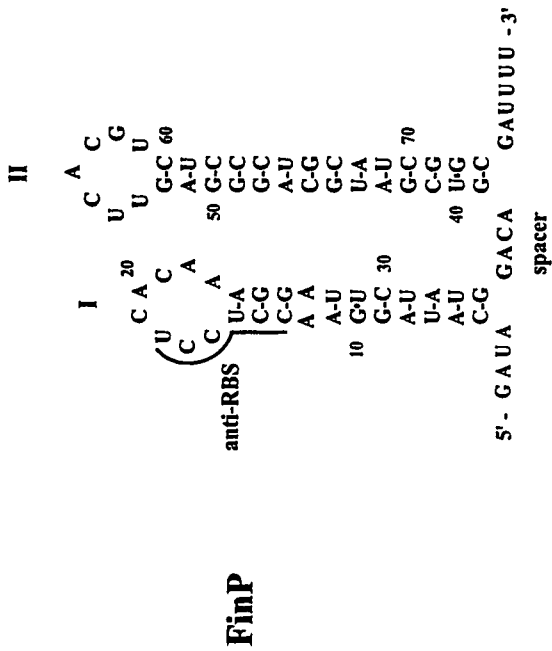
TraJ expression is subject to negative regulation by FinOP (discussed in the next section) and indirectly, by mutations that deregulate the Cpx signal transduction system (Silverman *et al.*, 1993). In response to cell envelope stress, the inner membrane sensor (CpxA) becomes autophosphorylated and transfers its phosphate to the response regulator (CpxR). Phosphorylated CpxR functions as a transcriptional activator of envelope stress-combative proteins, such as the periplasmic protease, DegP (Danese & Silhavy, 1998). Danese *et al.* (1995) have shown that *cpxA* missense mutations cause unregulated

phosphorylation of CpxR, due either to disrupted phosphatase activity or enhanced kinase activity of CpxA, resulting in hyperactivation of CpxR-regulated genes, including DegP. *cpxA* missense mutations are pleiotropic and result in decreased accumulation of the TraJ protein, leading to reduced *tra* gene expression, whereas deletion of the *cpx* genes has no effect (Silverman *et al.*, 1991). Danese *et al.* (1995) suggest that the effect of *cpxA* missense mutations on F transfer is indirect and results from aberrant properties (ie. DegP-mediated proteolysis of transfer proteins in the periplasm and secondary effects on TraJ) of the hyperactivated Cpx pathway. The transfer operon is also known to be sensitive to catabolite repression, as evidenced by the inhibitory effect of cyclic AMP (cAMP) on pilus formation in an *E. coli cya* mutant (Harwood & Meynell, 1975). Paranchych *et al.* (1986) identified a putative CRP (cAMP receptor protein) consensus binding sequence overlapping the *traJ* transcription initiation site and propose that in stationary phase (when cAMP levels increase), pilus synthesis is turned off by cAMP-CRP repression of *traJ* transcription.

#### 1.4.2 FinP antisense RNA

The most efficient means of regulating *tra* gene expression is through control of TraJ synthesis, which is accomplished by FinP and its corepressor FinO. The F *traJ* transcript contains a 105 base untranslated leader (Figure 1.3), whose secondary structure has been determined *in vitro* and consists of three stem-loop (SL) domains and an extensive 5' single-stranded region (Figure 1.4; van Biesen *et al.*, 1993). The *finP* gene is located within the *traJ* leader, but is transcribed in the opposite direction (Figure 1.3; Mullineaux & Willetts, 1985). Constitutive expression of *finP* from its own promoter

**Figure 1.4** Secondary structures of FinP antisense RNA and the first 117 bases of *traJ* mRNA. Stem-loops I and II of FinP are complementary to stem-loops Ic and IIc of *traJ* mRNA. The FinP sequence complementary to the *traJ* RBS is indicated (anti-RBS). The *traJ* mRNA has an extra stem-loop (III) and an extensive single-stranded region at its 5' end. Modified from van Biesen *et al.* (1993).



(Finlay *et al.*, 1986; Mullineaux & Willetts, 1985) results in the production of a ~79 base untranslated repressor RNA (FinP) that is antisense to part of the leader, ribosome binding site (RBS) and first two codons of the *traJ* mRNA. The FinP secondary structure forms two stem-loop domains *in vitro* (Figure 1.4; van Biesen *et al.*, 1993) which have the potential to base pair (duplex) with the *traJ* mRNA. Duplex formation between FinP and the *traJ* mRNA leader has been demonstrated *in vitro* (van Biesen *et al.*, 1993) and it is believed that such an interaction prevents translation of *traJ* by occlusion of its RBS.

Five alleles of FinP have been characterized (Finlay *et al.*, 1986) which exhibit near sequence identity within the stems but differ significantly in the two hairpin loops. Mutational analysis of plasmid R1 FinP (IncFII; Koraimann *et al.*, 1991, 1996) indicates that the loops define the allelic specificity (first suggested by Willetts & Maule, 1986) of FinP for its cognate *traJ* mRNA. Using a reporter *traJ-lacZ* fusion protein, Koraimann *et al.* (1996) provided the first evidence that FinP directly controls *traJ* expression. They found that *finP* expressed *in cis* or from a multicopy plasmid *in trans* reduced *traJ* expression 6- or 2000-fold, respectively, indicating that FinP activity is highly dosage-dependent. In the same study, the authors showed that base changes in the FinP loops dramatically reduce repressor activity, supporting a model in which FinP/*traJ* mRNA duplex formation is initiated by “kissing” of the sense/antisense RNA loops in a manner reminiscent of the RNA I/RNA II interaction that regulates ColE1 plasmid replication (described in section 1.5.1). It should be noted that rather than complete duplex formation, interaction of only the FinP/*traJ* loops might suffice to prevent *traJ* expression

because the sequence complementary to the *traJ* RBS lies partially in FinP loop I (Figure 1.4; van Biesen & Frost, 1993; Koraimann *et al.*, 1996).

Two FinP transcripts (approximately 74 and 135 bases) originating from the same promoter have been reported for the R100 plasmid (IncFII; Dempsey 1987, 1994a). The 74 base transcript represents the majority (95%) of the FinP signal obtained by ribonuclease (RNase) protection analysis, however Northern blots indicate that the ratio of the 74 base to the 135 base RNA varies from 4:1 to 1:2 (Dempsey, 1994a). Further work is required to address the differences obtained by these two techniques, which could benefit from the use of quantitative internal controls. Since both transcripts end with stem-loop structures characteristic of rho-independent terminators, Dempsey (1994a) proposes that the 135 base transcript results from “leaky” termination at the first site (74 bases), although it is also possible that the shorter transcript results from nucleolytic degradation of the longer transcript. Paranchych *et al.* (1986) suggested an alternate rho-dependent termination site for F FinP in the region complementary to *traJ* SLIII, but only one FinP transcript has been detected for F (Dempsey, 1987; Lee *et al.*, 1992), which appears to terminate at a rho-independent terminator (SLII).

Evidence for FinP/*traJ* mRNA duplex formation *in vivo* has been presented for R100-1, a spontaneous *finO*<sup>-</sup> mutant of R100 (Dempsey, 1994a). In this report, two sense/antisense duplexes, of sizes approximately equal to the FinP RNAs, were detected in a strain carrying a mutation in the host ribonuclease, RNase III. The presence of both FinP transcripts in the wild-type strain, in the absence of detectable *traJ*, indicated that FinP was present in excess and that *traJ* mRNA was removed by rapid destruction of the duplexes by RNase III. An unexpected result, which the author did not address, was the



finding that only trace amounts of the duplexes were produced from R100 (*finO*<sup>+</sup>) in the RNase III mutant. One possible explanation follows. In the absence of FinO, R100-1 produces additional sense transcripts that read into the *traJ* leader from two *traM*-associated promoters, *traM* and *finM* (Dempsey, 1989). The 3' ends of these transcripts, which are identical in sequence to the 5' end of *traJ*, provide additional substrates for duplex formation with FinP. Since *traJ* is the limiting factor for duplex formation, these additional *traM*-associated transcripts could account for the increased accumulation of duplexes from R100-1 seen in the RNase III mutant. Dempsey (1994b) proposes that these readthrough transcripts, which are not produced in the repressed plasmid R100, provide "decoy" RNA that attracts more FinP antisense RNA into pairing, resulting in less available FinP to prevent translation of complete *traJ* mRNA transcripts. This additional level of *traJ* regulation does not appear to operate in the naturally derepressed F plasmid, as *traM*-associated readthrough transcripts have not been detected.

Limited evidence has been obtained for *in vivo* duplex formation in F. Using primer extension analysis, van Biesen *et al.* (1993) showed that in the presence of FinO, the intracellular concentration of full-length *traJ* mRNA was reduced, while two truncated forms of *traJ*, with 5' ends located 12 and 24 bases from the 3' end of FinP, increased in concentration. They proposed that the truncated species might represent RNase III-mediated cleavage products but proof of this hypothesis awaits further more direct evidence. As noted earlier, full repression of conjugation by FinP requires the product of the *finO* gene, which is described in the following section.

### 1.4.3 The RNA-binding protein, FinO

FinO is the corepressor required for maximal repression of *traJ* (Finnegan & Willetts, 1971). The *finO* gene is located at the distal end of the *tra* region of F-like plasmids, adjacent to *traX* (Figure 1.2; Cheah *et al.*, 1984; McIntire & Dempsey, 1987). It is not presently known if *finO* is transcribed from its own promoter or as part of the *tra* operon, from pY. Conjugative transfer of F and R100-1 is deregulated due to inactivation of their *finO* genes by insertion of an IS3 element in the former and an A residue in the latter, both of which lead to premature termination of the open reading frames (Cheah & Skurray, 1986; Yoshioka *et al.*, 1987). Unlike the *finP* and *traJ* genes which are plasmid-specific, *finO* is exchangeable among F-like plasmids (Finnegan & Willetts, 1973). Willetts & Maule (1986) identified two alleles of *finO* based on their levels of repression of F-like plasmids. Although the sequences of the *finO* genes are highly conserved, the presence of a gene (*orf286/orfC*) upstream of Type I alleles stabilizes the *finO* mRNA and increases the FinO concentration (van Biesen & Frost, 1992), accounting for the 100-1000-fold repression of F transfer exhibited by Type I alleles (R100, R6-5), as compared to 20-50-fold for Type II (ColB2).

FinO is a 21.2 kDa (186 amino acid) cytoplasmic protein (McIntire & Dempsey, 1987; Yoshioka *et al.*, 1987) which seems to exert its coregulatory effect on *traJ* expression by increasing the intracellular concentration of FinP antisense RNA (Dempsey, 1987; Lee *et al.*, 1992; Koraimann *et al.*, 1991,1996). FinO does not increase transcription from the *finP* promoter (Mullineaux & Willetts, 1985), but instead elevates the steady-state level of FinP by preventing its decay (Frost *et al.*, 1989; Lee *et al.*, 1992; van Biesen & Frost, 1994). Lee *et al.* (1992) showed that, in the absence of *traJ*, the

chemical half-life of a cloned FinP-like intermediate RNA, derived from a longer (151 base) transcript induced from the *tac* promoter, could be extended from 2 to more than 40 minutes in the presence of FinO. In the same study the authors showed that decay of the 151 base and to a lesser extent, the FinP-like RNA, were stabilized at the nonpermissive temperature in a strain carrying a temperature-sensitive mutation in the gene encoding the host ribonuclease, RNase E, but not RNase III. However, because of the vector sequence that preceded FinP due to transcription from the *tac* promoter, it was unclear whether RNase E cleavage was reduced at a site within FinP or within the vector-encoded sequence. Two important goals of this thesis are to measure the effect of host RNases on FinP stability directly, in the presence and absence of *traJ* and to determine whether the FinO protein protects FinP from a specific RNase(s).

Koraimann's group (1996) has shown that the presence of FinO doubles the concentration of plasmid R1 FinP RNA, but this is insufficient to account for the concomitant ~300-fold increase in repression. A second function proposed for FinO is the enhancement of FinP/*traJ* duplex formation. Using a protein fusion between glutathione S-transferase (GST) and R6-5 FinO, van Biesen & Frost (1994) showed that FinO is an RNA-binding protein which increases the rate of duplex formation *in vitro* approximately 5-fold. The interaction between ColE1 plasmid RNA I and RNA II is also facilitated by a plasmid-encoded protein (Twigg & Sherratt, 1980; Tomizawa, 1990b, Eguchi & Tomizawa, 1990), known as Rop (*Repressor of Primer*) or Rom (*RNA One Modulator*). Unlike Rom, which binds to and stabilizes the sense/antisense RNA "kissing complex", FinO binds the RNAs individually, prior to duplex formation (van Biesen & Frost, 1994). Furthermore, Rom is dispensable for RNA-RNA hybrid formation, whereas

FinO activity is essential for complete repression of conjugative plasmids. In addition to the 2-fold increase in FinP antisense RNA concentration and the 5-fold increase in the rate of FinP/*traJ* duplex formation, RNA binding by FinO might stabilize the initial complex formed between FinP and its target, accounting for the full 300-fold increase in repression observed in the presence of FinO (Koraimann *et al.*, 1996).

The FinOP system has also been suggested to reduce *traM* expression in F and R100, through its negative effect on *traJ* translation, which in turn reduces *traY* expression, which is an activator of *traM* (Figure 1.3; Penfold *et al.*, 1996; Stockwell & Dempsey, 1997). For this reason R100 (*finO*<sup>+</sup>) does not express *traM/finM* transcripts and because the FinP concentration is increased by FinO, complete repression of *traJ* expression and plasmid transfer occurs.

The secondary structure of the FinO protein is predicted to consist of a basic N-terminal  $\alpha$ -helical domain (pI = 11.2) and an acidic C-terminal  $\alpha$ -helical domain (pI = 5.1; Sandercock, 1997; Sandercock & Frost, 1998). Regions of indeterminate structure followed by  $\beta$ -sheet domains are predicted to precede the N-terminal  $\alpha$ -helix and to span the central part of the protein. Although the FinO amino acid sequence does not share homology with any known binding motifs characteristic of other RNA-binding proteins (Mattaj, 1993), recent experiments have shown that the basic N-terminal domain (amino acids 1-73) possesses this activity (Sandercock, 1997; Sandercock & Frost, 1998). Characterization of GST-FinO deletion mutants has revealed that in addition to the N-terminal RNA-binding domain, two other functional domains exist in FinO: a central domain (amino acids 74-141) involved in sense/antisense RNA duplex formation and a

C-terminal (amino acids 142-186) RNA-protection domain (Sandercock, 1997; Sandercock & Frost, 1998).

The features of RNA that are recognized by FinO are less clear. Early studies with a class of dominant F *finP* mutants which were derepressed for transfer in the presence of R100 (Finnegan & Willetts, 1971, 1973), suggested that the defect was associated with the *FinO* site of action (*fisO*). Sequence analysis revealed that a single base mutation in SLI (C30:U), which reduced the intracellular concentration of FinP RNA, was responsible for the *fisO* phenotype (Frost *et al.*, 1989). Since the amount of FinP RNA did not increase in response to FinO, Frost *et al.* (1989) postulated that stabilization of FinP decay required FinO interaction with SLI. Subsequent *in vitro* studies revealed that GST-FinO recognition of FinP required SLII, but not SLI, although binding was observed between GST-FinO and a duplex formed between SLI and the complementary sequence in *traJ* and between FinP and the *traJ* mRNA leader (van Biesen & Frost, 1994). These findings suggest that FinO binds nonspecifically to A-form double-stranded RNA. The third, and final, goal of this thesis is to define the features of FinP RNA that are recognized by the FinO protein.

## **1.5 Regulation by other antisense RNA systems**

Several examples of gene regulation by natural antisense RNA transcripts have been found in prokaryotes (reviewed by Wagner & Simons, 1994) and more recently, in eukaryotes (reviewed by Knee & Murphy, 1997). For almost all systems characterized to date, the antisense RNAs act as negative regulators of biological activity. Currently, clinical trials are in progress to test the ability of synthetic antisense oligonucleotides to

act as specific inhibitors of gene expression in the control of diseases ranging from renal transplant rejection to the treatment of cancer and HIV infection (Wyngaarden *et al.*, 1997). In many instances, antisense constructs have been unsuccessful, necessitating a more thorough understanding of the mechanisms associated with natural antisense RNA control.

Eguchi *et al.* (1991) have classified antisense RNAs into two general types according to their mode of action. In Type I, binding of the antisense RNA disrupts the function of its target RNA directly, by blocking access to the region that is complementary to the antisense RNA. The best characterized example of the Type I mechanism is seen in the regulation of *IS10* transposition, where sense/antisense RNA pairing blocks the ribosome binding site, inhibiting translation of transposase (Ma & Simons, 1990). Type II antisense RNAs act indirectly by altering the structure of the target RNA. This may lead to masking of the RBS and/or the initiation codon, premature termination of transcription of the target RNA, increased susceptibility of the target RNA to degradation by RNases, or as in the case of ColE1 plasmid copy number control, prevention of primer maturation for DNA replication (Tomizawa, 1986).

### **1.5.1 Regulation of ColE1 plasmid replication by antisense RNA**

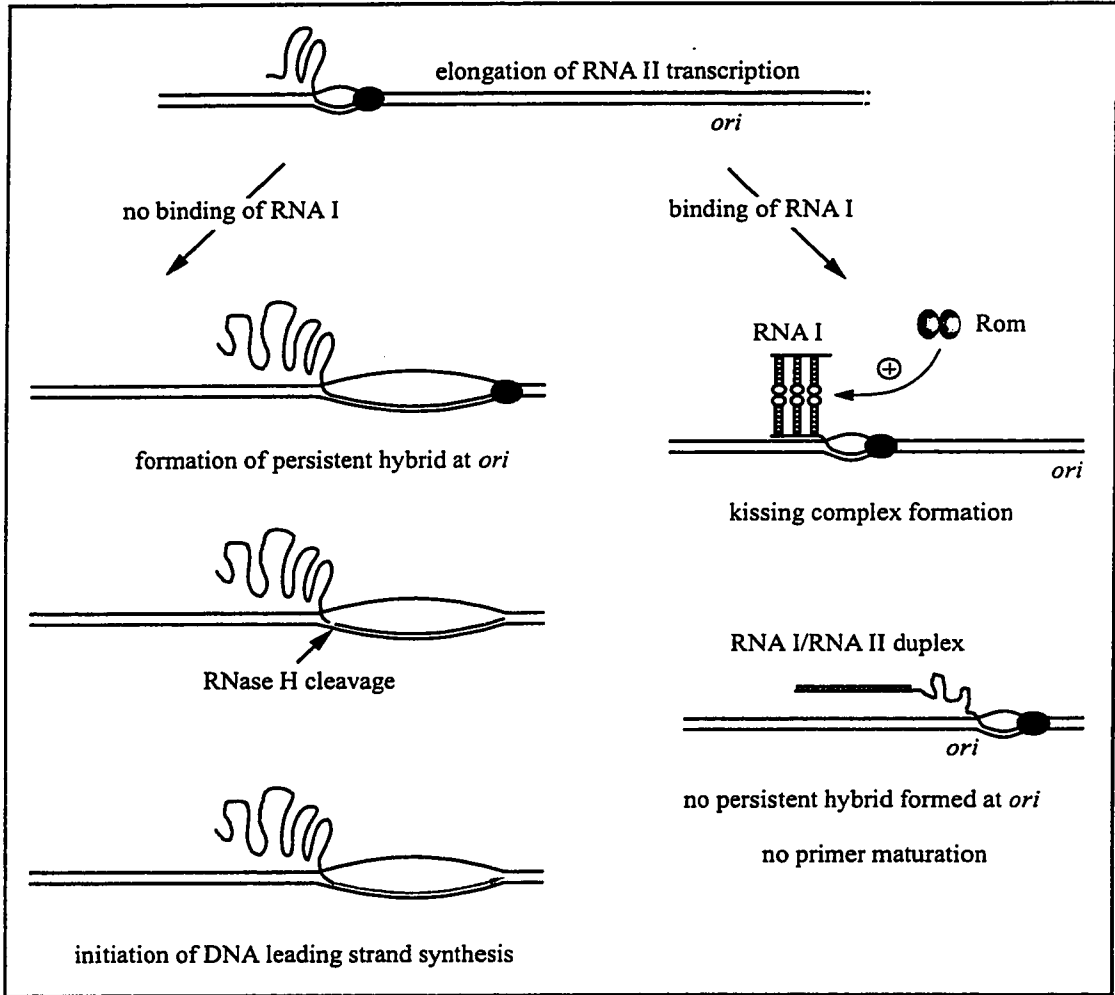
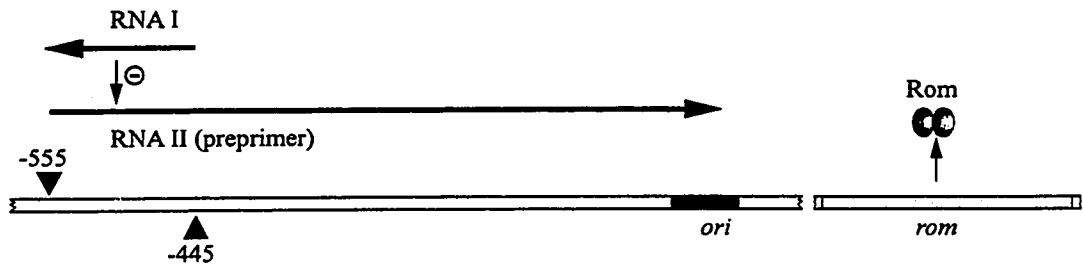
Natural antisense RNA control was first demonstrated in the small multicopy plasmid ColE1 (Lacatena & Cesareni, 1981). Replication of ColE1 and related plasmids (~10-30 copies per chromosome) is a tightly controlled, multi-step process that is dependent on host-encoded proteins. Initiation of DNA replication begins with the production of an immature RNA preprimer, RNA II, from a site 555 nucleotides upstream

of the plasmid origin of DNA replication (Itoh & Tomizawa, 1980; Figure 1.5a). Initially, the RNA II transcript is separated from the DNA template, but as RNA polymerase approaches the origin, an unusually persistent hybrid forms. The RNA strand of the RNA-DNA hybrid is cleaved by RNase H and the mature 3' end of RNA II serves as the primer for DNA synthesis by DNA polymerase I (Itoh & Tomizawa, 1980). In order to form a persistent hybrid with the template DNA, RNA II must fold into a unique structure which is subject to negative regulation by a plasmid-specified ~108 nucleotide RNA, RNA I (Tomizawa *et al.*, 1981; Tomizawa & Itoh, 1981; Lacatena & Cesareni, 1981). RNA I synthesis initiates 445 nucleotides upstream from the replication origin, but proceeds in the direction antisense to RNA II. Binding of RNA I to the complementary region within the 5' end of elongating RNA II prevents it from forming the conformation necessary for its hybridization to the template DNA (Masukata & Tomizawa, 1986), which inhibits primer maturation and replication and the plasmid copy number decreases (Tomizawa & Itoh, 1981; Tomizawa, 1984). The timing of sense/antisense RNA pairing is crucial, as the elongating RNA II transcript is susceptible to inhibition by RNA I only when it is between 100 and 360 nucleotides in length. After this time RNA II assumes a conformation that commits it to stable hybrid formation with the template DNA (Tomizawa, 1986).

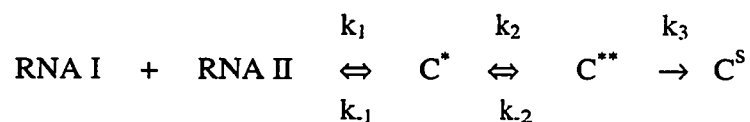
A second plasmid-encoded inhibitor, known as Rom or Rop, transcribed from a region downstream of the origin of replication, enhances the negative effect of RNA I on the frequency of replication initiation (Cesareni *et al.*, 1984; Lacatena *et al.*, 1984). Rom is a 63 amino acid protein which functions to enhance the binding of RNA I to RNA II. The kinetics of duplex formation between RNA I and RNA II, which proceeds through a

**Figure 1.5a** Antisense RNA control of plasmid ColE1 primer maturation. The elongating preprimer transcript, RNA II, forms a persistent hybrid with the template DNA near the replication origin (*ori*). The hybridized transcript is cleaved by RNase H and used as a primer for leading strand DNA synthesis. Association of antisense RNA I with elongating RNA II induces a conformational change that inhibits primer maturation. Rom protein binds to and stabilizes the RNA I/RNA II kissing complex. Adapted from Wagner & Simons (1994).





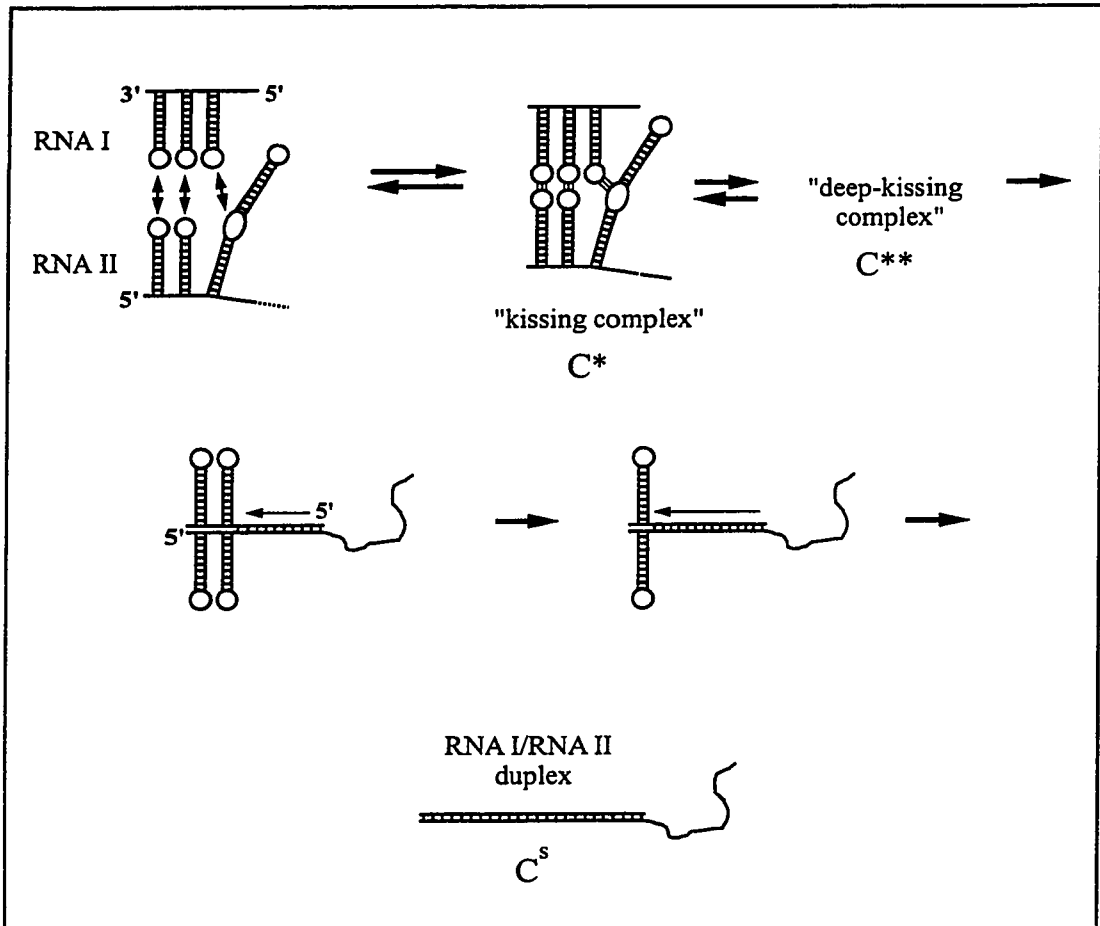
series of progressively more stable intermediates are well-characterized and are shown in Figure 1.5b. The initial interaction involves reversible base-pairing between a few nucleotides in the three complementary loops and forms the “kissing complex” ( $C^*$ ) (Tomizawa, 1985). This unstable intermediate is converted to a more stable “deep-kissing complex” ( $C^{**}$ ) by the inclusion of up to 7 nucleotides from each loop in the base-pairing reaction (Tomizawa, 1990a; Eguchi *et al.*, 1991). The 5' single-stranded region of antisense RNA I then becomes appropriately positioned to base-pair with the complementary region of RNA II allowing the two molecules to “zip” together as the “deep-kissing” intermediate progressively dissolves, producing the final stable duplex ( $C^S$ ). It has been shown that hybridization into the first stem-loops (SLIII/SLI of the sense/antisense RNA pair, respectively) is sufficient to inhibit primer formation (Tomizawa, 1984). The overall reaction for RNA I/RNA II pairing is:

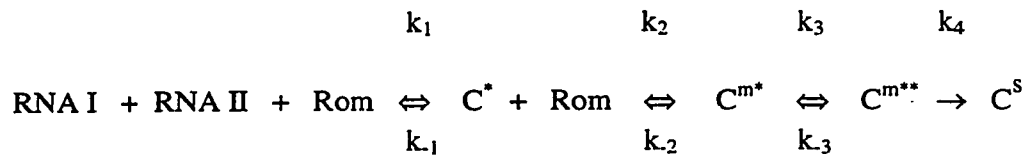


The rate limiting step in stable complex formation is kissing ( $k_1$ ) (Tomizawa, 1985; Tomizawa, 1990a). The exceptional stability of the duplex renders the value of the dissociation rate constant  $k_3$  insignificant. The apparent second order rate constant ( $k_{app}$ ) for duplex formation determined by Tomizawa (1984) is  $7.1 \times 10^5 \text{ M}^{-1}\text{s}^{-1}$ .

Rom creates a second pathway for stable RNA I/RNA II pairing, given by the following:

**Figure 1.5b** Pathway for duplex formation between ColE1 antisense RNA I and the replication preprimer, RNA II. An initial loose association between a few bases in the RNA loops leads to the formation and rapid dissociation of “kissing complexes”. The more stable, but reversible “deep-kissing” intermediates result from hydrogen bonding between all bases in the complementary loops. In the final steps, the unpaired 5’ leader of RNA I nucleates stable duplex formation by pairing to its complementary sequence in RNA II. Adapted from Wagner & Simons (1994).





where a single dimer of Rom binds to the kissing complex  $C^*$  and converts it to the more stable complex  $C^{m*}$  (Eguchi & Tomizawa, 1990), reducing the value of the dissociation constant  $k_{-1}$ , driving the formation of the “deep-kissing complex”  $C^{m^{**}}$  and finally the stable duplex  $C^S$ . Rom has no effect on the association rate constant  $k_1$  for kissing complex formation, nor on the subsequent propagation of pairing (Tomizawa, 1990b). As a result, Rom has only a moderate effect on the overall rate of duplex formation, doubling the  $k_{app}$  to  $1.0 \times 10^6 \text{ M}^{-1}\text{s}^{-1}$  (Tomizawa & Som, 1984), which corresponds well with the observed 2-fold increase in plasmid copy number associated with deletion of the *rom* gene (Twigg & Sherratt, 1980; Cesareni *et al.*, 1982). The high copy number of the pUC series of plasmids, which are based on the ColE1 origin of replication, is due to the absence of the *rop/rom* gene and a single base mutation in RNA II, which is predicted to alter its secondary structure and reduce its interaction with RNA I (Lin-Chao *et al.*, 1992).

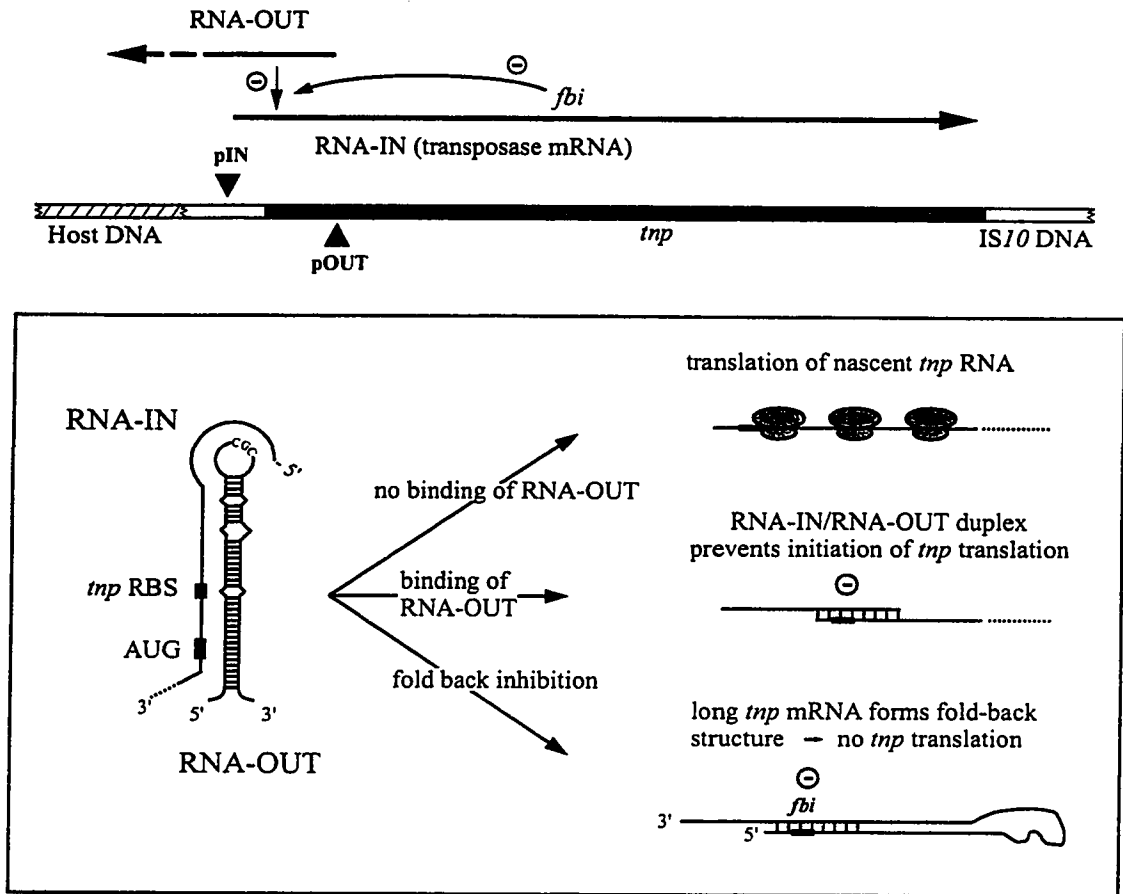
### 1.5.2 Antisense RNA control of *IS10* transposition

The tetracycline resistance transposon *Tn10* is flanked by inverted repeats of insertion sequence *IS10*. The rightward *IS10* encodes the transposase (*tnp*) function whose expression is rate-limiting for transposition (Figure 1.6a; Morisato *et al.*, 1983). Transcription from the pIN promoter yields the transposase mRNA, RNA-IN (Simons & Kleckner, 1983). Translation of *tnp* from RNA-IN is negatively regulated by an antisense

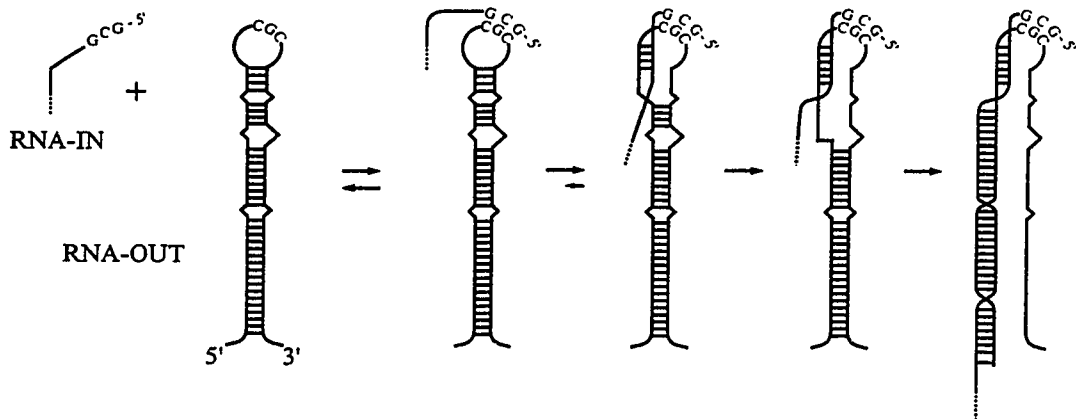
**Figure 1.6a** Regulation of *IS10* transposition by antisense RNA. Binding of RNA-OUT to the complementary region of the transposase (*tnp*) mRNA, RNA-IN, sequesters the RBS inhibiting its translation. Occlusion of the RBS can also be achieved by intramolecular base pairing (foldback inhibition (*fbi*)) if RNA-OUT does not bind before RNA-IN reaches 360 nucleotides in length. Adapted from Wagner & Simons (1994).

**Figure 1.6b** Pathway for duplex formation between *IS10* RNA-IN and RNA-OUT. The initial unstable complex involves the formation of three G-C base pairs between the 5' single-stranded end of RNA-IN and the loop of RNA-OUT. Nucleation propagates down the 5' side of RNA-OUT as the nascent duplex rotates around the disrupted stem. Adapted from Kittle *et al.* (1989).

a



b



RNA molecule, RNA-OUT, that is transcribed in the opposite direction to RNA-IN, from the pOUT promoter. The first 35 bases of RNA-OUT antisense RNA (69 bases) are complementary to part of the 5' end of RNA-IN that includes the *tnp* RBS and translation start codon. Binding of RNA-OUT to RNA-IN is believed to inhibit translation of *tnp* directly by blocking ribosomal access to the RBS. This proposal is supported by genetic studies whereby RNA-OUT has been shown to inhibit *tnp* expression from translational, but not transcriptional fusions (Simons & Kleckner, 1983). More direct evidence was obtained from an elegant *in vitro* study by Ma & Simons (1990) in which they used a sensitive "toe-print" assay to demonstrate that RNA-OUT prevents 30S (ternary) and complete 70S ribosomal pre-initiation complex formation specifically at the *tnp* translation initiation site only when it is paired to RNA-IN. Case *et al.* (1990) provided the first physical evidence that the RNA-IN/RNA-OUT pairing occurs *in vivo*. They also showed that a second effect of sense/antisense RNA pairing is destabilization of the RNA-IN transcript (and consequently RNA-OUT) due to cleavage of the duplex by RNase III. However the authors concluded that destabilization is not required for antisense RNA control because transposase expression (from a *tnp-lacZ* fusion) was not altered in an RNase III host when compared to the wild-type. Therefore occlusion of the ribosome binding site is the primary mechanism of antisense RNA-OUT action.

The secondary structure of RNA-OUT consists of a 28 base-pair stem domain topped by a 6 nucleotide loop (Kittle *et al.*, 1989). The region of complementarity to RNA-IN begins within the loop and extends down the 5' side of the RNA-OUT stem. Kittle *et al.* (1989) studied the process of duplex formation between wild-type and mutant pairs of RNA-IN and RNA-OUT *in vitro* and developed the pairing scheme shown in



Figure 1.6b. Pairing is thought to initiate by an interaction between the 5' terminal nucleotides (GCG) of RNA-IN with the complementary sequence in the loop of RNA-OUT. Following this rate-limiting step, nucleation proceeds down the 5' side of RNA-OUT by intertwining of the two complementary strands, which is achieved by rotation of the newly formed duplex around RNA-OUT. Mutations that close the loop are defective in duplex formation, likely because they prevent passage of RNA-IN through the loop.

In the model for RNA I/RNA II duplex formation, transient loop-loop interactions are followed by secondary pairing and nucleation at the single-stranded regions flanking the stems (Tomizawa, 1984). In contrast, RNA-OUT has only two unpaired nucleotides available for base-pairing on the 5' side of the stem and thus propagation of base-pairing must proceed down the 5' side of the RNA-OUT stem. An exhaustive mutational analysis carried out by Jain (1995) revealed that the internal loop nearest the top of the RNA-OUT stem is essential for antisense inhibition, as are the 4 G-U mismatches, which facilitate melting of the RNA-OUT stem. The apparent second order rate constant ( $k_{app}$ ) for RNA-IN/RNA-OUT duplex formation is  $3.0 \times 10^5 \text{ M}^{-1}\text{s}^{-1}$  (Kittle *et al.*, 1989), similar to that for RNA I/RNA II in the absence of Rom ( $7.1 \times 10^5 \text{ M}^{-1}\text{s}^{-1}$ ).

Interestingly, RNA-IN transcripts longer than 315 bases pair inefficiently to RNA-OUT (Wagner & Simons, 1994). This is due to the formation of secondary structure (called *fbi* for *fold-back inhibition*; Figure 1.6a) in the long RNA-IN transcripts that sequesters the RNA-IN 5' end and occludes entry to both the antisense RNA and ribosomes. Thus, as with the ColE1 system where RNA I must bind to the elongating RNA II transcript when it is between 100 and 360 nucleotides in length, the timing for RNA-IN/RNA-OUT pairing is critical.

## 1.6 mRNA degradation in *Escherichia coli*

mRNA turnover plays a central role in the control of gene expression. The lifetime of an RNA transcript is determined by a balance between its rates of synthesis and decay. In prokaryotes, the chemical half-life of mRNA, that is, the time necessary for degradation of 50% of the RNA molecules, varies from less than 30 seconds to more than 20 minutes (Ehretsmann *et al.*, 1992b). The stability of a given mRNA reflects its susceptibility to digestion by ribonucleases, which is determined by its sequence and structural features (Belasco & Higgins, 1988). On average, the lifetime of an mRNA in *E. coli* is approximately 2 to 3 minutes. It should be noted that “RNA degradation”, a catabolic activity in which the RNA molecule is destroyed, is distinct from “RNA processing”, an anabolic activity by which a precursor molecule undergoes specific modifications during its maturation to a functional form (Srivastava *et al.*, 1992; Deutscher, 1993). Examples of RNA processing include the separation of individual RNAs from polycistronic transcripts (ie. mRNA-mRNA, tRNA-tRNA, rRNA-rRNA, tRNA-mRNA and tRNA-rRNA) and mRNA splicing. This review will focus on the degradative enzymes and reactions that eliminate mRNA molecules from cells.

More than 20 RNases have been identified in *E. coli* and are divided into two classes on the basis of their mode of action. Exonucleases attack the free ends of an RNA molecule and endonucleases cleave the RNA internally.

### 1.6.1 *E. coli* exonucleases

Table 1.1 lists the RNases that have been implicated in mRNA degradation in *E. coli*. The two exonucleases, RNase II and polynucleotide phosphorylase (PNPase), are

**Table 1.1** *E. coli* RNases implicated in mRNA degradation.

<u>Ribonuclease</u>	<u>Gene</u>	<u>Reaction/Specificity</u>
<u>Exonucleases</u>		
RNase II	<i>mb</i>	RNA $\Rightarrow$ nucleoside (NS)-5'-monophosphates
PNPase	<i>pnp</i>	RNA + nPi $\Leftrightarrow$ n(NS-5'-diphosphate)
oligoribonuclease	<i>orn</i>	oligoribonucleotides $\Rightarrow$ NS-5'-monophosphates
<u>Endonucleases</u>		
RNase E	<i>rne;ams</i>	AU-rich single-stranded stretches $\Rightarrow$ 5'-P, 3'-OH ends
RNase III	<i>rnc</i>	double-stranded RNA $\Rightarrow$ 5'-P, 3'-OH ends
RNase I*	<i>rna</i>	unstructured RNAs and oligoribonucleotides $\Rightarrow$ 2',3'-cyclic mononucleotides ( $\Rightarrow$ NS-3'-monophosphates)
RNase M	?	pyrimidine-adenosine bonds $\Rightarrow$ 5'-OH, 3'-P ends

processive enzymes that degrade single-stranded RNA nonspecifically from the free 3' hydroxyl end towards the 5' phosphate end. No exonucleases functioning in the 5' to 3' direction have been identified in *E. coli*. RNase II mediates the step-wise hydrolysis of RNA releasing nucleoside-5'-monophosphates (Shen & Schlessinger, 1982) and is responsible for 90% of the exonucleolytic activity in *E. coli* extracts (Deutscher & Reuven, 1991). PNPase catalyzes the reversible, phosphorolytic degradation of RNA to nucleoside-5'-diphosphates (Littauer & Soreq, 1982). Both PNPase and RNase II slow down or stop when the oligonucleotide length is less than 10 nucleotides (Klee & Singer, 1968; Nossal & Singer, 1968) and are unable to bind or initiate degradation of short oligomers (Singer & Toburt, 1965; Coburn & Mackie, 1996a). A third processive 3'-5' exonuclease, oligoribonuclease (Niyogi & Datta, 1975; Zhang *et al.*, 1998), has been shown to co-purify with PNPase (Yu & Deutscher, 1995) and may serve to eliminate the small oligomers remaining from RNase II and PNPase activity. The presence of secondary structures, such as the *trp*t rho-independent terminator (Mott *et al.*, 1985) and the REP stem-loop from the *malE-malF* intergenic region of the maltose operon (McLaren *et al.*, 1991) have been shown to obstruct the processive activity of RNase II and to a lesser extent, PNPase. Strains with single mutations in either major exonuclease gene are viable and display normal mRNA decay (Donovan & Kushner, 1986), suggesting that RNase II and PNPase are functionally redundant. Conversely, an RNase II PNPase double mutant is inviable and accumulates mRNA decay intermediates, indicating that although these exonucleases play a major role in mRNA turnover, they do not participate in the rate-limiting step of decay for most messages.

### 1.6.2 *E. coli* endonucleases

The endonucleases, RNase III and RNase E, are moderately specific and participate in mRNA processing and degradation. Both RNases require divalent cations for catalysis and generate 3'-hydroxy termini, however RNase III degrades double-stranded RNA, whereas RNase E acts preferentially on single-stranded molecules. The RNase III dimer generally makes staggered, double-strand cleavages in duplex regions to yield a two base 3' overhang and leaves 5'-P and 3'-OH ends on the RNA products (Robertson *et al.*, 1968). RNase III cleaves extensive stretches (20–40 bases) of perfectly duplexed RNA nonspecifically and stem regions of mRNA that usually contain unpaired bases as bulges or internal loops, with a loosely defined consensus sequence (Krinke & Wulff, 1990). Although RNase III is involved in rRNA maturation and the degradation of a few selected phage, plasmid and bacterial mRNAs (reviewed in Court, 1993), it is not absolutely required for cell viability (Babitzke *et al.*, 1993) and therefore is unlikely to have a major role in mRNA decay. RNase E, on the other hand, is essential for cell growth (Gegenheimer *et al.*, 1977; Ghora & Apririon, 1978) and its inactivation has a stabilizing effect on bulk mRNA (Ono & Kuwano, 1979; Babitzke & Kushner, 1991; Mudd *et al.*, 1990), suggesting a central rate-determining role for this enzyme in mRNA degradation. RNase E was discovered initially as a rRNA processing enzyme (Misra & Apirion, 1979) and has since been shown to initiate the degradation of several *E. coli* mRNAs. Attempts to define an RNase E consensus recognition sequence have proven more difficult with each new site examined. The general conclusion is that RNase E cleavage is not determined by a simple consensus sequence but that single-stranded RNA substrates which are rich in A and/or U nucleotides are preferred (Mackie, 1991, 1992;

McDowall *et al.*, 1994; Lin-Chao *et al.*, 1994). Interestingly, RNase E has recently been shown to possess exonuclease activity, as demonstrated by its ability to degrade poly(A) and poly(U) homopolymer tails, releasing mononucleotides and to a lesser extent, 2-10 nucleotide oligomers (Huang *et al.*, 1998).

Based on an analysis of the 5' ends of RNA oligonucleotides generated in *E. coli*, Cannistraro and Kennell (1993) suggest that two broad-specificity endonucleases, RNase M and RNase I\*, participate in general mRNA decay. From their results, the authors conclude that RNase M, which preferentially cleaves pyrimidine-adenosine bonds, is a primary endonuclease for mRNA degradation and that RNase I\* accounts for most of the endonucleolytic degradation of very small oligonucleotides and almost all degradation of dinucleotides to mononucleotides. Evidence for the involvement of these two RNases in the degradation of specific mRNAs is limited. Sequence analysis of the 3' and 5' ends of endonucleolytic cleavage products from the *lac* mRNA invoke RNase M activity (Cannistraro *et al.*, 1986), whereas RNase I\* has been shown to be the principal RNase responsible for endonucleolytic degradation of hammerhead ribozymes (Wang *et al.*, 1996a).

### **1.6.3 The role of polyadenylation in mRNA degradation**

Like eukaryotes, many bacterial mRNAs harbour a polyadenylate (poly(A)) tail at their 3' ends (Nakazato *et al.*, 1975; Srinivasan *et al.*, 1975) but its function is very different. In prokaryotes, poly(A) tails have a destabilizing effect on mRNA (He *et al.*, 1993; Xu *et al.*, 1993; O'Hara *et al.*, 1995), whereas they are determinants of stability in eukaryotes (Sachs, 1993). Prokaryotic poly(A) tails are synthesized by template-

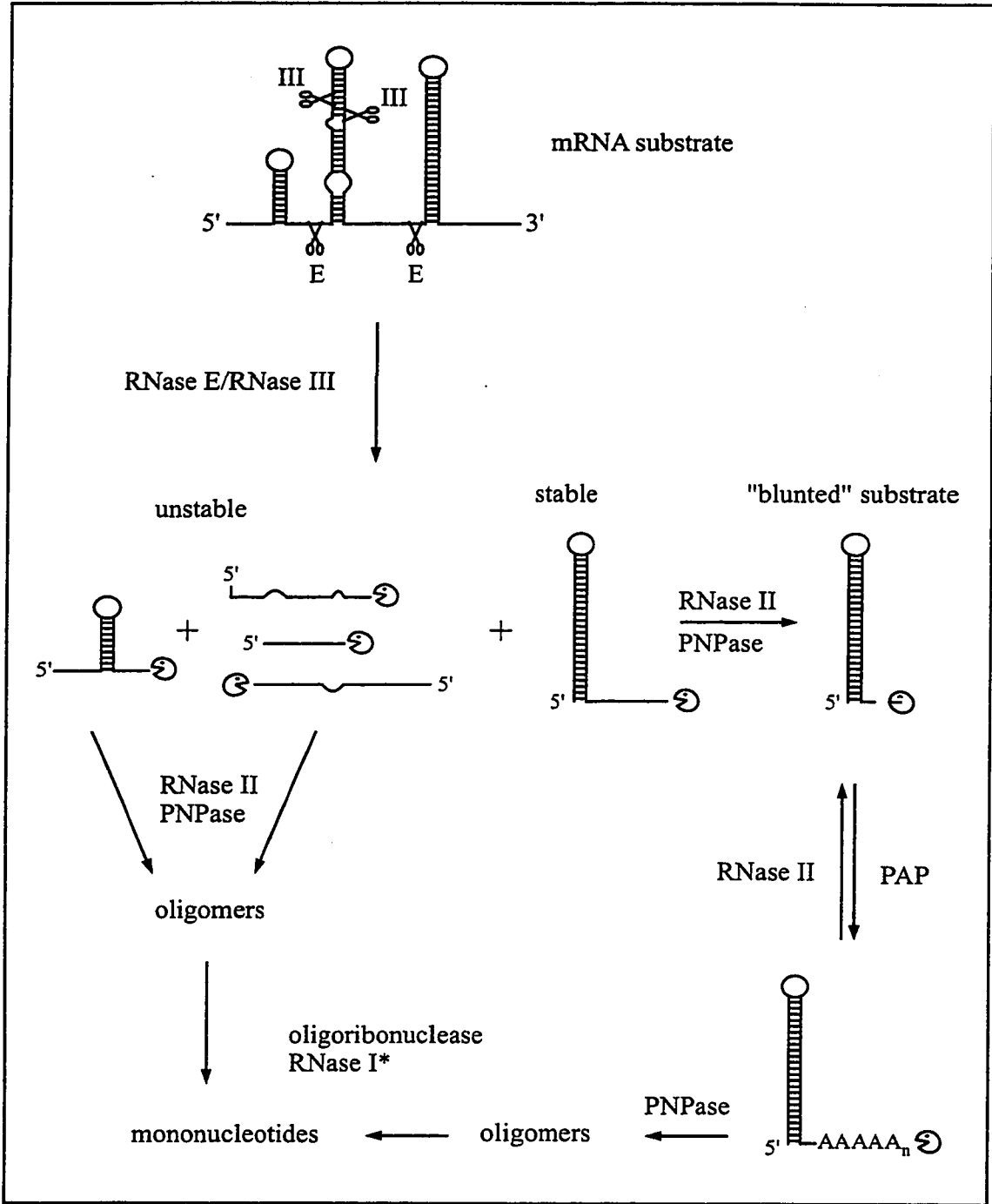
independent, stepwise addition of AMP residues to the 3'-OH end of RNAs catalyzed by poly(A)-polymerase (PAP). The *pcnB* gene encodes the major PAP in *E. coli*, PAP I (Cao & Sarkar, 1992), and a second PAP, PAP II, has been identified in a *pcnB* mutant (Kalapos *et al.*, 1994) indicating functional overlap. In wild-type *E. coli*, the poly(A) tail length of bulk mRNA ranges from 10 to 40 nucleotides; however, the number and size of the tails is significantly increased in a strain that lacks PNPase and has reduced RNase II activity (O'Hara *et al.*, 1995). These results, combined with the observation that mutation of the *pcnB* gene leads to stabilization of structured full-length mRNA and degradative intermediates (Haugel-Nielsen *et al.*, 1996; Mikkelsen & Gerdes, 1997; Söderbom *et al.*, 1997), suggest that poly(A) tails act as substrates for exonuclease activity, facilitating their progression through otherwise impeding 3' stem-loop structures. A subsequent study by Cao *et al.* (1997) showed that the exonucleases also affect poly(A) tail length by competing with PAP for the free 3' ends of mRNA.

#### **1.6.4 Mechanism of mRNA degradation in *E. coli***

The general scheme which has emerged for mRNA degradation in *E. coli* is dependent on the concerted action of endonucleases and exonucleases and is shown in Figure 1.7. The model assumes that segments of mRNA are accessible to RNases and are not masked by ribosomes or other RNA-binding proteins. The initial (and often rate-limiting) step involves endonucleolytic cleavage of the mRNA by RNase E or occasionally, RNase III. The linear and loosely-structured endonuclease-derived products would be further degraded by RNase II and PNPase. Products with secondary structures followed by a stretch of single-stranded residues could be bound by PNPase or RNase II.

**Figure 1.7** Model for mRNA degradation in *E. coli*. Endonucleases are indicated by scissors and exonucleases by the pacman. This mRNA substrate is cleaved once by RNase III and twice by RNase E. Unstable degradative intermediates are eliminated by RNase II and PNPase activity, followed by oligoribonuclease and/or RNase I\*. The 3' single-stranded end is removed from the stable intermediate by RNase II or PNPase. A strong stem-loop will cause stalling and dissociation of RNase II and possibly PNPase. A poly(A) tail is added to the "blunted" substrate by PAP and can be bound by RNase II or PNPase. RNase II will degrade the tail, stall at the stem-loop and dissociate once again. PNPase, which is less sensitive to secondary structure, will degrade the tail and continue through the stem-loop structure.





If RNase II cannot progress through the secondary structure, it stalls, dissociates from the substrate and reassociates with another substrate containing a free 3' end (Coburn & Mackie, 1996a). The “blunted” substrate which has lost its single-stranded 3' end is also inaccessible to PNPase and must be modified through the addition of a poly(A) tail by PAP. The poly(A)-modified substrate can be rebound by RNase II, which then removes the poly(A) tail, or preferably by PNPase, which is less sensitive to secondary structure than RNase II and may be able to overcome it (McLaren *et al.*, 1991). RNAs with very stable stem-loops would require successive rounds of PAP/PNPase activity to weaken base pairing within the stem-loop structure (Coburn & Mackie, 1998). Small, highly structured RNAs which are not substrates for RNase E or RNase III would depend exclusively on this polyadenylation/exonuclease pathway. Finally, oligoribonuclease and/or RNase I\* would eliminate any short oligomers remaining from PNPase and RNase II activity.

The characterization of a multi-enzyme complex termed the “degradosome”, composed of RNase E, PNPase, RhIB RNA helicase, enolase and polyphosphate kinase (PPK), suggests a mechanism for achieving spatially coordinated mRNA degradation in *E. coli* (Blum *et al.*, 1997; Carpousis *et al.*, 1994; Miczak *et al.*, 1996; Py *et al.*, 1994, 1996). It is proposed that binding of the degradosome complex to the substrate RNA allows for an initial endonucleolytic cleavage by RNase E and positions PNPase for subsequent exonucleolytic attack of the newly formed 3' end. RhIB may function to unwind RNA structures that impede PNPase activity. PPK is believed to modulate degradosome activity by maintaining the correct microenvironment by removing ADP and poly(P), which are inhibitory to mRNA degradation, through their conversion to

ATP, which is necessary for RhlB helicase activity (Blum *et al.*, 1997). The role of enolase, a glycolytic enzyme, in the degradasome is unknown. Most recently, Bessarab *et al.* (1998) have identified degradasome-associated 16S and 23S rRNA fragments that appear to be RNase E-generated decay intermediates, implicating the degradasome in the decay of rRNA.

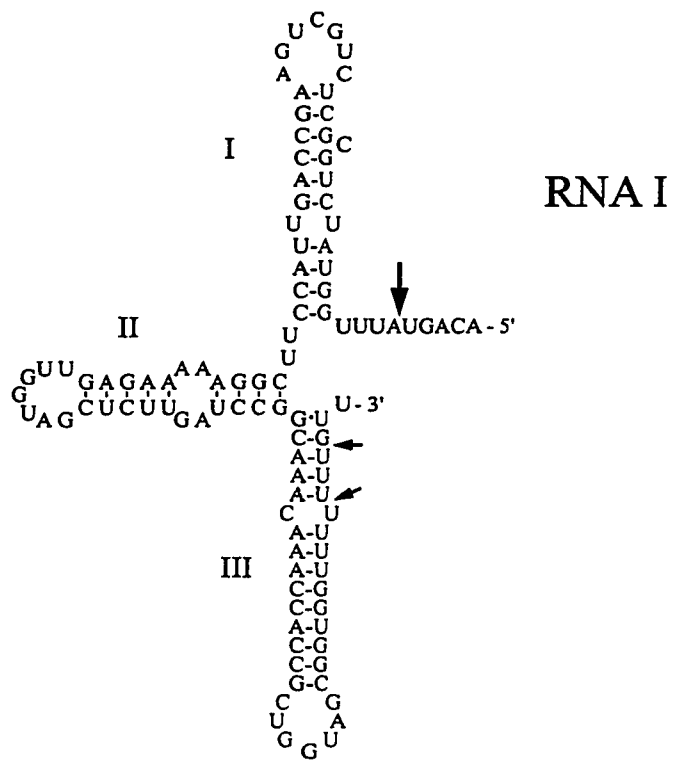
#### 1.6.5 Degradation of ColE1 RNA I

RNA I, the antisense RNA regulator of ColE1 plasmid replication, is transcribed from a strong promoter (Lin-Chao & Bremer, 1987), but is rapidly turned over to allow for adjustment to rapid changes in plasmid copy number. Investigation of RNA I decay from a number of ColE1-related plasmids indicates that its short half-life (~2 minutes) is determined by RNase E cleavage within the 9 base single-stranded 5' leader sequence (Figure 1.8a; Tomcsanyi & Apirion, 1985; Lin-Chao & Cohen, 1991; He *et al.*, 1993). Subsequent PAP I-mediated polyadenylation of the RNase E cleavage product, RNA I<sub>5</sub>, accelerates its decay by the exonucleolytic activity of PNPase and perhaps RNase II (Xu & Cohen, 1995). Full-length RNA I is also polyadenylated, but this does not influence its half-life, which is determined by RNase E (Xu *et al.*, 1993). An unexpected finding was that mutation of the *pnp* gene encoding PNPase decreased exonucleolytic degradation from the 3' end of RNA I and RNase E cleavage at the 5' end (Xu & Cohen, 1995). In order to explain this result, the authors propose that RNase E and PNPase interact both physically (within the "degradasome" complex) and functionally and that mutation of PNPase somehow affects RNase E function.

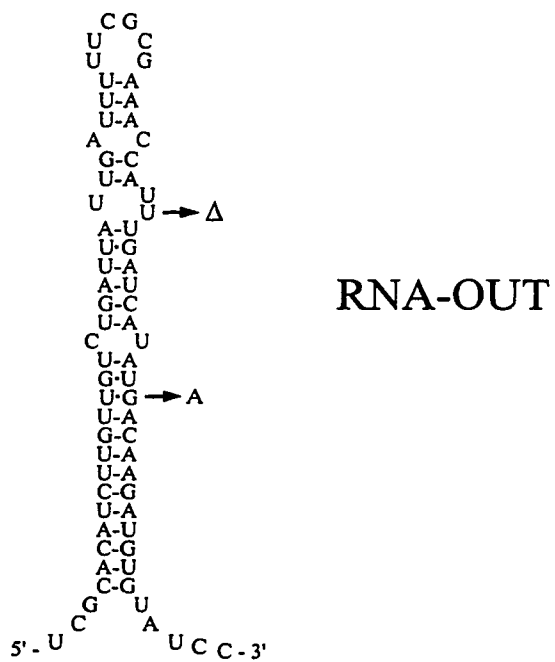
**Figure 1.8a** Secondary structure of pBR322 RNA I antisense RNA (Helmer-Citterich *et al.*, 1988). The major site of RNase E cleavage is indicated by the large arrow and the two minor sites within SLIII are shown by small arrows.

**Figure 1.8b** RNA-OUT secondary structure (Kittle *et al.*, 1989). The two mutations (U deletion and G:A transition) that cause RNase III susceptibility are shown.

a



b



A thorough analysis of the decay intermediates produced in a PAP I strain revealed the presence of two additional RNase E cleavage sites in RNA I, within mismatched and double-stranded regions of SLIII (Figure 1.8a; Kaberdin *et al.*, 1996). Using a ribonuclease-accessibility footprinting analysis of RNA I complexed with the RNase E RNA binding domain (RBD), the authors showed that the RBD destabilizes RNA I structure and propose that this might facilitate access of the RNase E catalytic domain to regions of the RNA previously engaged in hydrogen bonding interactions. The accumulation of multiple RNase E intermediates in the PAP I strain suggests they are destabilized by polyadenylation in wild-type *E. coli* and consequently undergo rapid degradation by PNPase and possibly, RNase II and thus escape detection. Earlier data presented by He *et al.* (1993) suggest that cleavage events within SLIII do not make an important contribution to the functional inactivation of RNA I. They showed that the major RNase E intermediate that accumulates in a *pcnB* mutant is RNA L<sub>5</sub> and that only minor amounts of low molecular weight products (likely due to RNase E cleavage within SLIII) are seen. Furthermore, they demonstrate that *pcnB* mutation results in a 10-fold increase in the RNA L<sub>5</sub> half-life with a corresponding 10-fold decrease in ColE1 plasmid copy number. These results indicate that since RNA L<sub>5</sub> is able to inhibit replication in the absence of polyadenylation, subsequent RNase E cleavage of this intermediate must be minimal.

#### **1.6.6 The unusual stability of IS10 antisense RNA, RNA-OUT**

RNA-OUT, the antisense RNA that regulates IS10 transposition, folds into a single stem-loop structure (Figure 1.8b) that is optimized for metabolic stability.

Expression of RNA-OUT from a modest promoter (Simons & Kleckner, 1983) and its exceptional stability (half-life of ~60 minutes; Case *et al.*, 1989) are well-suited for a regulator whose concentration can respond slowly to gradual increases in *IS10* copy number. Despite its predominantly double-stranded character, RNA-OUT is not cleaved by RNase III, unless it is part of a duplex with its target, RNA-IN (Case *et al.*, 1990). RNA-OUT is also resistant to RNase E attack and thus its eventual slow degradation is entirely dependent on the activity of exonucleases (Pepe *et al.*, 1994).

Two groups (Case *et al.*, 1989; Pepe, *et al.*, 1994) examined the effects of 17 single and double base mutations on RNA-OUT decay and found that base pairing within the stem-domain is the most important determinant of RNA-OUT's stability. Single base mutations that disrupted base pairing severely destabilized RNA-OUT by increasing PNPase, and to a lesser extent, RNase II cleavage *in vivo*, whereas second-site mutations that re-established base pairing restored its half-life. Mutations that reduced RNA-OUT's predicted thermodynamic stability, equally reduced its *in vivo* stability. Unexpectedly, RNA-OUT was more sensitive to PNPase attack in the absence of RNase II, suggesting that RNase II protects RNA-OUT from PNPase. The authors suggest that this might be achieved if RNase II binds to, but does not degrade the substrate, physically blocking access to PNPase. Coburn & Mackie (1996a) propose that the observed stabilization by RNase II is more likely due to removal of the 3' single-stranded tail, which prevents binding and subsequent degradation by PNPase. Both hypotheses require that RNA-OUT receive a poly(A) tail, a feature which has not yet been explored. Two mutations, one that changed a G-U mismatch to an A-U pair and a second that deleted a base from an imperfect bulge, destabilized RNA-OUT by rendering it susceptible to RNase III. Thus,

the sequence of the RNA-OUT stem imposes structural features that make it naturally resistant to RNase III and retards the activity of exonucleases.

### **1.7 RNA-binding proteins**

RNA-binding proteins and their nucleic acid targets possess unique structural features that allow for specific, high-affinity binding. Opportunities for specific recognition of RNA are commonly found in single-stranded regions such as terminal (hairpin) loops and junctions between helices. RNA helices are A-form and have a very deep, narrow major groove and a wide, shallow minor groove. Base pairs in the accessible minor groove present a poorly distinguishable collection of hydrogen bond donors and acceptors. Conversely, base pairs in the major groove are more easily distinguished but are less accessible to amino acid side chains. Nonetheless, examples of specific protein interactions with both the major and minor groove are known (Steitz, 1993). Contacts with bases in the major groove are often made next to internal loops, bulges or distortions produced by noncanonical pairs or with bases at the end of a helix (Weeks & Crothers, 1993). Proteins can also induce conformational changes in the target RNA that increase its binding affinity and specificity (Draper, 1995). The protein structures recognizing RNA are as variable as the targets themselves. Protein families have been described based on the presence of RNA-binding amino acid sequence “motifs” (Mattaj, 1993). The most common of these are the ribonucleoprotein (RNP), double-stranded RNA binding domain (dsRBD), K-homologous (KH), arginine-rich motif (ARM) and the RGG-box, which is characterized by Arg-Gly-Gly repeats. Membership in a family can be predictive of the secondary structure of the RNA-binding



domain of the protein and of the amino acids that might contact the RNA. It does not reveal the structure of the substrate RNA because a single RNA-binding motif is capable of binding structurally diverse targets.

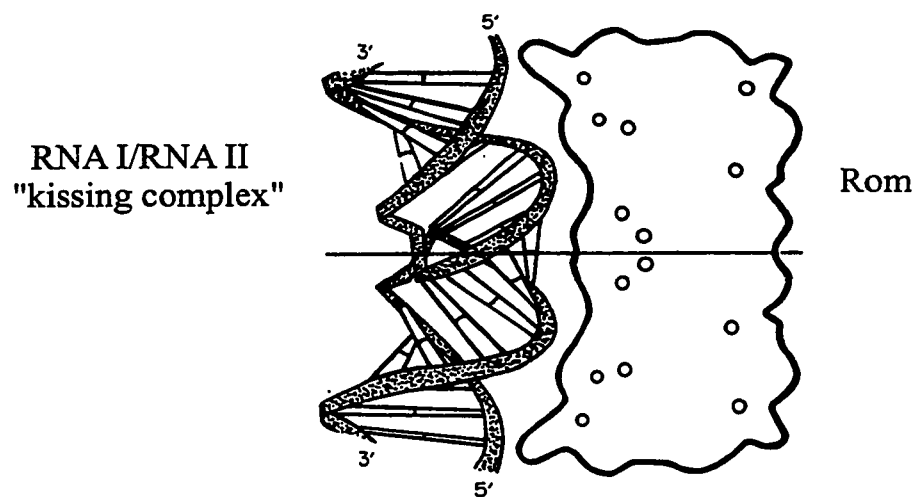
### 1.7.1 Rom/Rop protein of plasmid ColE1

ColE1 plasmid-encoded Rom is an RNA-binding protein that binds to and reduces the dissociation of the unstable “kissing” complex formed between RNA I and RNA II (Tomizawa, 1990b). Rom does not bind either member of the RNA pair individually prior to “kissing” and has no affinity for the A-form duplex end product (Eguchi & Tomizawa, 1991). Rom binds with high affinity to the interacting loops of any stem-loop pair as long as there is complete Watson-Crick base-complementarity in the loop sequences. Rom is unaffected by the size or sequence of the loops and stems, indicating that it recognizes the structure rather than the specific sequence of its target (Eguchi & Tomizawa, 1990b, 1991; Gregorian & Crothers, 1995). A structural model for the RNA I/RNA II kissing complex proposed by Eguchi & Tomizawa (1990, 1991) and confirmed by NMR spectroscopy (Marino *et al.*, 1995) is shown in Figure 1.9a. The overall structure is similar to linear A-form double-stranded RNA (dsRNA) with a bend at its centre and an axis of dyad symmetry. The phosphate backbone of each RNA kinks at the 5' end of the loop, which accommodates pairing between all of the loop bases and permits co-axial helical stacking. A convex protein-binding surface is formed that becomes increasingly distorted and protected from alkylation by bound Rom (Eguchi & Tomizawa, 1990). The preference by Rom for the loop-loop complex over linear A-form dsRNA suggests that the pre-formed bend in the RNA target facilitates formation of the

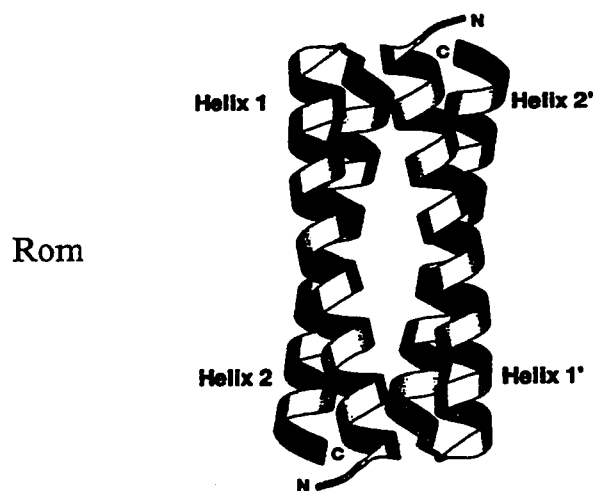
**Figure 1.9a** Model for the RNA I/RNA II “kissing complex” and its interaction with the Rom dimer. The horizontal line indicates the axis of dyad symmetry (disregarding sequence). Circles inside Rom indicate positions of basic amino acids. It is proposed that the convex surface of the associated RNA molecules and the concave surface of the Rom dimer facilitate RNA/protein interactions. Adapted from Eguchi & Tomizawa (1991).

**Figure 1.9b** Ribbon diagram of the Rom dimer. The 4-helix bundle is formed by the association of two identical helix-turn-helix monomers. The N- and C-termini are indicated. Adapted from Predki *et al.* (1995).

a



b



final RNA-protein complex (Marino *et al.*, 1995). Rom binds with similar affinity to a deformed “kissing” complex formed between HIV-2 TAR RNA and its complement (Chang & Tinoco, 1997).

The Rom protein shows no structural or sequence homology to other RNA-binding proteins. It is a dimer composed of two identical 63 amino acid subunits that form an antiparallel four-stranded coiled coil with connecting loops at opposite sides of the structure (Figure 1.9b; Banner *et al.*, 1987). Rom is relatively acidic but contains several solvent-exposed basic amino acids along one face (helix 1/1'). Predki *et al.* (1995) mutated each of these basic residues to alanine and determined the ability of the Rom mutants to bind an RNA I/RNA II “kissing” complex. They found that mutation of Asn-10, Phe-14, Gln-18 and Lys-25 completely abolished RNA binding and mutation of Lys-3 decreased binding 3-fold. Furthermore, they demonstrated that each of these residues must be present in both helix 1 and helix 1', indicating that the RNA-binding site is symmetrical. Mutation of the few positively charged residues in the acidic helix 2/2' had no effect on RNA binding. The authors propose that this side of the protein acts as an “electrostatic rudder” that steers the 1/1' face into the RNA target. None of the alanine mutations studied caused changes in the structure or stability of the proteins as measured by circular dichroism. Thus, residues whose mutation blocked RNA binding are involved in direct contact with the RNA and form a thin stripe down the centre of helix 1/1'. This side of the dimer has a concave surface (Eguchi & Tomizawa, 1990; Figure 1.9a) that is appropriately shaped for interaction with the convex protein-binding surface on the RNA target. It is proposed that Phe-14/14' and Gln-18/18' interact with

the loops of the hairpin RNA pair and the other essential basic residues interact with the stems (Predki *et al.*, 1995).

### 1.7.2 Rev protein of HIV-1

Rev is a 116 amino acid nuclear phosphoprotein that promotes the cytoplasmic accumulation and expression of singly spliced and unspliced human immunodeficiency virus type 1 (HIV-1) mRNAs encoding virion structural proteins (Cullen, 1992). Rev binds to a highly structured 351 base region of all intron-containing viral mRNAs called the Rev responsive element (RRE; Figure 1.10). Although Rev binds with highest affinity to the purine-rich bubble in Stem IIB (Heaphy *et al.*, 1990), the entire RRE sequence is required for full biological activity of Rev *in vivo* (Mann *et al.*, 1994). Nuclease protection analysis of Stem I truncations indicates that binding of a Rev monomer to the high affinity site (Stem IIB) nucleates the highly cooperative oligomerization of eight to ten additional monomers to lower affinity sites along Stem I (Mann *et al.*, 1994). Rev activity is abolished *in vivo* by deletion of the RRE high-affinity binding site (Bartel *et al.*, 1991) or by mutations in Rev that prevent its oligomerization (Malim & Cullen, 1991). Thus cooperative binding allows Rev to function as a “molecular rheostat” that detects Rev levels during the HIV-1 growth cycle and limits virus growth when there is insufficient Rev (Mann *et al.*, 1994).

The sequence requirements within the high affinity site necessary for Rev binding have been examined in detail. Footprinting data show that Rev covers 10-14 base pairs that are positioned asymmetrically with respect to the bubble (Kjems *et al.*, 1992). NMR spectroscopy studies indicate that the bubble is stabilized by non-Watson-Crick G48-G71

**Figure 1.10** Secondary structure of the RRE. The sequence is marked with a dot every ten bases. The high affinity Rev binding site within Stem IIB is outlined and is shown enlarged below. Specific interactions between the Rev peptide and Stem IIB are indicated as follows: black arrows = base contacts; open arrows = phosphate backbone contacts; arcs = van der Waals contacts. The thick boxes and black circles indicate important nucleotides and phosphates, respectively. Adapted from Battiste *et al.* (1996) and Mann *et al.* (1994).



and G47-A73 base pairs that, together with a bulged-out uridine (U72), open the major groove of the A-form double helix (Bartel *et al.*, 1991; Heaphy *et al.*, 1991; Iwai *et al.*, 1992). The G48-G71 base-pair is essential for Rev binding but does not make direct hydrogen bond contacts with the protein, as evidenced by toleration of A-A, but not Watson-Crick pairing at this site (Bartel *et al.*, 1991; Iwai *et al.*, 1992). This finding suggests that the purine-purine pair provides a critical structural feature for specific binding. Similarly, base substitutions (Iwai *et al.*, 1992) or replacement of the essential extrahelical nucleotide U72 by an abasic propyl linker (Heaphy *et al.*, 1991) do not reduce Rev affinity, indicating that U72 acts as a single-stranded spacer. By contrast, Rev makes specific contacts with the G47-A73 pair and with Watson-Crick base pairs flanking the bulge (Heaphy *et al.*, 1991). Ethylation interference studies have shown that Rev also makes phosphate contacts on both sides of the duplex (Kjems *et al.*, 1992).

Rev belongs to the arginine-rich motif (ARM) family of RNA-binding proteins because it contains a 17 amino acid (aa) RNA-binding domain that includes 10 arginine residues (Lazinski *et al.*, 1989). The complete Rev protein possesses 50%  $\alpha$  helix and 25%  $\beta$  sheet structure (Daly *et al.*, 1990); however, the N-terminal 17 aa ARM which serves as a nuclear/nucleolar localization signal and as the RNA-binding domain, functions as an  $\alpha$  helix (Tan *et al.*, 1993). The isolated arginine-rich  $\alpha$  helix binds to the high affinity site within the RRE with the same affinity and specificity as the full-length protein (Tan *et al.*, 1993) and has, therefore, been used to model Rev-RRE RNA-protein interactions. NMR studies indicate that the Rev peptide binds to the major groove of the distorted Stem IIB bubble, causing a significant change in the RNA conformation (Peterson & Feigon, 1996). The sugar-phosphate backbone undergoes a reversal at G71



as the entire nucleotide is turned upside-down. The bulged U72 facilitates this kink, causing the major groove to become wider and more underwound than the free RNA. Four amino acids have been identified that make important base-specific contacts in the major groove (Figure 1.10, inset; Battiste *et al.*, 1996). On one side of the groove, Arg35 and Arg39 interact with U66, G67 and G70. On the opposite side, Asn40 and Arg44 interact with U45, G47 and A73. Since mutation of any of these arginines to lysine abrogates Rev binding *in vivo* (Tan & Frankel, 1994), it is proposed that these residues form hydrogen bonds rather than electrostatic contacts. Other residues make hydrogen bond or electrostatic contacts with backbone phosphates (Arg38, Arg41, Arg42, Arg43, Thr34) or van der Waals contacts (Gln36, Ala37, Arg 43, Trp45, Arg50) that allow orientation-specific docking of the  $\alpha$  helix in the major groove. Unlike the Rom protein where essential amino acid contacts localize to one face of the protein, the amino acids critical for Rev activity are distributed around the  $\alpha$  helix which suggests that the RNA may wrap around the peptide helix (Tan & Frankel, 1994).

### **1.7.3 Histone mRNA stem-loop binding protein (SLBP)**

Eukaryotic histone mRNAs lack introns and poly(A) tails, but instead are terminated by a highly conserved 26 base stem-loop structure (Figure 1.11; Marzluff, 1992). Specific interaction between the stem-loop and an RNA-binding protein, appropriately named the stem-loop binding protein (SLBP), is required for efficient histone pre-mRNA processing in the nucleus (Pandey *et al.*, 1994), mature histone mRNA transport to the cytoplasm and localization to polyribosomes (Williams *et al.*, 1994) and regulation of cytoplasmic histone mRNA degradation (Pandey & Marzluff,

**Figure 1.11** Consensus structure of the histone mRNA 3' end. Bases in the stem and loop which have been 100% conserved are boxed or circled, respectively. The loop sequence is numbered and bases essential for SLBP binding are shown in bold. Adapted from Williams *et al.* (1994).



1987; Williams *et al.*, 1994). The recently cloned human SLBP consists of 269 amino acids with a predicted molecular mass of 31 kDa (Wang *et al.*, 1996b), although it migrates as a 45 kDa protein on SDS-polyacrylamide gels (Pandey *et al.*, 1991; Hanson *et al.*, 1996; Wang *et al.*, 1996b). Like Rom, it is not a basic protein (predicted pI of 7.4) and does not contain any of the sequence motifs found in other RNA-binding proteins. A moderately basic RNA-binding domain (20% lysine + arginine) has been localized to 73 central amino acids (residues 125-197; Wang *et al.*, 1996b), but the secondary structure of this region and the amino acid contacts made with the RNA have not been determined.

The RNA target consists of a six base pair stem and a four base loop structure (Figure 1.11). Several bases have been highly conserved in metazoans (Marzluff, 1992) and include the UYUN sequence of the loop (Y = pyrimidine, N = any nucleotide), the U-A and G-C base pairs in the stem and the three pyrimidine-purine pairs between them. In addition, the stem-loop is usually preceded by at least two A's and followed by AC. Mutational analysis of the SLBP target revealed that conserved bases in the stem, loop and flanking sequences are required for high affinity SLBP binding (Williams & Marzluff, 1995). Specifically, mutations that increased the size of the loop to 5 or 6 bases reduced SLBP binding about 5-fold whereas changes in the loop sequence (U1:A, U3:A) lowered the affinity 20-fold. Interestingly, SLBP binding was not affected by cleavages in the loop, indicating that the conformation of the loop is unimportant for binding. Reversal of the stem sequence or an increase in stem-length abolished detectable binding indicating that the conserved 6 base stem-length and sequence are critical. The authors also showed that the three bases 5' and 3' of the stem are necessary for high affinity binding and suggest that, together with the stem-loop, form the complex structure

recognized by the SLBP. The SLBP-RNA complex is extremely stable (half-life > 4 hours; Williams & Marzluff, 1995) which suggests that once the SLBP associates with the histone pre-mRNA, it remains bound for the lifetime of RNA, fitting with its roles in both the nucleus and cytoplasm.

## 1.8 Summary and research objectives

FinP is a Type-I antisense RNA that, like *IS10* RNA-OUT, is believed to directly block access of ribosomes to the mRNA target, *traJ*, and prevent its translation. FinP, RNA-OUT and RNA I antisense RNAs all exhibit a high degree of secondary structure. However, unlike RNA-OUT which interacts with a single-stranded region of RNA-IN, the FinP and RNA I target sites consist of complex stem-loop structures. FinP/*traJ* mRNA duplex formation is likely initiated by interaction of the sense/antisense RNA loops as occurs with RNA I/RNA II. The Rom protein enhances duplex formation by stabilizing the preformed RNA I/RNA II “kissing” complex, but is unable to bind the RNAs individually. Like Rom, the FinO protein also enhances duplex formation but is capable of binding FinP and *traJ* mRNA both prior to their association and as an RNA duplex. Binding of FinO to free FinP is thought to be necessary to prevent its degradation. Whereas the Rom protein binds to RNA in a sequence-independent, structure-dependent manner, Rev and the SLBP contact specific bases in their RNA targets. Preliminary studies indicate that FinO binds to the second stem-loop domain of FinP with moderate specificity and may have a nonspecific affinity for double-stranded RNA.

The primary goal of this thesis is to define the mechanism by which the FinO protein protects FinP antisense RNA from decay. The first objective was to characterize the pathway of FinP degradation in the absence of FinO. Chapter 3 examines FinP decay in a series of ribonuclease-deficient strains in the presence and absence of *traJ*. The results indicate that similar to RNA I, the chemical half-life of FinP is determined by RNase E. Full-length FinP is not a substrate for either exonuclease, RNase II or PNPase, and like RNA-OUT, FinP is not cleaved by RNase III unless it is part of a duplex with its target RNA.

The second objective was to determine whether the FinO protein could protect FinP from degradation. In Chapter 4, the pattern of RNase E cleavage is mapped on FinP synthesized *in vitro* in the presence and absence of FinO. A major RNase E cleavage site within the single-stranded spacer between stem-loops I and II and a secondary site near the 5' end of FinP were found in the absence of FinO. Mutation of the spacer sequence prolonged the FinP half-life *in vivo* and RNase E cleavage at both sites was prevented in the presence of the GST-FinO fusion protein *in vitro*. These results suggest that FinO protects FinP from RNase E. The FinP mutant (*finP305*) which has a single base mutation in stem I shows a decreased chemical half-life, increased RNase E cleavage *in vitro*, and reduced protection by GST-FinO as detailed in Chapter 5.

The third objective was to define the RNA features that are recognized by the FinO protein. In Chapter 6, RNA mobility shift analysis was used to study the interaction between GST-FinO and a series of synthetic FinP and *traJ* mRNA variants. The results show that, like the SLBP, single-stranded regions flanking FinP stem-loop II (or *traJ* stem-loop IIc) are required for high affinity FinO binding. Weaker binding was achieved

with stem-loop I (accompanied by 5' and 3' unpaired nucleotides) and multiple band shifts were apparent on nondenaturing gels at higher protein concentrations. Thus, like the Rev/RRE interaction, FinO may bind FinP in a step-wise manner, which is initiated at a high-affinity site. No evidence for sequence-specific contacts was found, indicating that like Rom, FinO recognizes the overall shape of the RNA.

## **Chapter 2**

### **Materials and Methods**



## 2.1 Bacterial strains, growth media and plasmids

The *Escherichia coli* strains used in this study are listed in Table 2.1. Strains N3431, N3433 (provided by Dr. C. Higgins, University of Oxford) and IBPC5321, IBPC5321-*mc*<sup>o</sup>, N3433 $\Delta$ *pcnB* (provided by Dr. E.G.H. Wagner, Swedish University of Agricultural Sciences) were grown in trypticase soy broth (TSB) and DH5 $\alpha$  was grown in Luria Bertani (LB) broth. Strains MG1693, SK5665, SK5689, SK5691 and SK5704 (provided by Dr. S. Kushner, University of Georgia) were grown in LB broth supplemented with 50  $\mu$ g/ml thymine. Colonies were grown on LB medium or MacConkey agar (Difco) plus lactose (10 g/L). Antibiotics were used at the following concentrations: ampicillin (Ap), 50  $\mu$ g/ml; chloramphenicol (Cm), 50  $\mu$ g/ml; tetracycline (Tc), 10  $\mu$ g/ml; kanamycin (Km), 25  $\mu$ g/ml.

The plasmids used in this study are listed in Table 2.2. The relevant sequence in each construct was confirmed by dideoxy sequencing (section 2.2). Plasmids pLT180, pLT185 and pLT350.1 were constructed so that FinP, *finP305* (FinP with a C30:U mutation) and *traJ* mRNA could be expressed free of external promoters on moderate copy number plasmids. The *EcoRI/HindIII* fragment from pSQ180 (containing a 180 base pair [bp] *RsaI-BglIII* insert from the *traJ/finP* region of the F plasmid; Lee *et al.*, 1992) was cloned into pT7.3 (Ap<sup>r</sup>; Tabor & Richardson, 1985) digested with *EcoRI* and *HindIII*, creating pLT180. The *RsaI* site interrupts the *traJ* promoter sequence, such that pLT180 expresses only the *finP* gene. The *EcoRI/HindIII* fragment from pSQ350.1 (containing a 350 bp *HpaII-BglIII* F plasmid fragment; Lee *et al.*, 1992) was cloned into pT7.3 digested with *EcoRI* and *HindIII*, creating pLT350.1, which expresses both *finP*

**Table 2.1** *E. coli* strains used in this study

Strain	Genotype	Reference
DH5 $\alpha$	<i>hsdR17, <math>\Delta</math>lacU169<math>\phi</math>80, lacZ<math>\Delta</math>M15, recA1, supE44</i>	Hanahan (1983)
IBPC5321	F', <i>thi-1, argG6, argE3, his-4, mtl-1, xyl-5, tsx-29, rpsL, <math>\Delta</math>lacX74</i>	Plumbridge <i>et al.</i> (1985)
IBPC5321- <i>rnc</i> <sup>o</sup>	as IBPC5321, except <i>rnc-14::Tn10</i>	Hjalt & Wagner (1995)
MG1693	F', <i>thyA715, lambda</i> <sup>-</sup>	Arraiano <i>et al.</i> (1988)
SK5665	F', <i>thyA715, lambda</i> <sup>-</sup> , <i>rne-1(ts)</i> <sup>a</sup>	Arraiano <i>et al.</i> (1988)
SK5689	F', <i>thyA715, lambda</i> <sup>-</sup> , <i>rnb-500(ts)</i>	Arraiano <i>et al.</i> (1988)
SK5691	F', <i>thyA715, lambda</i> <sup>-</sup> , <i>pnp-7</i>	Arraiano <i>et al.</i> (1988)
SK5704	F', <i>thyA715, lambda</i> <sup>-</sup> , <i>pnp-7, rne-1(ts), rnb-500(ts)</i>	Arraiano <i>et al.</i> (1988)
N3433	<i>HfrH, lacZ43, lambda</i> <sup>-</sup> , <i>spoT1, thi-1</i>	Goldblum & Apririon (1981)
N3431	as N3433, except <i>rne-3071(ts)</i>	Goldblum & Apririon (1981)
N3433/ $\Delta$ <i>pcnB</i>	as N3433, $\Delta$ <i>pcnB</i> (replaced by kanamycin cassette)	Söderbom <i>et al.</i> (1997)

<sup>a</sup> temperature-sensitive mutation

**Table 2.2** Plasmids used in this study. Relevant phenotypes and promoters are indicated. Clones were constructed from fragments obtained by parental restriction digests unless otherwise stated.

Plasmid	Phenotype	Promoter(s)	Parent	Vector	Reference/Source
pT7.3	Ap <sup>r</sup>	T7 $\Phi$ 10	-	-	Tabor & Richardson (1985)
pUC18	Ap <sup>r</sup>	<i>lac</i>	-	-	Vieira & Messing (1982)
pTTQ18	Ap <sup>r</sup>	<i>lac</i>	pUC18	-	Stark (1987)
pNY300	Ap <sup>r</sup> FinP <sup>+</sup> TraJ <sup>+</sup>	<i>lac, finP, traJ</i>	F	pUC18	Frost <i>et al.</i> (1989)
pSQ180	Ap <sup>r</sup> FinP <sup>+</sup>	<i>lac, finP</i>	pNY300	pTTQ18	Lee <i>et al.</i> (1992)
pLT180	Ap <sup>r</sup> FinP <sup>+</sup>	<i>finP</i>	pSQ180	pT7.3	This study
pUC180	Ap <sup>r</sup> FinP <sup>+</sup>	<i>lac, finP</i>	pSQ180	pUC18	This study
pUC180cc	Ap <sup>r</sup> <i>finPcc</i> <sup>+</sup>	<i>finPcc</i>	pUC180 (PCR)	-	This study
pLT180cc	Ap <sup>r</sup> <i>finPcc</i> <sup>+</sup>	<i>finPcc</i>	pUC180cc	-	This study
pSQ350.1	Ap <sup>r</sup> FinP <sup>+</sup> TraJ153 <sup>+</sup>	<i>lac, finP, traJ</i>	pNY300	pT7.3	Lee <i>et al.</i> (1992)
pLT350.1	Ap <sup>r</sup> FinP <sup>+</sup> TraJ153 <sup>+</sup>	<i>finP, traJ</i>	pSQ350.1	pT7.3	This study
pNY305	Ap <sup>r</sup> <i>finP305</i> <sup>+</sup>	<i>lac, finP305, traJ</i>	EDFL68	pUC18	Frost <i>et al.</i> (1989)
pLT185	Ap <sup>r</sup> <i>finP305</i> <sup>+</sup>	<i>finP305</i>	pNY305	pT7.3	This study
pT7.300	Ap <sup>r</sup> FinP <sup>+</sup> TraJ <sup>+</sup>	<i>finP, traJ</i>	F	pT7.3	Frost, unpublished
pUC19	Ap <sup>r</sup>	-	-	-	Vieira & Messing (1982)
pOX38-Km	Km <sup>r</sup> FinP <sup>+</sup> TraJ <sup>+</sup>	<i>finP, traJ</i>	F	-	Chandler & Galas (1983)
pLJ5-13	Ap <sup>r</sup> FinP <sup>+</sup>	T7 $\Phi$ 10	pOX38-Km (PCR)	pUC19	This study
pLJ305	Ap <sup>r</sup> <i>finP305</i> <sup>+</sup>	T7 $\Phi$ 10	pNY305 (PCR)	pUC19	This study
pGEX-2T	Ap <sup>r</sup> GST <sup>+</sup>	<i>lac</i>	-	-	Pharmacia
pGEX-FO2	Ap <sup>r</sup> GST-FinO <sup>+</sup>	<i>lac</i>	pGEX-2T	-	van Biesen & Frost (1994)
pACYC184	Tc <sup>r</sup> Cm <sup>r</sup>	-	-	-	Chang & Cohen (1978)
pSnO104	Cm <sup>r</sup> FinO <sup>+</sup>	?	-	pACYC184	Lee <i>et al.</i> (1992)
pBluescript KS <sup>+</sup>	Ap <sup>r</sup>	-	-	-	Stratagene
pQF50	Ap <sup>r</sup>	none	-	-	Ronald <i>et al.</i> (1990)
pLQ1	Ap <sup>r</sup> $\beta$ -galactosidase <sup>+</sup>	<i>finP</i>	pNY300 (PCR)	pQF50	This study
pRS27	Tc	<i>finP, traJ</i>	F	pSC101	Skurray <i>et al.</i> (1978)

and the first 153 bases of the *traJ* mRNA. The 180 bp *RsaI* fragment of pNY305 (containing a 1.1 kb *BglIII* F plasmid insert; Frost *et al.*, 1989) was moved into the *SmaI* site of pUC18 (Vieira & Messing, 1982), creating pUC185. pUC185 was then digested with *EcoRI* and *HindIII* and the *finP305*-containing fragment was ligated to *EcoRI/HindIII*-digested pT7.3, creating pLT185. The 1076 bp *BglIII* fragment of F was cloned into *BamHI*-linearized pT7.3, creating pT7.300. pSnO104 expresses the R6-5 *finO* gene from a 4.0 kb *PstI* fragment cloned into pACYC184 (Cm<sup>r</sup>; Lee *et al.*, 1992). pBluescript II KS<sup>+</sup> (Stratagene) was used as a DNA template for the *in vitro* synthesis of RNA size markers.

Plasmids pLJ5-13 and pLJ305 were designed to allow for the synthesis of FinP and *finP305* RNA, respectively, using bacteriophage T7 RNA polymerase. Primers LJE5 and LJE6 (Table 2.3) were used to amplify the *finP* or *finP305* gene from pOX38-Km or pNY305 (Chandler & Galas, 1983) and link it downstream of the bacteriophage T7 promoter (bolded in LJE6 sequence). Each fragment was individually cloned into pUC19 digested with *EcoRI/SmaI* (Ap<sup>r</sup>; Vieira & Messing, 1982), using the *EcoRI* site provided in primer LJE6, creating pLJ5-13 and pLJ305.

pUC180 was constructed by inserting the 180 bp *EcoRI/HindIII* fragment containing the *finP* gene from pSQ180 (Lee *et al.*, 1992) into pUC18 (Ap<sup>r</sup>; Vieira & Messing, 1982). pGEX-2T (Pharmacia) and pGEX-FO2 (van Biesen & Frost, 1994) were used for expression of glutathione S-transferase (GST) and a protein fusion between R6-5 FinO and GST (GST-FinO), respectively. pLQ1 expresses  $\beta$ -galactosidase activity from the *finP* promoter and was constructed as follows. The *finP* promoter sequence was amplified by PCR from pRS27 (Skurray *et al.*, 1978) using primers A and TVB14. The

**Table 2.3** PCR primers used in this study. Base changes are underlined and the T7 promoter sequence is shown in bold.

<b>Primer</b>	<b>Sequence</b>
A (LFR21)	GAGGTTCCCTATGTAT
D	TTACGTGGTTAATG
LJE1	ATACATAGGAACCTC
LJE5	AAAATCGCCGATGCAGGG
LJE6	TCGAATTCTAATACGACTCACTATAGATACATAGGAACCTCCTCCTCACAAAGG
LJE7	CGGAATTCTAATACGACTCAC
LJE8	CATAGAA <u>ACC</u> TTTGTGAGGA
LJE9	AAAATCGC <u>A</u> GATG <u>A</u> AGGGAG
LJE10	AAAATCGCCGATGC <u>TTT</u> AG
LJE11	GCCGATGCAGGGAGAC
LJE12	TCGAATTCTAATACGACTCACTATAGGTCGATGCAGGGAGTTC
LJE13	<u>TTTT</u> TCGCCGATGCAGGG
LJE14	AAAATCCATAGAATCCTTTGTGAGGA
LJE15	AACAAAAAAACCACCGCTAC
LJE16	CGGAATTCTAATACGACTCACTATAGACAGTATTTGGTATCTGCG
LJE17	TGTCCATAGAATCCTTTGTGAGGA
LJE19	TCGCCGATGCAGGGAGAC
LJE20	AATCGCCGATGCAGGGAG
LJE21	TGTCGCCGATGCAGGGAG
LJE22	TCGAATTCTAATACGACTCACTATAGCATAGGAACCTCCTCACAAAGG
LJE24	AAAATCT <u>AAT</u> ATGCAGGGAGACG
LJE25	GACAGTCGATGCAGGGAG
LJE26	GATTCTATGG <u>CC</u> GTTCGATGCAG
LJE27	AAAAGGGCCGATGCAGGGAG
LJE28	CGATGCAGGGAGTTCACG
TVB14	CCTGAATAACTGCCGTCAG
TVB15	TCGAATTCTAATACGACTCACTATAGACGTGGTTAATGCCACG
TVB18	CATAGAATCCTTTGTGAGGA
TVB24	TCGAATTCTAATACGACTCACTATAGGACAGTCGATGCAGGGAGTTC

89 bp PCR product was digested with *Bgl*II and cloned into the promoter probe vector pQF50 (Ronald *et al.*, 1990) digested with *Sma*I/*Bgl*II.

## 2.2 DNA sequencing

Double-stranded template DNA (~1 µg) was denatured in 0.2 N NaOH/0.2 mM EDTA for 5 min at room temperature (Kraft *et al.*, 1988). The denatured DNA was precipitated for 20 min on dry ice with 2.5 volumes of 95% ethanol in the presence of 0.3 M sodium acetate. The DNA was then washed twice with 70% ethanol, dried under vacuum and sequenced using a Sequenase<sup>TM</sup> version 2.0 kit (USB) in the presence of [ $\alpha$ -<sup>35</sup>S]dATP (Mandel Scientific). Reactions were heat-denatured for 5 min at 85°C and loaded onto a denaturing (6M urea) 6% polyacrylamide gel (38:1 acrylamide:bis-acrylamide) and electrophoresed (1600 V, 40 Watts) for 1-2 hours. Sequencing gels were dried and autoradiographed overnight at room temperature using Kodak X-Omat AR film.

## 2.3 Site-directed mutagenesis of *finP*

Mutagenesis was performed to change the sequence of the FinP spacer (nucleotides 35-38) from GACA to GCCC, according to the method of Frost *et al.* (1989). All enzymes were from Boehringer Mannheim unless otherwise stated. Briefly, ~1 µg of pUC180 cut with *Eco*RI and *Hind*III or *Ava*II alone, the DNA was purified from agarose, extracted 2X with phenol/chloroform and ethanol precipitated. One hundred picomoles of mutagenic oligonucleotide LJE26 was end-labelled using 0.1 units of T4

polynucleotide kinase in the presence of 0.3 mM ATP. The phosphorylated mutagenic oligonucleotide was mixed with *EcoRI/HindIII* and *AvaII*-digested pUC180 in annealing buffer (50 mM Tris-HCl [pH 7.5], 10 mM MgCl<sub>2</sub>). The mixture was boiled for 3 min and then chilled on ice for 2 h. Extension and ligation reactions were carried out at 37°C for 1 h, followed by overnight incubation at room temperature in buffer containing 20 mM Tris-HCl (pH 7.5), 10 mM MgCl<sub>2</sub>, 10 mM dithiothreitol (DTT) with 5 units of Klenow fragment and 6 units of T4 DNA ligase in the presence of 0.5 mM dNTPs. The DNA was phenol/chloroform extracted, ethanol precipitated and one fifth of the product was used to transform electrocompetent DH5 $\alpha$ . The resulting Ap<sup>r</sup> colonies were transferred to Hybond-N nylon membranes (Amersham Life Science) and probed overnight at 37°C with [<sup>32</sup>P]-labelled LJE26 in buffer containing 4X SSC, 0.1% SDS, 1 mM EDTA, 5X Denhardt's Solution. The membranes were washed (in 5X SSC, 0.1% SDS) 1X each at 37°C, 45°C, 50°C, 55°C, 60°C and 65°C and then autoradiographed on a Molecular Dynamics PhosphorImager 445 SI. Positive clones were confirmed by sequencing and one representative clone was subcloned into *EcoRI/HindIII* digested pT7.3, creating pLT180cc.

#### 2.4 $\beta$ -galactosidase assay

$\beta$ -galactosidase activity was assayed from DH5 $\alpha$  harbouring pQF50 or pLQ1 in the presence/absence of pSnO104 according to the method of Miller (1992). Cultures were grown to an A<sub>600</sub> of 1.2 at 37°C in LB medium supplemented with appropriate antibiotics and then chilled on ice for 20 min. Five hundred microlitres of cells were

mixed with an equal volume of chilled Z buffer (60 mM Na<sub>2</sub>HPO<sub>4</sub>-7H<sub>2</sub>O, 40 mM NaH<sub>2</sub>PO<sub>4</sub>-H<sub>2</sub>O, 10 mM KCl, 1 mM MgSO<sub>4</sub>-7H<sub>2</sub>O, 50 mM β-mercaptoethanol). The cells were then lysed with 2 drops of chloroform, 1 drop of 0.1% SDS and vortexed for 10 sec. After a 5 min incubation at 28°C, 0.2 ml of freshly prepared ONPG solution (*o*-nitrophenyl β-D-galactopyranoside; 4 mg/ml in Z buffer) was added and the tube was shaken for a few sec. The reaction was allowed to proceed for 40 min, the cell debris was removed by centrifugation and the A<sub>420</sub> (due to *o*-nitrophenol produced by β-galactosidase-mediated ONPG hydrolysis) was taken for each sample. The increase in *o*-nitrophenol per minute per bacterium, expressed as β-galactosidase units was calculated as follows:

$$\text{units of } \beta\text{-galactosidase} = (1000 \times A_{420}) / (t \times v \times A_{600})$$

where the A<sub>600</sub> reflects the cell density just before the assay, t = the time of the reaction in minutes and v = the volume of the culture (ml) used in the assay. Each culture was grown in duplicate and triplicate samples were assayed from each culture.

## 2.5 Isolation of total cellular RNA

Ten millilitre cultures of strains transformed with appropriate plasmids, were grown at 37°C to mid-log phase (A<sub>600</sub> = 0.75). For temperature-sensitive strains and their wild-type isogenic counterparts, cells were grown at 30°C to mid-log phase and then shifted to the non-permissive temperature (44°C) for 20 min. At time zero, rifampicin (200 μg/ml final concentration; Sigma) was added to stop the initiation of new rounds of



transcription. One ml samples were withdrawn at timed intervals and total cellular RNA was isolated using a modified hot-phenol method (Frost *et al.*, 1989). The cells were pelleted, frozen on dry ice and then resuspended in 300  $\mu$ l of lysis buffer (0.5% SDS; 10 mM Tris-HCl pH 7.5; 1 mM EDTA). An equal volume of phenol was added and the mixture was vortexed for 30 sec, followed by a 10 min incubation at 65°C. The phases were separated by centrifugation at 4°C for 15 min, after which the aqueous phase was removed and the RNA was precipitated with ethanol. The pelleted RNA was then dried and dissolved in 40  $\mu$ l diethyl-pyrocabonate (DEPC)-treated water. One microlitre samples were mixed with 1.5 ml fluorometer buffer (5 mM Tris-HCl; 1 mM EDTA, pH 8; 0.5  $\mu$ g/ml ethidium bromide) and the amount of total cellular RNA was determined using a Sequoia-Turner Model 450 fluorometer. RNA was stored at -70°C.

## **2.6 Northern analysis and chemical half-life determination**

Thirty microgram samples of total cellular RNA were denatured in formamide load dye (90% deionized formamide, 0.5X TBE, 0.05% BPB, 0.05% xylene cyanol) at 95°C for 3 min and then electrophoresed on 8 M urea 8% polyacrylamide gels at 350 V for 2 h. The RNA was transferred to Zeta-Probe nylon membrane (Bio-Rad Laboratories) for 30 min at 20V, using a Bio-Rad semi-dry blotting apparatus and UV cross-linked to the membrane in a Bio-Rad GS Gene-Linker. Blots were prehybridized for 3 h at 37°C in 5X Denhardt's Solution, 2.5X SSC, 0.5% SDS, 90 mM Tris-HCl (pH 7.5), 0.9 M NaCl, 6 mM EDTA, 100  $\mu$ g/ml of *E. coli* strain W tRNA type XX (Sigma) and 100  $\mu$ g/ml heat-denatured calf thymus DNA (Sigma). Blots were hybridized with 10 pmol of the

appropriate [<sup>32</sup>P]-end-labelled oligomer probe for 12-14 h at 37°C and then washed for 20 min at 37°C using each of the following conditions: 5X SSC, 1% SDS; 1X SSC, 0.1% SDS; 0.1X SSC, 0.1% SDS. Autoradiography was done at -70°C in the presence of an intensifying screen, using Kodak X-Omat AR film. Membranes which were to be reprobbed, were stripped by boiling the blot in 0.1% SDS for 15 min and then cooling the mixture to room temperature. Blots were then prehybridized and reprobbed as described above. The bands were quantified by phosphorimager analysis and the RNA chemical half-lives were obtained from plots of the percentage transcript remaining over time.

## 2.7 Generation of DNA templates for *in vitro* transcription

Plasmids pLJ5-13 and pLJ305 contain a 105 base pair PCR product with the *finP* and *finP305* gene, respectively, fused to the T7 promoter sequence in pUC19. During the construction of pLJ5-13, seven spontaneous mutant clones were obtained with single base mutations in stem II (G42:A, G45:A, C46:T, A47:G, G48:A, G49:A, A51:G) and one clone with a double mutation in stem II (C41:T C46:T). RNAs were generated by *in vitro* transcription from *Bam*HI-linearized pLJ305, pLJ5-13 and pLJ5-13 mutant plasmids which led to the addition of 7 vector-derived bases (GGGGAUC) to their 3' ends. All other RNAs were transcribed directly from gel purified PCR products prepared with Vent<sup>TM</sup> DNA polymerase (New England Biolabs) using the appropriate primers and DNA templates, as detailed in Table 2.4.

**Table 2.4** RNAs derived by *in vitro* transcription from PCR-generated templates

RNA	5' primer	3' primer	PCR template
FinP	LJE7	LJE5	pLJ5-13
FinP G66:U G71:U	LJE7	LJE9	pLJ5-13
FinP C46:U G66:U G71:U	LJE7	LJE9	pLJ5-13 C46:T
FinP C41:U C46:U G66:U G71:U	LJE7	LJE9	pLJ5-13 C41:T C46:T
FinP C62:A C63:A C64:A	LJE7	LJE10	pLJ5-13
FinP C70:A G71:U G72:U C73:A	LJE7	LJE24	pLJ5-13
FinP G75:C A76:C	LJE7	LJE27	pLJ5-13
FinP $\Delta$ A2,U3,A4	LJE22	LJE5	pLJ5-13
spacer-SLII-GAUUUU	TVB24	LJE5	pLJ5-13
spacer-SLII-GAUU	TVB24	LJE20	pLJ5-13
spacer-SLII-GACA	TVB24	LJE21	pLJ5-13
spacer-SLII-GA	TVB24	LJE19	pLJ5-13
spacer-SLII	TVB24	LJE11	pLJ5-13
SLII-GAUUUU	LJE12	LJE5	pLJ5-13
SLII-GAAAAA	LJE12	LJE13	pLJ5-13
SLII	LJE12	LJE11	pLJ5-13
SLI	LJE7	TVB18	pLJ5-13
SLI A12:U	LJE7	LJE8	pLJ5-13
SLI-spacer	LJE7	LJE17	pLJ5-13
SLI-tail	LJE7	LJE14	pLJ5-13
<i>traJ</i> 184	TVB15	TVB14	pOX38-Km
<i>traJ</i> 110	TVB15	LJE1	pOX38-Km
<i>traJ</i> 77	TVB15	LJE25	pOX38-Km
<i>traJ</i> 71	TVB15	LJE28	pOX38-Km
ColB2	LJE6	LJE5	ColB2
R100-1	LJE6	LJE5	R100-1
RNA I	LJE16	LJE15	pLJ5-13

## 2.8 *In vitro* transcription of RNA

RNA was synthesized *in vitro* by run-off transcription from the appropriate template DNA, according to the method of Hjalt & Wagner (1992). 5' end-labelled RNA for use in RNase E cleavage assays was synthesized as follows. Non-radioactive FinP-G<sub>4</sub>AUC (FinP carrying the 7 base vector-derived extension) and *finP305*-G<sub>4</sub>AUC RNA were synthesized overnight at 37°C in a reaction mixture containing 1X T7 RNA polymerase buffer (Boehringer Mannheim); 0.5 mM rNTPs, 0.01% Triton X-100, 10 mM DTT, 1.0 unit/μl RNaguard (Pharmacia), 2 μg *Bam*HI-linearized pLJ5-13/pLJ305 DNA and 0.5 units/μl T7 RNA polymerase (Boehringer Mannheim). Thirty units of RNase-free DNase I (Boehringer Mannheim) were added to the cold RNA and incubated for 15 min at 37°C. The DNA-free RNA was phenol/chloroform extracted, ethanol precipitated and dissolved in DEPC-treated H<sub>2</sub>O. One fifth the volume of formamide load dye was added and the *in vitro* synthesized RNA was denatured at 95°C for 3 min and then electrophoresed (1.5 h at 250 V) on an 8 M urea 8% polyacrylamide gel. Full-length (86 base) transcripts were identified by ethidium bromide (EtBr) staining and cut out of the gel. The gel slice was crushed and the RNA eluted overnight at 37°C in DEPC-treated elution buffer (0.5 M NH<sub>4</sub>OAc, 0.1 mM EDTA). The RNA was phenol extracted (once each with phenol, phenol/chloroform, chloroform) and then ethanol precipitated, dried and dissolved in 10 mM Tris-HCl (pH 8.0). This was followed by dephosphorylation at 50°C for 45 min with 2 units of calf intestinal alkaline phosphatase (Boehringer Mannheim). The RNA was phenol extracted (as above) and then ethanol precipitated, dried and dissolved in 10 μl DEPC-treated H<sub>2</sub>O. The RNA concentration was determined

by fluorometry and 10 pmol of RNA was end-labelled at 37°C for 1 h, using 0.1 units of polynucleotide kinase (Boehringer Mannheim) in the presence of 1 unit/ $\mu$ l RNAGuard and 50  $\mu$ Ci [ $\gamma$ -<sup>32</sup>P]ATP (Mandel Scientific). Five microlitres of formamide load dye was added and the end-labelled RNA was gel purified as above, except that the full-length transcript was detected by autoradiography and the eluted RNA was dissolved in 20  $\mu$ l DEPC-treated H<sub>2</sub>O. Labelled RNA was stored at -20°C for 1 week without noticeable degradation.

For gel-shift analysis, uniformly-labelled RNA was prepared by *in vitro* transcription of DNA templates (pLJ5-13, pLJ5-13 mutants or PCR products) in reaction mixtures containing 1X T7 RNA polymerase buffer (Boehringer Mannheim), 1 unit/ $\mu$ l RNAGuard (Pharmacia), 10  $\mu$ Ci of [ $\alpha$ -<sup>32</sup>P]UTP (Mandel Scientific), 0.5 mM GTP, ATP, CTP and 0.02 mM UTP at 37°C for 1 hour. One microlitre aliquots were withdrawn for scintillation counting to determine the initial radioactivity (pre-cpm/ $\mu$ l) added to the reaction. DNA was removed with 10 units of RNase-free DNase I (Boehringer Mannheim) for 15 min at 37°C and the labelled RNA was gel purified as described. One  $\mu$ l aliquots of purified RNA were subjected to scintillation counting to determine the amount of radioactivity incorporated into product (post-cpm). The amount of uniformly-labelled RNA synthesized was calculated according to the following:

$$\text{pmol product} = (\text{post-cpm})/(\text{SA})(\# \text{ of Us})$$

where specific activity (SA) = (pre-cpm/ $\mu$ l)( $V_t$ )/pmol U.  $V_t$  is the total volume (30  $\mu$ l) and pmol U is the amount (400 pmol) of uridine used for each reaction. The number of uridines varied with the RNA synthesized.

## 2.9 Purification of GST and GST-FinO proteins

GST and GST-FinO (from R6-5) were purified using glutathione agarose affinity as described (van Biesen & Frost, 1994; Sandercock, 1997; Sandercock & Frost, 1998). One litre of DH5 $\alpha$  (pGEX-2T or pGEX-FO2) was grown in LB medium containing 2% glucose and 50  $\mu$ g/ml Ap at 37°C from an overnight seed culture (1/50 inoculum) started from a single colony. At an  $A_{600}$  of 1.0, IPTG (Sigma) was added to a final concentration ( $C_f$ ) of 0.5 mM to induce the production of protein for 5 hours. One hundred millilitre aliquots of cells were pelleted and stored at -20°C until needed.

The cell pellet was thawed on ice and resuspended in 4 mg/ml lysozyme (Sigma) in STE buffer (10 mM Tris-HCl pH 8.0, 150 mM NaCl, 1 mM EDTA) and incubated for 30 min on ice. DTT ( $C_f$  = 4.6 mM) was added and while vortexing, Sarkosyl (N-laurylsarcosine dissolved in STE buffer; Sigma) was added to a final concentration of 1.5%. The cell suspension was lysed using a French Press (American Instrument Company) at a constant pressure of 1300 kPa. Following the addition of Triton X-100 ( $C_f$  = 2%), the cell lysate was vortexed and then incubated on ice for 30 min. The insoluble cell debris was removed by centrifugation at 10,000 x g for 10 min at 4°C. One hundred microlitre of a 50% glutathione agarose-bead slurry (S-linked; Sigma) in PBS (137 mM NaCl, 1.5 mM KH<sub>2</sub>PO<sub>4</sub>, 2.8 mM Na<sub>2</sub>HPO<sub>4</sub>·7H<sub>2</sub>O, 2.7 mM KCl, pH 7.2) was

added to the supernatant and binding was allowed to proceed for 90 min on a rocking platform at 4°C. The beads were carefully pelleted at ~500 x g and washed three times with 20 ml TEB (50 mM Tris-HCl pH 8.0, 1 mM EDTA, 100 µg/ml RNase/DNase free BSA). GST/GST-FinO protein was eluted from the beads for 10 min with 20 mM reduced glutathione (Sigma) dissolved in TEB. The beads were pelleted at ~500 x g and the protein-containing supernatant was removed. The protein was stored in 10 µl aliquots supplemented with glycerol ( $C_f = 10\%$ ) at -70°C for several months without noticeable loss of activity. Protein yields (typically 50 µg per 100 ml of starting culture) were determined by comparison of a 10 µl aliquot with a range of BSA concentrations run on a 15% SDS polyacrylamide gel (35 mA for 3 h).

## 2.10 *In vitro* RNase E cleavage of FinP-G<sub>4</sub>AUC and *finP305*-G<sub>4</sub>AUC RNA

RNase E was kindly provided by Dr. George Mackie (UBC). The enzyme was purified from strain GM402 (BL21[DE3]/pGM102; Cormack *et al.*, 1993), which overexpresses a protein of apparent size ~180 kDa, corresponding to RNase E and is largely free of exonucleases (Mackie & Masterman, personal communication). The extract was supplied at a concentration of 5.1 µM and was diluted 1:30 as recommended for use in cleavage reactions.

The RNase E cleavage sites were mapped *in vitro* according to the method of Mackie (1991). 5' end-labelled FinP-G<sub>4</sub>AUC (~0.6 pmol) or *finP305*-G<sub>4</sub>AUC RNA (1.8 pmol) was denatured for 2 min at 50°C in 2X RNase E assay buffer (50 mM Tris-HCl pH 7.8, 10 mM MgCl<sub>2</sub>, 200 mM NH<sub>4</sub>Cl, 120 mM KCl, 10% glycerol, 0.2 mM EDTA and 0.2

mM DTT), shifted to 37°C for 10 min and then chilled on ice for 5 min. The annealed RNA was digested in a total volume of 30  $\mu$ l at 30°C with RNase E extract (5.1 pmol for FinP-G<sub>4</sub>AUC; 1.6 pmol for *finP305*-G<sub>4</sub>AUC RNA) in the presence of 8% PEG 6000, 0.06% Triton X-100. Aliquots (4  $\mu$ l) were removed from the reaction at timed intervals and quenched in formamide load dye (12  $\mu$ l). Products were denatured at 95°C for 3 min and then separated on an 8 M urea 12% polyacrylamide gel. The bands were visualized by autoradiography and quantified by phosphorimager analysis.

RNA size standards were prepared by two methods. *In vitro* run-off transcription was used to synthesize [<sup>32</sup>P]-labelled RNA markers of 39, 59 and 81 bases from pBluescript II KS<sup>+</sup> template DNA digested with *Xba*I, *Pst*I and *Hind*III, respectively. A second size standard was generated by alkaline hydrolysis of [<sup>32</sup>P]-labelled Fin-G<sub>4</sub>AUC (van Biesen *et al.*, 1993). Hydrolysis of ~0.2 pmol (10,000 cpm) Fin-G<sub>4</sub>AUC was achieved by boiling the RNA in alkaline buffer (0.05 M NaOH, 1 mM EDTA) for 10-20 sec, followed by the addition of equal volumes of neutralizing buffer (8 M urea, 80 mM NaOAc, 1% glacial acetic acid) and formamide load dye.

### **2.11 Assay for FinO protection of RNA cleavage by RNase E**

The assay was carried out as detailed for RNase E cleavage with the following changes. Approximately 0.4-0.5 pmol of annealed 5' end-labelled RNA was incubated with 0, 3, 10, or 21 pmol of GST-FinO or 21 pmol GST, in the presence of 1.3 pmol RNase E extract. Samples were taken 1, 5 and 30 minutes later and electrophoresed on a denaturing (8M urea) 12% polyacrylamide gel. As a control, the annealed RNA was incubated with 21 pmol GST-FinO in the absence of RNase E.

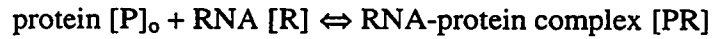


## 2.12 Gel-shift analysis of RNA-protein interactions

The ability of GST-FinO to bind FinP and a series of RNA variants was assessed by RNA mobility shift analysis. A step of RNA denaturation-renaturation did not improve or modify the binding affinity of the protein, therefore gel-purified *in vitro*-transcribed RNA was used directly for analysis. Seven and one half femtomoles of uniformly-labelled RNA was incubated with increasing amounts of GST-FinO (0 - 31.9 pmol) for 30 min at room temperature in buffer containing 50 mM Tris-HCl, pH 8.0, 1 mM EDTA, 10 mM (or 83.5 mM as indicated) NaCl, 100 µg/ml BSA (RNase/DNase free; Boehringer Mannheim), 7.6 Units RNAGuard (Pharmacia), 10% glycerol. A range of divalent cation concentrations (0.1 - 10 mM MgCl<sub>2</sub>) was also tested. As controls, GST protein (5.3 - 192 pmol) was incubated with either FinP, SLI or SLII. For competition assays, competitor RNA (0.0003-30 µg of tRNA or poly(U); Sigma) was mixed with FinP prior to the addition of GST-FinO. Samples were loaded onto a continuously running (150 V) 6% or 8% non-denaturing polyacrylamide gel in 1X TBE buffer and electrophoresed at room temperature for 1.5 hours. Bands were visualized by autoradiography and quantified by phosphorimager analysis.

The ability of RNase E to bind wild-type FinP was determined as described above except that binding was carried out for 1, 5, 10 or 30 min. Competition between GST-FinO and RNase E for binding to FinP (7.5 fmol) was assessed by mixing 10 pmol of GST-FinO with increasing amounts of RNase E (0.1, 1.1, 2.1, 5.3 and 10.6 pmol) prior to their addition to FinP.

The equilibrium association constant ( $K_a$ ) for each RNA-protein interaction was calculated from the protein concentration that caused 50% of the labelled RNA to shift in the gel (Tsai *et al.*, 1990; van Biesen & Frost, 1994) given by the following:



where  $K_a = [PR]/[P]_o[R]$ . At 50% binding, the free RNA [R] and complexed RNA [PR] concentrations are equal, therefore the  $K_a$  can be directly calculated as  $K_a = 1/[P]_o$ , where  $[P]_o$  is the initial concentration of protein added to the reaction. For RNA variants that gave more than one band shift,  $K_a$ s were calculated by considering all bound RNA as a single species. Except where noted,  $K_a$  values were calculated from 3 independent determinations.

## Chapter 3

### Characterization of FinP antisense RNA degradation *in vivo*\*

\*A version of this chapter has been accepted for publication in the *Journal of Molecular Biology*. Jerome, L.J., van Biesen, T. & Frost, L.S.

### 3.1 Introduction

Antisense RNA control of biological function by post-transcriptional regulation is a common theme among prokaryotes (reviewed in Wagner & Simons, 1994). The FinOP fertility inhibition system of F-like plasmids uses an antisense RNA to regulate the frequency of plasmid transfer by controlling expression of the *traJ* gene. The *traJ* gene encodes a 27 kDa protein required for the initiation of high levels of transcription from the major F transfer region promoter, pY. Expression of *traJ* is negatively regulated by the combined actions of the *finO* and *finP* gene products. The *finP* gene encodes a plasmid-specific 79 base antisense RNA molecule that is complementary to part of the 5' untranslated region of *traJ* mRNA (Mullineaux & Willetts, 1985; Finlay *et al.*, 1986; Dempsey, 1987). Binding of FinP to its target region within the *traJ* mRNA leader is believed to sequester the *traJ* RBS, preventing its translation and leading to repression of F plasmid transfer.

The product of the *finO* gene is a 21.2 kDa protein (van Biesen & Frost, 1992), which is essential for effective repression of transfer by FinP. The *finO* gene in F is interrupted by an IS3 element (Cheah & Skurray, 1986; Yoshioka *et al.*, 1987), rendering F plasmid-containing cells constitutive for transfer. This mutation in F can be complemented by the *finO* product of related plasmids, such as R100 (Finnegan & Willetts, 1973) or R6-5 (van Biesen & Frost, 1992). Earlier work has shown that FinO has two important effects on FinP. *In vitro*, a GST-FinO fusion protein binds to stem-loop II of FinP and *traJ* mRNA and promotes duplex formation (van Biesen & Frost, 1994). *In vivo*, FinO blocks FinP antisense RNA decay, increasing its effective concentration (Frost *et al.*, 1989; Lee *et al.*, 1992). FinO does not act on the *finP*

promoter (Mullineaux & Willetts, 1985), but rather acts post-transcriptionally. The combined actions of FinO (from R100 or R6-5) and FinP repress F transfer by 100- to 1000-fold (Willetts & Maule, 1986).

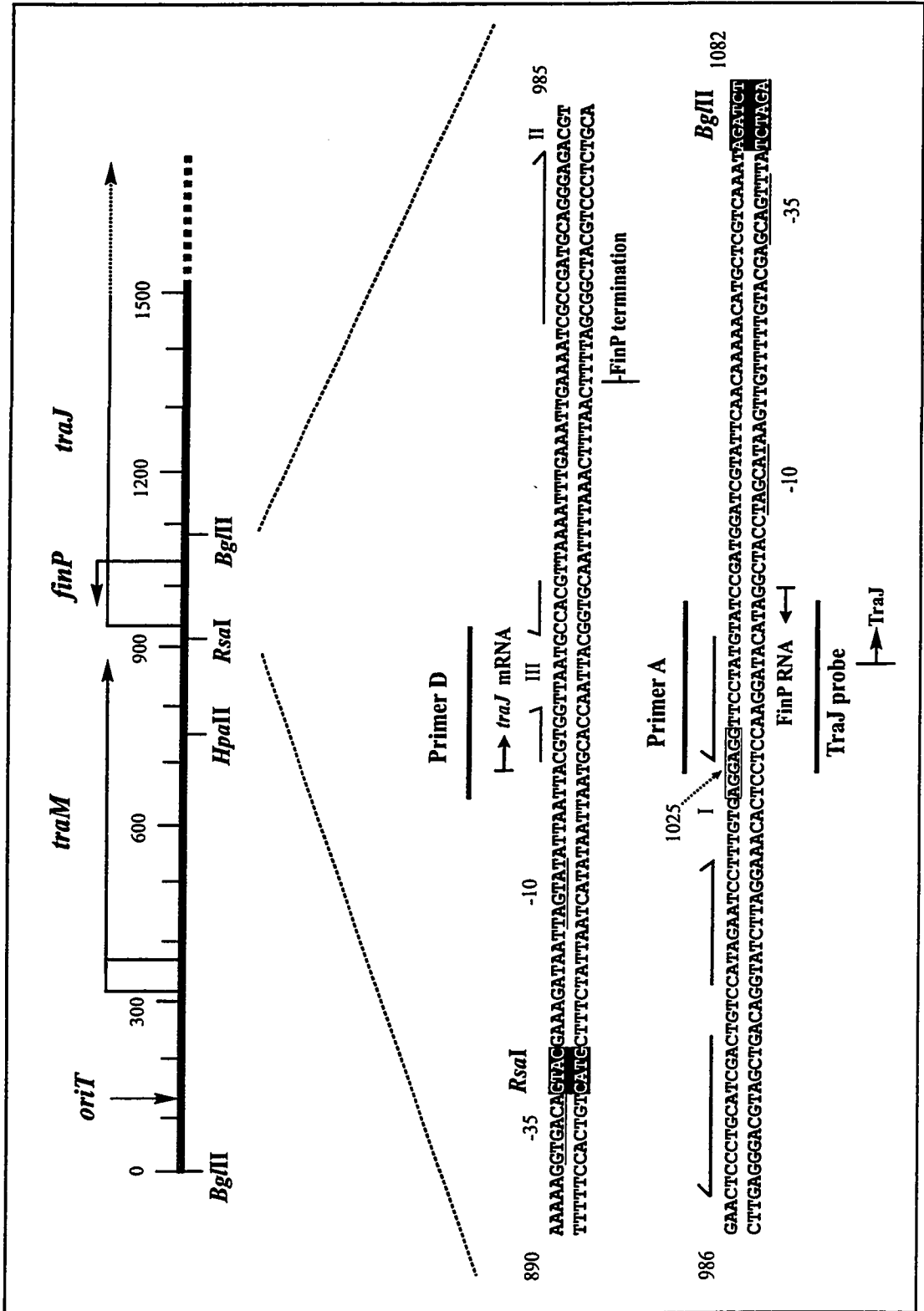
The present study was initiated as a prelude to determining how FinO protects FinP from decay. Four major ribonucleases (RNases) have been implicated in mRNA decay in *E. coli* and could potentially be involved in FinP degradation. These include the endonucleases RNase III and RNase E and the 3' exonucleases RNase II and PNPase. Some highly structured RNAs also require addition of a polyadenylate tail by PAP I, which facilitates their subsequent exonucleolytic degradation (Cohen, 1995; Hajnsdorf *et al.*, 1995; Haugel-Nielsen *et al.*, 1996; Coburn & Mackie, 1996b). In this chapter FinP degradation is examined by Northern blot analysis, in the presence and absence of *traJ* mRNA, in a series of strains deficient in each of these enzymes.

## 3.2 Results

### 3.2.1 Full-length FinP antisense RNA accumulates in RNase E-deficient strains

In order to investigate the intracellular degradation of FinP antisense RNA, the chemical half-life of FinP was examined in wild-type and RNase-deficient strains. FinP was expressed from a moderate copy number plasmid, pLT180, which contains the *RsaI*-*Bgl*III fragment of F (Figure 3.1). The *RsaI* site interrupts the *traJ* promoter, allowing FinP decay to be monitored in the absence of transcription of *traJ*. To allow comparison of mRNA half-lives between wild-type and temperature-sensitive strains, RNA was extracted from all strains under identical growth conditions. Cultures were grown to mid-log phase ( $A_{600} = 0.75$ ) at 30°C, shifted to the non-permissive temperature (44°C) for 20

**Figure 3.1** Map of the origin of transfer (*oriT*) region of F (modified from Lee *et al.*, 1992). Distances from the *Bgl*III site upstream of *oriT* (Frost *et al.*, 1994) are indicated and the relevant restriction sites are shown. The horizontal arrows indicate the direction and length of transcripts, with the *traJ* mRNA extending to position ~1760, beyond the region shown in the diagram. The sequence of the *finP* gene and *traJ* 5'-untranslated region are shown below the map. The *Rsa*I and *Bgl*III sites used for cloning are shown in bold. The transcriptional start sites for FinP RNA and *traJ* mRNA are indicated and their respective promoters are underlined. Inverted repeats which allow FinP and *traJ* mRNA to form stem-loop structures, are indicated by arrows above the sequence. The start of TraJ translation and the termination of FinP transcription are shown. The *traJ* ribosome binding site (RBS) is boxed. Oligonucleotide probes (Primer A, Primer D and TraJ probe) used for Northern analysis are positioned above or below the opposite strand to which they anneal.



minutes and then rifampicin was added to stop transcription (time 0). Samples were withdrawn at various times after the addition of rifampicin and total cellular RNA was extracted and subjected to Northern blot analysis. FinP RNA was detected with Primer A (Figure 3.1), which hybridizes to the 5' side of stem-loop I. Bands were quantified by phosphorimager analysis and the relative amount of FinP at each time point was expressed as a percentage of the highest value obtained. Chemical half-lives were determined from plots of the percentage transcript remaining over time.

In the wild-type strain (MG1693), in the absence of FinO (Figure 3.2, RNase E<sup>+</sup> FinO<sup>-</sup>), the full-length FinP transcript had a chemical half-life of 14 min (Table 3.1). In the presence of FinO (RNase E<sup>+</sup> FinO<sup>+</sup>), FinP was stable over the 4 h time course of the experiment, suggesting that FinO protects FinP from nucleolytic degradation, as previously proposed (Lee *et al.*, 1992). In order to assess the role of RNase E in FinP degradation, the decay of FinP in the absence of FinO was followed in a strain (SK5665) carrying a temperature-sensitive mutation within the gene encoding RNase E (*rne-1*; G736:A). At the non-permissive temperature, the chemical half-life of FinP increased to 104 min in this strain (RNase E<sup>-</sup> FinO<sup>-</sup>). The FinP half-life was also increased in a strain (N3431) carrying an alternative temperature-sensitive RNase E mutation (*rne-3071*; C742:T) as seen in Figure 3.3. In this isogenic pair, the FinP half-life was extended from 14 minutes in the wild-type (N3433) to 64 minutes in the RNase E mutant (Table 3.1). No shorter FinP intermediates could be detected in either RNase E mutant, suggesting that RNase E acts on and initiates degradation of full-length FinP RNA. Products of RNase E cleavage were not observed in the wild-type strains indicating that degradation occurred too rapidly to allow their detection, suggesting that exonucleases are involved.



**Figure 3.2** FinP decay is dependent on RNase E and is stabilized by FinO. FinP was expressed from pLT180 (in the absence of *traJ*) in a wild-type strain (MG1693) in the absence (RNase E<sup>+</sup> FinO<sup>-</sup>) and presence of FinO (RNase E<sup>+</sup> FinO<sup>+</sup>) and from a temperature-sensitive RNase E mutant (*rne-1*; SK5665) in the absence of FinO (RNase E<sup>-</sup> FinO<sup>-</sup>). Samples were withdrawn at the times indicated (min) after the addition of rifampicin at 44°C. Thirty microgram samples of total cellular RNA were electrophoresed on denaturing (8M urea) 8% polyacrylamide gels and then transferred to nylon membranes, as described in Materials and Methods (section 2.6). Blots were hybridized with Primer A (Figure 3.1).

RNase E<sup>+</sup> FinO<sup>-</sup>

0  
15  
30  
60  
120  
180  
240



RNase E<sup>-</sup> FinO<sup>-</sup>

0  
15  
30  
60  
120  
180  
240



RNase E<sup>+</sup> FinO<sup>+</sup>

0  
15  
30  
60  
120  
180  
240

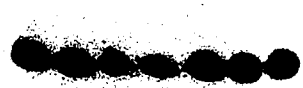


**Table 3.1** FinP RNA half-life in wild-type and mutant strains.

<b>Strain Phenotype</b>	<b>RNA half-life (min)<sup>a</sup></b>
wild-type	14
wild-type + FinO	>240
RNase E <sup>-</sup> ( <i>rne-1</i> )	104
RNase E <sup>-</sup> ( <i>rne-3071</i> )	64 <sup>b</sup>
RNase II <sup>-</sup>	15
PNPase <sup>-</sup>	13
RNase II <sup>-</sup> PNPase <sup>-</sup> RNase E <sup>-</sup> ( <i>rne-1</i> )	64 <sup>b</sup>
PAP I <sup>-</sup>	18 <sup>b</sup>

<sup>a</sup> RNA half-lives (at 44°C) were determined from plots of the percent transcript remaining over time and are averages from three experiments unless otherwise indicated.

<sup>b</sup> Half-life determined from a single experiment.

**Figure 3.3** The half-life of FinP is also extended in an *rne-3071* mutant. FinP was expressed from pLT180 in a wild-type strain (N3433) and from a second temperature-sensitive RNase E mutant (*rne-3071*; N3431) in the absence of FinO. Samples were withdrawn at the times indicated (min) after the addition of rifampicin at 44°C and 30 µg samples of total cellular RNA were subjected to Northern analysis as described in Figure 3.2. Blots were hybridized with Primer A (Figure 3.1).

**N3433**  
**Wild-type**

**N3431**  
***rne-3071***

**0 15 30 60 120 240**

**0 15 30 60 120 240**

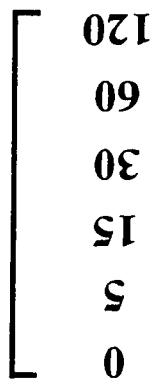


### 3.2.2 RNase II, PNPase and PAP I are not involved in the degradation of full-length FinP

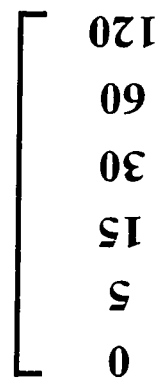
The effect of mutations in RNase II (SK5689; *rnb-500(ts)*) and polynucleotide phosphorylase (PNPase; SK5691; *pnp-7* nonsense mutation) on the decay of FinP expressed from pLT180 were examined by Northern analysis, as described above. The chemical half-life of full-length FinP at the non-permissive temperature (44°C) was not affected by mutations in either of the exonucleases (Figure 3.4, Table 3.1). A similar decay pattern was observed in a strain deficient in both exonucleases (data not shown). In agreement with these findings, the half-life of FinP was not increased in an RNase II PNPase<sup>-</sup> RNase E<sup>-</sup> triple mutant (SK5704; Figure 3.4, Table 3.1) over that seen in the single RNase E<sup>-</sup> mutants. These results suggest that the well-characterized 3' exonucleases, RNase II and PNPase, are not able to degrade the highly-structured, full-length FinP antisense RNA. The FinP half-life in the triple mutant (which carries the *rne-1* mutation) was lower than in the single *rne-1* mutant suggesting that this strain, which lacks 3 of the 4 major RNases, might have activated a weaker compensatory degradation pathway. FinP decay was also examined in a strain (N3433/ $\Delta$ *pcnB*) deficient in PAP I. Although the amount of FinP detected in this mutant was significantly reduced when compared to the wild-type, its half-life was essentially unaltered (14 min in the wild-type vs 18 min in the PAP I<sup>-</sup> strain; Figure 3.5, Table 3.1), suggesting that degradation of the full-length FinP transcript is not dependent on PAP I. The decrease in FinP concentration in the PAP I mutant was not unexpected since it has been shown previously that the *pcnB* mutation decreases ColE1 plasmid copy number 10-fold due to stabilization of the copy

**Figure 3.4** FinP decay is not dependent on 3' exonucleases. FinP was expressed from pLT180 in exonuclease-deficient strains SK5689 (RNase II<sup>-</sup>) and SK5691 (PNPase<sup>-</sup>) and from the triple mutant SK5704 (RNase II<sup>-</sup> PNPase<sup>-</sup> RNase E<sup>-</sup>). Samples were withdrawn at the times indicated (min) after the addition of rifampicin at 44°C and 30 µg samples of total cellular RNA were subjected to Northern analysis as described in Figure 3.2. The FinP transcript was detected with the Primer A (Figure 3.1).

RNase II



PNPase



RNase II PNPase RNase E

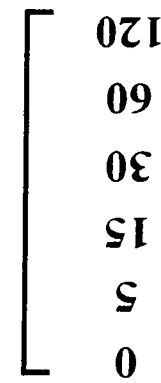




**Figure 3.5** Mutation of the gene encoding PAP I does not affect the half-life of FinP. FinP was expressed from pLT180 in the isogenic pair N3433 (wild-type) and N3433/ $\Delta$ *pcnB* (PAP I). Samples were withdrawn at the times indicated (min) after the addition of rifampicin at 44°C and 30  $\mu$ g samples of total cellular RNA were subjected to Northern analysis as described in Figure 3.2. The FinP transcript was detected with the Primer A (Figure 3.1).

**PAPI<sup>+</sup>**

**0 15 30 60 120**

**PAPI<sup>-</sup>**

**0 15 30 60 120**



number regulator RNA I (He *et al.*, 1993) and the vector used to express FinP (pT7.3) in this study uses the ColE1 origin of replication.

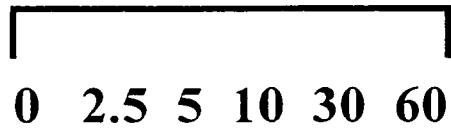
No shorter transcripts were detected with this probe (Primer A), which anneals to the 5' end of FinP, in either exonuclease mutant or the PAP I mutant. Therefore 5' intermediates of RNase E cleavage do not require polyadenylation by PAP I prior to their degradation, which can occur independent of RNase II and PNPase. Probes directed at the 3' end of FinP (within SLII) hybridized very poorly to full-length FinP (data not shown) indicating that SLII was resistant to denaturation and thus detection of 3' intermediates was not possible.

### 3.2.3 FinP is degraded by RNase III when duplexed with *traJ* mRNA

The previous sections examined FinP decay in the absence of *traJ*. Plasmid pLT350.1 was constructed to allow comparison of FinP decay in the presence of *traJ*. pLT350.1 contains the *HpaII-BglIII* fragment of F (Figure 3.1), which expresses the first 153 bases of *traJ* mRNA. pLT180 and pLT350.1 were separately introduced into IBPC5321 (wild-type) and grown at 37°C to mid-log phase ( $A_{600} = 0.75$ ). A 60 minute time course experiment was performed as described above and FinP was detected with the Primer A probe. In the absence of FinO, FinP expressed from pLT180 had a half-life of 15 minutes (FinP<sup>+</sup> TraJ<sup>-</sup> FinO<sup>-</sup>; Figure 3.6), as reported in previous sections. When FinP was co-expressed with *traJ* there was no detectable FinP transcript (FinP<sup>+</sup> TraJ<sup>+</sup> FinO<sup>-</sup>; Figure 3.6), suggesting that either FinP was not expressed from this construct or it was destabilized by *traJ*. To ensure that the FinP expressed from pLT350.1 was functioning normally, its decay in the presence of FinO was tested (Figure 3.7a). As with

**Figure 3.6** FinP is destabilized when co-expressed with *traJ* mRNA. pLT180 (FinP<sup>+</sup> TraJ<sup>-</sup> FinO<sup>-</sup>) and pLT350.1 (FinP<sup>+</sup> TraJ<sup>+</sup> FinO<sup>-</sup>) were introduced into the wild-type strain, IBPC5321. Samples were withdrawn at the indicated times (min) after the addition of rifampicin at 37°C and 30 µg samples of total cellular RNA were subjected to Northern analysis as described in Figure 3.2. FinP RNA was detected with Primer A (Figure 3.1).

**FinP<sup>+</sup> TraJ<sup>-</sup> FinO<sup>-</sup>**



**FinP<sup>+</sup> TraJ<sup>+</sup> FinO<sup>-</sup>**

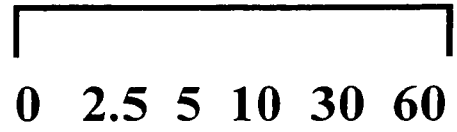
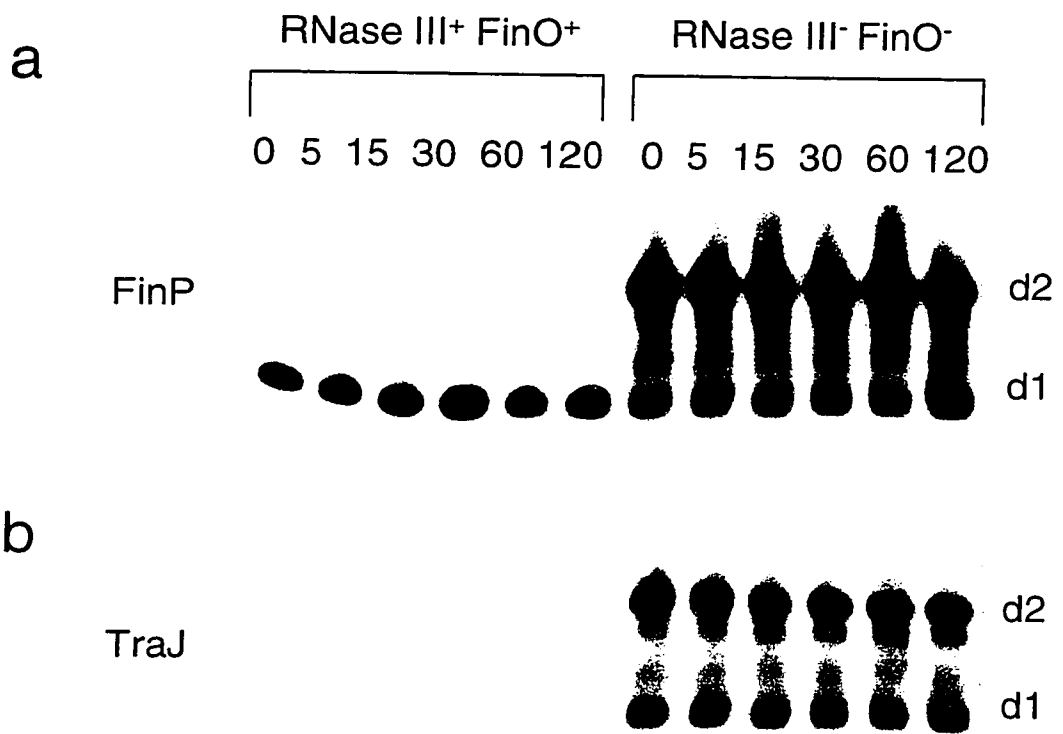


**Figure 3.7** Two *FinP/traJ* duplexes (d1 and d2) are stabilized in the absence of RNase III. Northern analysis of *FinP* and *traJ* mRNA expressed from pLT350.1 in a wild-type strain (IBPC5321), in the presence of *FinO* (RNase III<sup>+</sup> *FinO*<sup>+</sup>) and in an RNase III mutant (IBPC5321-*rnaseIII*<sup>o</sup>) in the absence of *FinO* (RNase III<sup>-</sup> *FinO*<sup>-</sup>). Samples were withdrawn at the indicated times (min) after the addition of rifampicin at 37°C and resolved on a denaturing 8% polyacrylamide gel. Single-stranded RNA corresponding to *FinP* was detected in (a) with Primer A (Figure 3.1). The complementary single-stranded *traJ* mRNA derived from the duplex was detected in (b) by stripping the blot in (a) and rehybridizing with the *TraJ* Probe (Figure 3.1).



pLT180 which does not express *traJ* (Figure 3.2), the FinO protein fully stabilized FinP in the wild-type strain (RNase III<sup>+</sup> FinO<sup>+</sup>) when co-expressed with *traJ*. Thus, FinP was expressed from pLT350.1 but was destabilized by *traJ* in the absence of FinO.

van Biesen *et al.* (1993) previously detected truncated *traJ* mRNA species that they propose originated by RNase III-mediated cleavage of a FinP/*traJ* mRNA duplex. To examine the contribution of RNase III to the degradation of FinP, pLT350.1 was introduced into a strain (IBPC5321-*rnc*<sup>o</sup>) carrying a Tn10 insertion within the gene encoding RNase III (*rnc-14::Tn10*). In the RNase III mutant in the absence of FinO, the 79 base FinP transcript (d1) and an additional higher molecular weight band (d2) were detected (RNase III<sup>-</sup> FinO<sup>-</sup>; Figure 3.7a). In order to determine whether the observed stabilization of FinP in the RNase III mutant was due to its participation in a duplex with *traJ* mRNA, the blot was stripped and rehybridized with the TraJ probe (Figure 3.1). In the wild-type strain expressing FinO, there was no detectable *traJ* at all time points (Figure 3.7b). In the absence of RNase III and FinO, two major *traJ* bands corresponding to d1 and d2 were visible at the same positions as those detected for FinP, suggesting that d1 and d2 represent FinP/*traJ* duplexes. Similar results were obtained when the FinO protein was supplied *in trans* (data not shown).

The absence of FinP/*traJ* mRNA duplexes in the wild-type strain is, therefore, due to degradation by RNase III. The continued presence of FinP in the wild-type strain implies that it was present in excess of *traJ* mRNA due to its stabilization by FinO. In order to determine if FinP itself was a target for RNase III cleavage, FinP was expressed from pLT180 (in the absence of *traJ*) in the RNase III mutant without FinO. As seen in



Figure 3.8a, FinP was not stabilized in the absence of RNase III and the longer transcript present in d2 was not detected.

To ensure that the observed duplexes resulted from pairing between FinP and *traJ* mRNA and not a vector-initiated counter-transcript, FinP expression was followed from pT7.300, which contains the entire *Bgl*III fragment of F (1076 bp; Figure 3.1) including 930 bp upstream of the *traJ* mRNA start site. The same pattern of duplex stabilization occurred with this plasmid (Figure 3.8b), indicating that the duplexes were not artifacts caused by transcription from vector promoters in pLT350.1. Similar results (not shown) were obtained with F itself, but the amounts of duplex were greatly reduced because of the low copy number of F.

The longer FinP transcript present in the RNase III mutant might be due to either transcription initiation upstream of the reported *finP* promoter or transcriptional readthrough at the rho-independent terminator (SLII) at the 3' end of FinP. To determine which of these possibilities was correct, the blot in Figure 3.8b was stripped and reprobed with Primer D (Figure 3.1), which anneals to the region complementary to the 5' end of the *traJ* mRNA leader. The longer transcript (d2) hybridized to Primer D (Figure 3.8c) suggesting that a portion of FinP is extended at its 3' end by readthrough beyond the SLII terminator in the RNase III mutant.

### **3.2.4 FinO does not affect transcription from the *finP* promoter**

The results obtained thus far suggest that the half-life of FinP can be extended either by the presence of FinO or the mutation of RNase E. It is therefore tempting to speculate that FinO increases the steady-state concentration of FinP by preventing its

**Figure 3.8** (a) FinP is not degraded by RNase III in the absence of *traJ* mRNA. Northern analysis of FinP expressed from pLT180 in an RNase III-deficient strain at 37°C. Samples were withdrawn at the indicated times (min) after the addition of rifampicin and FinP was detected with Primer A (Figure 3.1). (b) FinP decay from pT7.300 (expressing F sequences upstream of *traJ*) in an RNase III mutant at 37°C. FinP was detected with Primer A (Figure 3.1). (c) The blot in (b) was stripped and reprobed with Primer D (Figure 3.1), which hybridizes downstream of the natural FinP terminator, indicating that the longer FinP transcript is extended at its 3' end.

**a**

pLT180

RNase III<sup>-</sup> FinO<sup>-</sup> TraJ<sup>-</sup>

0 1 2.5 5 10 20



**b**

pT7.300

RNase III<sup>-</sup> FinO<sup>-</sup> TraJ<sup>+</sup>

0 1 2.5 5 10 20



d2

d1

**c**

pT7.300

RNase III<sup>+</sup> FinO<sup>-</sup> TraJ<sup>+</sup>

0 1 2.5 5 10 20



d2

d1

Primer A

Primer A

Primer D

degradation by RNase E. To ensure that FinO had no effect on FinP transcription from the clones (pLT180 and pLT350.1) used for chemical half-life determinations, the DNA sequence starting within the *finP* gene (nucleotide 1025; Figure 3.1) and extending to the *finP* promoter (*Bgl*III site; nucleotide 1082) was amplified by PCR and cloned into the promoter-probe vector pQF50. The resulting clone, pLQ1, was used to determine the effect of FinO on *finP*-driven  $\beta$ -galactosidase activity. pLQ1 was introduced with or without pSnO104 (expressing R6-5 FinO) into DH5 $\alpha$  and the transformants were selected on MacConkey-lactose (1%) agar with the appropriate antibiotics. pQF50 was introduced into DH5 $\alpha$  as a negative control. On MacConkey-lactose plates, there was no detectable  $\beta$ -galactosidase activity from the vector control (DH5 $\alpha$ /pQF50) which grew as white colonies (Table 3.2). The *finP* promoter-*lacZ* transcriptional fusion produced colonies with red centres surrounded by a white halo (pLQ1, Table 3.2), suggestive of low level  $\beta$ -galactosidase activity. The colony morphology was identical in the presence of FinO (pLQ1 + pSnO104).

Quantitative assays which measure  $\beta$ -galactosidase-mediated ONPG hydrolysis were performed according to the method of Miller (1992). Values are expressed as units of  $\beta$ -galactosidase (Table 3.2) which correspond to the increase in *o*-nitrophenol per minute per bacterium. A very low level of activity ( $4.6 \pm 0.39$  units) was obtained from the vector control which represents spontaneous ONPG hydrolysis in the absence of  $\beta$ -galactosidase. The *finP* promoter conferred a low level of  $\beta$ -galactosidase activity ( $12.4 \pm 0.28$ ), suggestive of weak promoter activity. This value was not increased by the presence of the FinO protein ( $11.8 \pm 1.2$ ) indicating that FinO does not act to alter *finP*

**Table 3.2** Effect of FinO on *finP*-driven  $\beta$ -galactosidase activity in DH5 $\alpha$ .

Plasmid	Phenotype	Colony color <sup>a</sup>	Units $\beta$ -galactosidase <sup>b</sup>
pQF50	no promoter, FinO <sup>-</sup>	white	4.6 $\pm$ 0.39
pLQ1	<i>finP</i> promoter, FinO <sup>-</sup>	red centre with white halo	12.4 $\pm$ 0.28
pLQ1 + pSnO104	<i>finP</i> promoter, FinO <sup>+</sup>	red centre with white halo	11.8 $\pm$ 1.20

<sup>a</sup> determined on MacConkey-lactose agar.

<sup>b</sup> average  $\pm$  standard deviation of six samples (see Materials and Methods).

promoter activity, in agreement with an earlier study by Mullineaux & Willetts (1985). Therefore the FinO-mediated increase in FinP half-life observed in the previous sections is due to an increase in FinP stability, rather than an increase in FinP expression.

### 3.3 Discussion

Lee *et al.* (1992) previously examined the decay of a 151 base *lacZ*-FinP RNA induced from the *tac* promoter. They found that the 151 base transcript was shortened to a FinP-like intermediate which had a half-life of 2 minutes and could be stabilized by FinO. They also found that the *rne-3071* mutation stabilized both the 151 base *lacZ*-FinP transcript and the FinP-like intermediate, however they were unable to conclude whether this was due to reduced RNase E cleavage within FinP or within the vector sequence preceding FinP. The results of the present study suggest that the degradation of authentic FinP is initiated by endonucleolytic RNase E cleavage. FinP expressed from its own promoter (pLT180) had a moderate chemical half-life of 14 minutes. The shorter half-life (2 minutes) of the FinP-like intermediate observed previously was therefore the result of its association with *lacZ* (see below). In the present study, the FinP half-life increased ~5-fold and ~7-fold in the *rne-3071* and *rne-1* strains, respectively. Both mutations have been mapped to the N-terminal catalytic domain of RNase E (McDowall *et al.*, 1993; McDowall & Cohen, 1996), however the *rne-3071* allele is not as strong as *rne-1* (Nierlich & Murakawa, 1996; Dr. S. Kushner, personal communication). The small discrepancy in FinP half-lives observed in these two strains is therefore attributable to differences in RNase E thermolability. Since Lee *et al.* (1992) observed stabilization of both the *lacZ-finP* fusion and the FinP-like intermediate in the *rne-3071* strain, this

indicates that sites within both *lacZ* and *finP* were subject to cleavage by RNase E. Mackie *et al.* (1997) propose that for substrates with more than one RNase E site, initial recognition, cleavage and retention of the product from the first site by one subunit of an RNase E dimer facilitates recognition and cleavage at subsequent sites by the other subunit. Thus, the rapid degradation of the FinP-like intermediate was most likely influenced by a prior RNase E cleavage event in the upstream *lacZ* portion of the fusion, accounting for its shorter half-life.

The finding that inactivation of RNase E stabilized full-length FinP suggests that RNase E initiates degradation of the full-length transcript and that FinP is a poor substrate for other endonucleases and 3' exonucleases. The latter conclusion is supported by the finding that mutations in the well-characterized 3' exonucleases, RNase II and PNPase, did not alter the FinP chemical half-life (Table 3.1). Full-length FinP does not appear to require polyadenylation by PAP I prior to its degradation since mutation of the *pcnB* gene did not significantly alter the FinP half-life (18 minutes); however, the involvement of PAP II cannot be ruled out. Intermediates of RNase E cleavage were not observed using Primer A to detect the 5' end of FinP and probes directed at the 3' end of FinP hybridized very poorly. Therefore the effects of RNase II, PNPase and PAP I mutations on the subsequent degradation of 3' intermediates of RNase E cleavage are not known. The lack of detectable 5' intermediates in all mutant strains tested suggests that they may be eliminated by an alternate degradation pathway.

In a previous study, van Biesen *et al.* (1993) showed that FinP forms a duplex with the *traJ* transcript *in vitro*, with similar kinetics to that observed for other sense/antisense RNA systems. They also used primer extension analysis to demonstrate

the existence of truncated *traJ* mRNA transcripts, which they suggest may originate from RNase III-mediated cleavage of the FinP/*traJ* mRNA duplex *in vivo*. Two stable FinP/*traJ* mRNA duplexes (d1 and d2) were detected in the RNase III-deficient strain in the present study. The shorter duplex d1 likely results from pairing between FinP (79 bases) and *traJ*, with removal of the extended regions of the *traJ* mRNA by exonuclease and endonuclease activity. The size of d1 would therefore be limited by the size of FinP (79 bases). The longer duplex (d2) could form only in the event of transcriptional readthrough at the rho-independent terminator (SLII) in FinP. Thus the size of d2 is defined by the length of the *traJ* mRNA leader region. Both duplexes are degraded by RNase III, as evidenced by their absence in the wild-type strain, but whether this is necessary for repression of conjugation was not examined.

The 3' extended form of F FinP in d2 is not detected in the RNase III mutant in the absence of *traJ* expression (Figure 3.8a) or in the wild-type strain when *traJ* is expressed (Figure 3.7a). These results suggest that in the absence of *traJ*, the longer FinP is not produced. However, in its presence, this transcript is somehow produced (see below) and forms a duplex with *traJ*, but is rapidly degraded by RNase III and escapes detection. Large amounts of FinP RNA are produced in the presence of FinO, resulting in excess, unreacted FinP in the wild-type strain (compare amounts of FinP and *traJ* in RNase III<sup>+</sup> FinO<sup>+</sup> strain in Figure 3.7). Why is the longer form of FinP seen only in the duplex? One hypothesis (Dr. E.G.H. Wagner, personal communication) is as follows. When FinP is co-transcribed with *traJ* mRNA, some of the time, FinP and *traJ* mRNA begin to duplex before *finP* transcription is complete. If part or all of the stem-loop II sequence duplexes before it has a chance to form a stem-loop structure (terminator),



transcription continues, leading to the longer transcript seen in the RNase III mutant. This FinP transcript may end at the putative rho-dependent termination site (sequence complementary to *traJ* mRNA SLIII) proposed by Paranchych *et al.* (1986) or terminate at a site further downstream. Since the longer transcript is already duplexed with *traJ* mRNA (as required for its production), it will be readily degraded by RNase III and will not be detected in the wild-type (Figure 3.7a). When there is no counter-transcript being produced, as is the case with pLT180, termination occurs at the rho-independent terminator and the longer transcript is not made (Figure 3.8a). Clearly, further experiments are required to test this hypothesis.

Like IS10 antisense RNA, FinP itself is not a substrate for RNase III (Figure 3.8a). SLI consists of only 7 continuous bp and SLII is a continuous duplex of 14 bp, neither of which is of sufficient length for RNase III cleavage. Overall the results of this study suggest that the primary enzyme involved in FinP degradation is RNase E. FinO increased the steady-state concentration of FinP (Figure 3.2), but had no effect on the *finP* promoter when fused to *lacZ* (Table 3.2), in corroboration with earlier studies (Mullineaux & Willetts, 1985; Frost *et al.*, 1989; Lee *et al.*, 1992). The results of this study (Table 3.2) and those of Mullineaux & Willetts (1985) suggest that FinP is transcribed constitutively from a weak promoter. Conversely, *traJ* mRNA is transcribed constitutively from a promoter that is 50 to 100 times stronger than the *finP* promoter (Mullineaux & Willetts, 1985; Sandercock, 1997; Sandercock & Frost, 1998). Under such conditions, the concentration of *traJ* mRNA would be expected to greatly exceed that of FinP and conjugation would be continuously derepressed. An important part of FinO function may be to protect FinP from degradation by RNase E, increasing its steady-

state concentration to a level that represses conjugation. Evidence supporting this proposal is presented in Chapter 4.

## **Chapter 4**

### ***In vitro* analysis of FinP cleavage by RNase E\***

\*A version of this chapter has been accepted for publication in the *Journal of Molecular Biology*. Jerome, L.J., van Biesen, T. & Frost, L.S.

## 4.1 Introduction

Transfer of F-like conjugative plasmids is regulated by the FinOP fertility inhibition system which controls the expression of *traJ*, a positive regulator of the transfer operon. FinP is a 79 base antisense RNA molecule, consisting of 2 stem-loop domains (Figure 4.1), complementary to the 5' untranslated region (UTR) of *traJ* mRNA. Binding of FinP to the *traJ* UTR is believed to sequester the *traJ* ribosome binding site, preventing its translation and repressing plasmid transfer. FinP works in concert with a second essential factor, the FinO protein, to exert its negative effect on *traJ*. van Biesen & Frost (1994) showed that a GST-FinO fusion protein, which represses conjugation *in vivo*, binds to stem-loop II of FinP and *traJ* mRNA *in vitro* and increases the rate of duplex formation 5-fold (van Biesen & Frost, 1994). FinP/*traJ* mRNA duplex formation independent of FinO has been demonstrated *in vivo* (Chapter 3) and occurs at a rate similar to other sense/antisense pairs *in vitro* (van Biesen & Frost, 1994), suggesting that this is not the primary function of FinO.

FinP is expressed from a weak promoter (Mullineaux & Willetts, 1985; Chapter 3) and has a moderate half-life of approximately 14 minutes (Chapter 3). *In vivo*, FinO has been shown to extend the chemical half-life of FinP RNA to greater than 240 minutes (Chapter 3), increasing its effective concentration (Dempsey, 1987; Frost *et al.*, 1989; Lee *et al.*, 1992) by a mechanism that does not involve alteration of *finP* promoter activity (Mullineaux & Willetts, 1985; Chapter 3). Koraimann *et al.* (1996) and Dempsey (1994b) have shown that R1 and R100 FinP expressed from multicopy plasmids efficiently repress conjugation (~2000-fold) without the assistance of FinO. This indicates that FinP activity is highly dosage-dependent and that the principal role of FinO

**Figure 4.1** Secondary structure of FinP antisense RNA (van Biesen *et al.*, 1993). Stem-loops I and II are labelled. The vector-derived bases added to the 3' end of FinP by *in vitro* transcription are shown in brackets. The regions complementary to the *traJ* mRNA RBS (anti-RBS) and start codon (anti-AUG) are indicated. Large arrows labelled I1 and I2 represent RNase E cleavages (*in vitro*) within the vector sequence and the spacer region of FinP, respectively. Small arrows (at ~10 bases and I3) within stem I indicate minor RNase E cleavage sites.



may be to raise the steady-state concentration of FinP to a level that blocks translation of all *traJ* mRNAs.

The results obtained in the previous chapter (Chapter 3) suggest that the primary enzyme involved in FinP decay is RNase E. The present *in vitro* study was performed to determine whether FinO stabilizes FinP by protecting it from RNase E. Using purified RNase E and synthetic FinP, the sites of RNase E cleavage are mapped on FinP and the effect of GST-FinO on FinP binding and cleavage by RNase E is examined.

## 4.2 Results

### 4.2.1 FinP RNA is cleaved *in vitro* by RNase E

The sites of RNase E cleavage were mapped on *in vitro* synthesized FinP RNA. Transcription of *Bam*HI-linearized pLJ5-13 template DNA using T7 RNA polymerase resulted in an 86 base product (termed FinP-G<sub>4</sub>AUC), composed of FinP (79 bases) with a 7 base 3' tail (Figure 4.1) derived from the *Bam*HI site. A time course experiment of FinP-G<sub>4</sub>AUC cleavage using purified RNase E (generously provided by Dr. George Mackie, UBC), is shown in Figure 4.2. The amount of RNase E necessary for cleavage of >90% of the full-length transcript in 30 min was experimentally determined (data not shown) using the method of Mackie (1991). Based on these pilot experiments, ~0.6 pmol of annealed 5' end-labelled FinP-G<sub>4</sub>AUC was incubated with 5.1 pmol of RNase E extract at 30°C. Aliquots were withdrawn at the times indicated, denatured by boiling the samples for 3 min in formamide load dye, and then electrophoresed on a 12% denaturing (8M urea) polyacrylamide gel. Radioactive bands were sized by comparison with the

**Figure 4.2** RNase E cleavage of *in vitro* synthesized 5' end-labelled FinP-G<sub>4</sub>AUC. At timed intervals after the addition of RNase E (1, 2.5, 5, 10, 30, 60 and 90 min), samples were withdrawn and electrophoresed on a 8 M urea 12% polyacrylamide gel. 5'-labelled products were sized by comparison with the 81, 59 and 39 base RNA markers (lane M) and with 10 (L2) and 20 (L1) second hydrolysis ladders, obtained from 5' end-labelled FinP-G<sub>4</sub>AUC. The locations of intermediates I1, I2 and I3 are indicated on the left.





synthetic RNA markers (39, 59 and 81 bases), in conjunction with a hydrolysis ladder obtained from 5' end-labelled FinP-G<sub>4</sub>AUC.

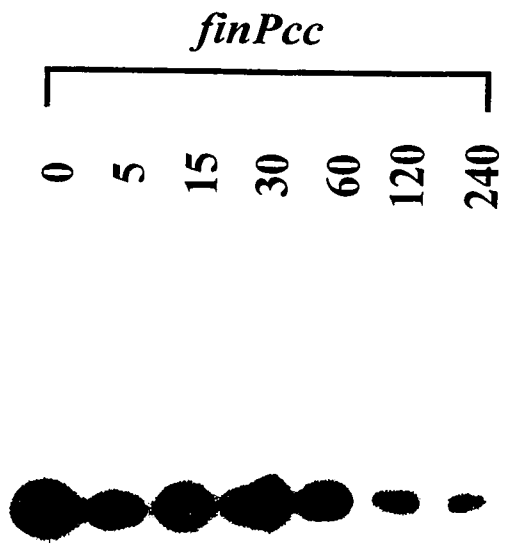
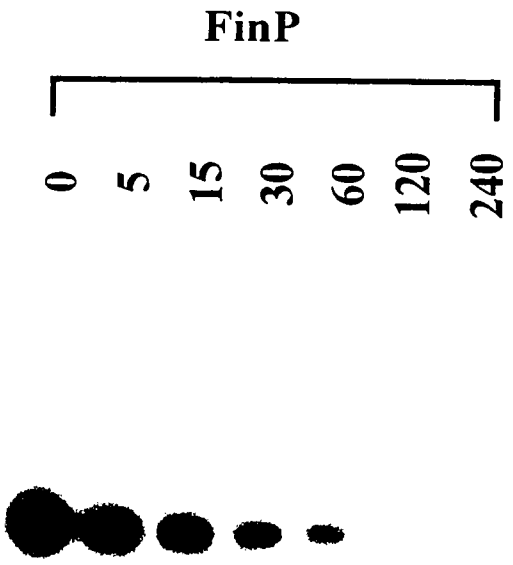
Cleavage of the full-length (86 base) transcript yielded two prominent intermediates, I1 and I2 of approximately 81 and 36 bases, respectively. I1 resulted from cleavage within the 7 base extension at the 3' end of FinP-G<sub>4</sub>AUC. The faint series of bands between I1 and I2 suggested that over time, I1 was trimmed to successively shorter products and that an undefined 3' exonuclease activity was present. Since the buffer used in this assay contained no phosphate, this activity could not be attributed to PNPase which copurifies to some extent with RNase E (Carpousis *et al.*, 1994; Py *et al.*, 1994). Instead, its origin could be RNase II or RNase E itself, which was recently implicated in shortening RNA 3' tails containing poly(A) or poly(U) (Huang *et al.*, 1998). The major cleavage product of FinP itself, I2 (36 bases), resulted from RNase E digestion within the single-stranded spacer region between stem-loops I and II (Figure 4.1). A very minor cleavage product, I3 (~29 bases) was observed, which could result either from rare RNase E cleavage events at this position within stem-loop I or from degradation of I2. Interestingly, I3 accumulates in the FinP mutant, *finP305*, harboring a C:U transition at position 30 within stem-loop I (Chapter 5). A series of short 5'-labelled products (<10 bases), which were successively shortened over time, were suggestive of RNase E cleavage approximately 10 bases from the 5' end of FinP, followed by exonucleolytic trimming. RNase E cleavage at the 5' end of FinP occurred at the same time as or immediately following cleavage at I2, since a very small amount of I2 was detectable at 1 min, whereas the 5' products first appeared at 2.5 min. Results with FinP RNA generated from a PCR product lacking the 7 base, 3' extension were identical except that RNase E

activity at the 3' end of the transcript was not observed (data not shown). Thus the major site of cleavage by RNase E in FinP is within the single-stranded spacer between stems I and II with subsequent cleavage within the first 10 bases of the FinP RNA.

#### **4.2.2 Mutation of the single-stranded spacer stabilizes FinP *in vivo***

Several attempts were made to map the sites of RNase E cleavage more precisely by primer extension analysis of both synthetic FinP-G<sub>4</sub>AUC and cellular RNA. As mentioned in Chapter 3, probes targeted at the 3' end of FinP hybridized very poorly, indicating that stem-loop II was resistant to denaturation. All procedures (changing reverse transcription conditions and positioning of primers) failed to yield any products other than very small amounts of full-length RNA. Positions where RNase E intermediates were expected, were masked by a ladder of reverse transcriptase stall/dissociation sites (data not shown). To demonstrate that the major site of RNase E cleavage determined *in vitro* was relevant to FinP decay *in vivo*, the sequence of the FinP spacer was mutated from GACA to GCCC by site-directed mutagenesis, which did not alter the secondary structure as predicted by computer algorithms. The decay patterns of wild-type FinP and the mutant, *finPcc* RNA, were then compared by Northern analysis (Figure 4.3). At 37°C, the half-life was increased from 14 min for FinP to 48 min for *finPcc* RNA. This confirmed that the spacer region was the site of cleavage by RNase E and that the sequence of the spacer was important for FinP decay *in vivo*.

**Figure 4.3** Mutation of the spacer from GACA to GCCC stabilizes FinP, as determined by Northern analysis of wild-type FinP and *finPcc* RNA. Samples were withdrawn at the indicated times (min) after the addition of rifampicin at 37°C, as described in Materials and Methods (section 2.6) and RNA was detected with Primer A (Figure 3.1).



### 4.2.3 GST-FinO protects FinP from RNase E cleavage *in vitro*

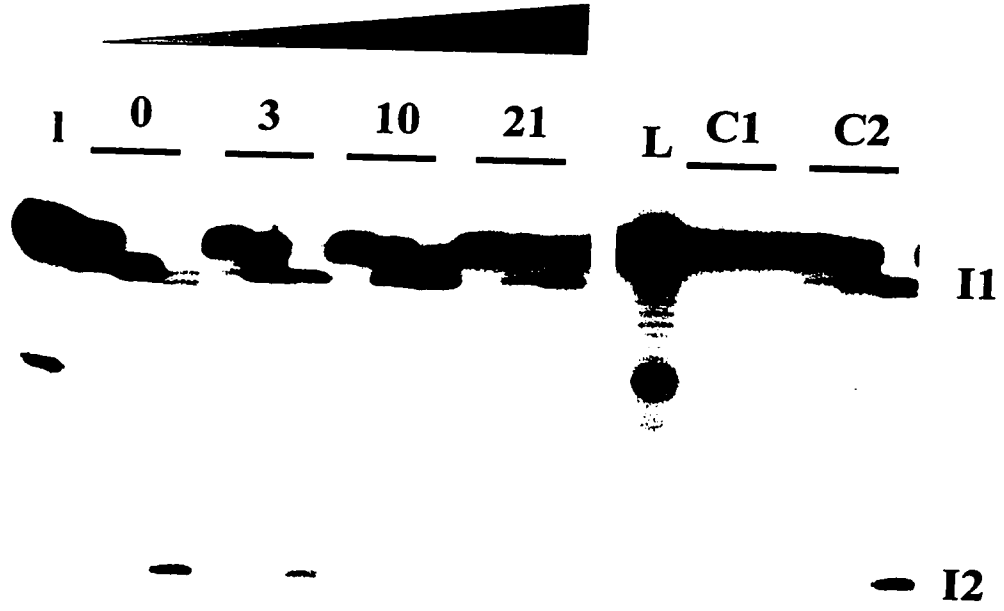
Since RNase E appeared to have a role in FinP decay both *in vivo* (Chapter 3) and *in vitro* and since FinO is known to stabilize FinP *in vivo*, it was reasoned that FinO might protect FinP from degradation by RNase E. To test this hypothesis, the ability of a given amount of RNase E to cleave FinP in the presence and absence of the GST-FinO fusion protein or GST was determined *in vitro*. GST and GST-FinO (from R6-5) were purified using glutathione agarose affinity (van Biesen & Frost, 1994; Sandercock, 1997; Sandercock & Frost, 1998). RNase E (1.3 pmol) and GST-FinO (3-21 pmol) or GST (21 pmol) were premixed, added to 0.4 pmol of annealed 5'-labelled FinP-G<sub>4</sub>AUC and incubated at 30°C. Aliquots were withdrawn 1, 5 and 30 minutes later and electrophoresed on a denaturing 12% polyacrylamide gel. The autoradiogram shown in Figure 4.4a was under-exposed to sharpen the bands for full-length FinP-G<sub>4</sub>AUC and I1. Thus, I3, the series of minor bands between I1 and I2, and the short oligomers (<10 bases) seen in Figure 4.2 are not visible here.

As seen in Figure 4.4a, the presence of increasing amounts of GST-FinO led to a reduction of I1 and I2 produced by RNase E. The production of smaller cleavage products (~10 bases) was also reduced. RNA incubated with 21 pmol of GST-FinO without RNase E did not yield any cleavage products (lanes C1) and the presence of 21 pmol of GST did not inhibit RNase E cleavage (lanes C2). These controls indicate that the protection conferred by GST-FinO is specific. The percent inhibition of RNase E activity by GST-FinO was determined from the level of I2 produced at each GST-FinO concentration (3, 10, 21 pmol) as compared to the level of I2 produced in the absence of GST-FinO (Figure 4.4b). The presence of 3 pmol of GST-FinO (a 2.3:1 molar ratio of

**Figure 4.4a** GST-FinO protects FinP from RNase E cleavage *in vitro*. Approximately 0.4 pmol of 5'-labelled FinP-G<sub>4</sub>AUC was incubated with 0, 3, 10 or 21 pmol of GST-FinO in the presence of 1.3 pmol RNase E extract and aliquots were withdrawn 1, 5 and 30 min later. Samples were electrophoresed on a 12% polyacrylamide gel containing 8 M urea. C1, RNA incubated with 21 pmol GST-FinO in the absence of RNase E. C2, RNA incubated with 21 pmol GST in the presence of 1.3 pmol RNase E. 1, L indicate 10 and 20 second alkaline hydrolysis ladders, respectively. RNase E intermediates I1 and I2 are indicated on the right.

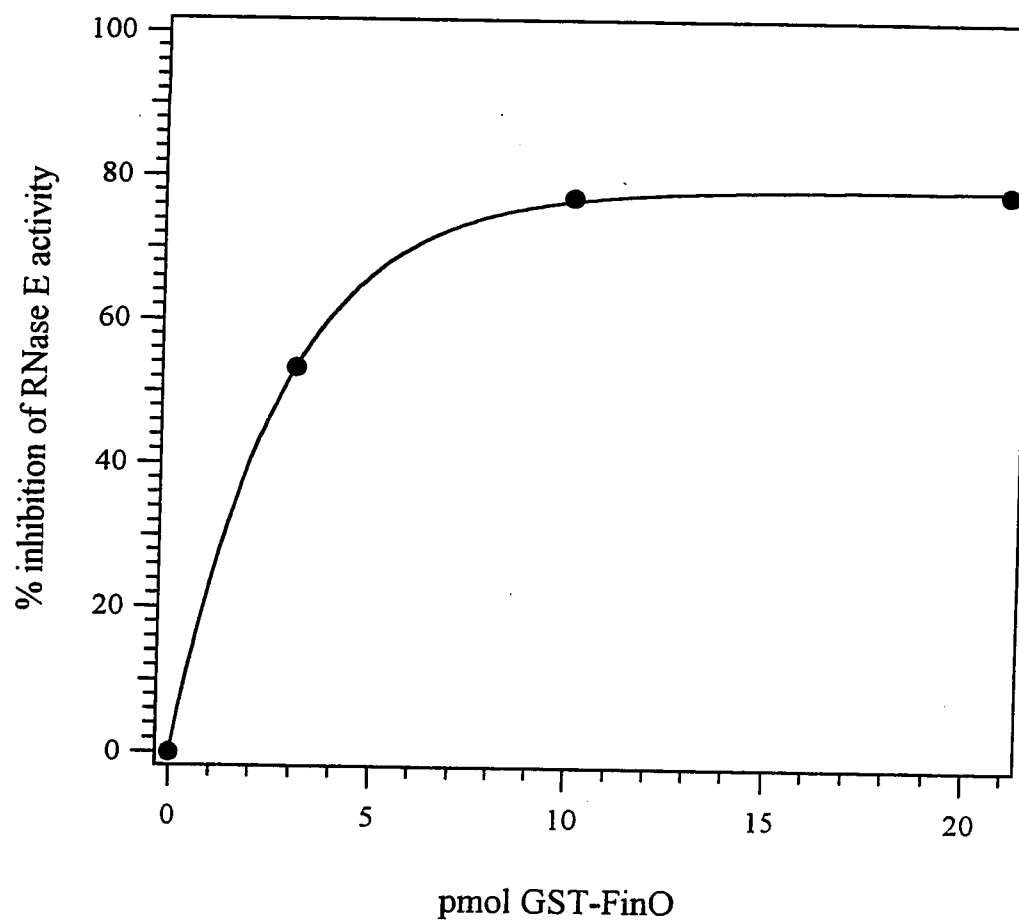
**a**

pmol GST-FinO





**Figure 4.4b** The percent I2 present at 30 minutes relative to the full-length substrate at time zero was calculated for each concentration of GST-FinO from (a). The percent inhibition of RNase E activity was calculated as  $(\% \text{ I2 produced at each GST-FinO concentration}) / (\% \text{ I2 produced in the absence of GST-FinO})$  and is shown graphically.

**b**

GST-FinO:RNase E) reduced the amount of I2 produced by more than 50%. Maximum inhibition (~80%) of RNase E cleavage was achieved with 10 pmol of GST-FinO (a ratio of 3:1).

#### 4.2.4 GST-FinO and RNase E compete for binding to FinP *in vitro*

van Biesen and Frost (1994) have shown previously that the GST-FinO protein binds to FinP with moderate specificity *in vitro*. Thus FinO may prevent RNase E cleavage of FinP by steric interference. RNA mobility shift analysis was performed to determine whether GST-FinO could bind to FinP in the assay buffer used for RNase E cleavage in the previous section. Seven and a half femtomoles of uniformly-labelled FinP RNA was incubated for 30 min at room temperature with increasing amounts of GST-FinO (0.11-5.3 pmol) in either the buffer used by van Biesen & Frost (Buffer A; 50 mM Tris-HCl pH 8.0, 1 mM EDTA, 10 mM NaCl, 100 µg/ml BSA, 10% glycerol) or the buffer used for the RNase E assay (Buffer B; 25 mM Tris-HCl pH 7.8, 0.1 mM EDTA, 60 mM KCl, 5 mM MgCl<sub>2</sub>, 100 mM NH<sub>4</sub>Cl, 0.1 mM DTT, 100 µg/ml BSA, 10% glycerol). Seven point six units of RNAGuard was added to each reaction mixture to minimize RNA degradation. Samples were loaded onto a continuously running, nondenaturing 8% polyacrylamide gel and electrophoresed in 1X TBE. The equilibrium association constant ( $K_a$ ) of GST-FinO binding to FinP in each buffer was determined from the protein concentration that caused 50% of the labelled RNA to shift in the gel (see Materials & Methods).

GST-FinO bound to FinP in both buffers tested (Figure 4.5), although its binding constant ( $K_a$ ) was reduced 2-fold ( $1.0 \times 10^7 \text{ M}^{-1}$ ) in the RNase E assay buffer. This means that 50% of the RNA in the reaction was bound by  $1.0 \times 10^{-7} \text{ M}$  GST-FinO. The amount of GST-FinO necessary to inhibit RNase E cleavage within the FinP spacer by 50% (determined from Figure 4.4b) was 2.7 pmol (in 30  $\mu\text{l}$  total volume) or  $0.9 \times 10^{-7} \text{ M}$ . These results are in perfect agreement (ie. an equivalent amount of GST-FinO blocks RNase E binding and RNase E cleavage by 50%) and suggest that GST-FinO binding directly blocks access of RNase E to FinP. To further test this hypothesis, the ability of RNase E to bind FinP under similar conditions was examined *in vitro*. To minimize RNase E cleavage of FinP, binding was carried out in Buffer A in the presence of 7.6 units of RNAGuard. Figure 4.6 shows saturation of FinP by 2.1 pmol of RNase E at 1 or 5 min. The 30 min assays displayed “smearing” of the RNA which may indicate release of full-length or degraded FinP by RNase E. Subsequent assays were performed for 10 min to reduce this effect. The RNase E/FinP complex migrated very slowly as compared to the GST-FinO/FinP complex (Figure 4.5), although both gels were run under equivalent conditions and likely reflects the large difference in the size of the two proteins (GST-FinO = 47.2 kDa and RNase E = 118 kDa).

Next, the ability of RNase E to bind FinP in the presence of a fixed amount of GST-FinO was examined. A saturating amount of GST-FinO (10 pmol) was mixed with increasing amounts of RNase E and then limiting FinP (7.5 fmol) was added. In the absence of RNase E (Figure 4.7, lane 1) FinP was shifted to a discrete position by GST-FinO. GST-FinO binding predominated until the molar ratio of GST-FinO:RNase E was

**Figure 4.5** RNA mobility shift analysis of GST-FinO binding to FinP. Seven and a half femtomoles of uniformly-labelled FinP was mixed with increasing amounts (lanes 1-5 and 6-10 = 0, 0.11, 1.1, 2.1, 5.3 pmol) of GST-FinO in assay Buffer A (50 mM Tris-HCl pH 8.0, 1 mM EDTA, 10 mM NaCl, 100 µg/ml BSA, 10% glycerol; van Biesen & Frost, 1994) or Buffer B (25 mM Tris-HCl pH 7.8, 0.1 mM EDTA, 60 mM KCl, 5 mM MgCl<sub>2</sub>, 100 mM NH<sub>4</sub>Cl, 0.1 mM DTT, 100 µg/ml BSA, 10% glycerol; used in the RNase E cleavage assay) in a total volume of 30 µl. Samples were loaded onto a continuously running, nondenaturing 8% polyacrylamide gel and electrophoresed in 1X TBE. The equilibrium association constant ( $K_a$ ) of GST-FinO binding to FinP in each buffer was determined from the protein concentration that caused 50% of the labelled RNA to shift in the gel (see Materials & Methods). The locations of free FinP and the GST-FinO/FinP complex are indicated.

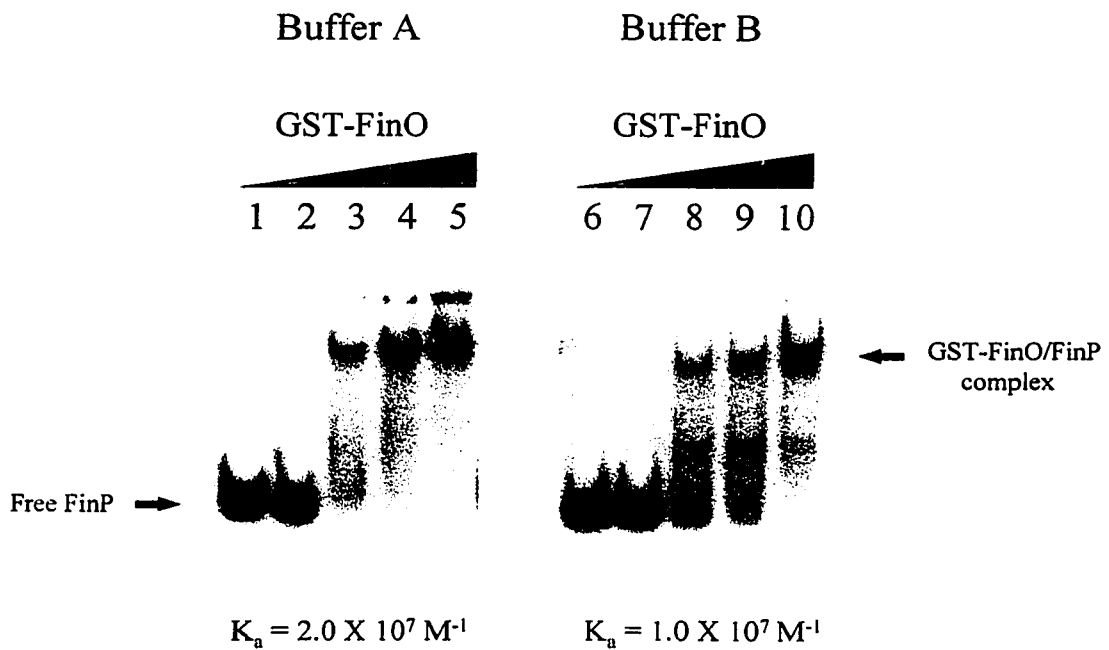


**Figure 4.6** RNA mobility shift analysis of RNase E binding to FinP. Seven and a half femtomoles of uniformly-labelled FinP was mixed with 2.1 or 5.3 pmol RNase E in Buffer A (total volume = 30  $\mu$ l) and incubated at room temperature for the indicated times (min). Samples were loaded onto a continuously running, nondenaturing 8% polyacrylamide gel and electrophoresed in 1X TBE. The locations of free FinP and the RNase E/FinP complex are indicated.

time (min)	30	30	30	5	1	5	1	5
pmol RNase E	0	2.1	5.3	0	2.1	2.1	5.3	5.3



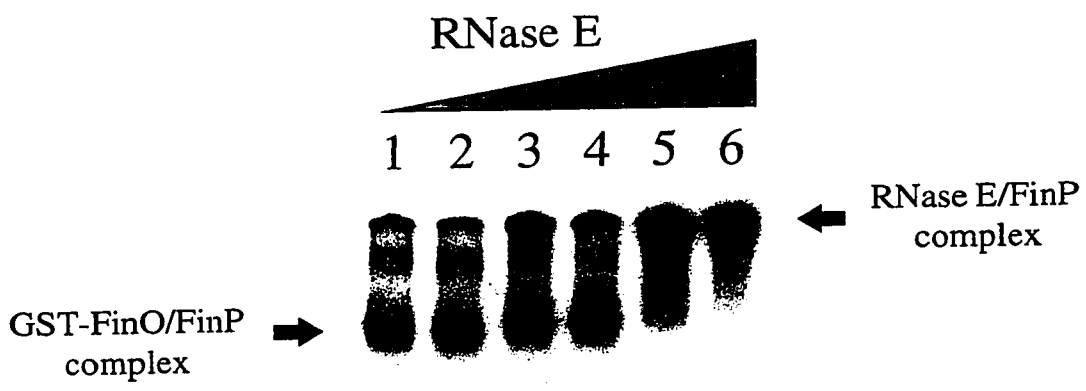
RNase E/FinP  
complex

free FinP





**Figure 4.7** RNase E and GST-FinO compete for binding to FinP. Uniformly-labelled FinP (7.5 fmol) was incubated with 10 pmol GST-FinO in the presence of increasing amounts of RNase E (0, 0.1, 1.1, 2.1, 5.3 and 10.6 pmol; lanes 1-6) in a total volume of 30  $\mu$ l for 10 min at room temperature. Samples were loaded onto a continuously running, nondenaturing 8% polyacrylamide gel and electrophoresed in 1X TBE. The locations of GST-FinO/FinP and RNase E/FinP complexes are marked with arrows.



2:1 (lane 5). At this point, the labelled RNA was shifted into the well, indicating that FinP was either bound by RNase E alone, or by GST-FinO and RNase E. At least twice the amount of RNase E was required for FinP saturation by RNase E in the presence of GST-FinO, as compared to its absence (Figure 4.6). This suggests that GST-FinO functions as a specific inhibitor of RNase E binding *in vitro*. In the previous section, a similar ratio of GST-FinO:RNase E (3:1) was found to inhibit RNase E cleavage activity by 80%. Since the amounts of active GST-FinO and RNase E in the extracts was not determined, these ratios are only useful for the purpose of comparing the inhibitory effects of GST-FinO on RNase E activity and RNase E binding. Furthermore, it is not known if GST-FinO binds to FinP as a monomer or as a multimer, although gel exclusion chromatography suggests that the fusion protein exists as a monomer in solution (van Biesen & Frost, 1994). While these results are preliminary, they do provide evidence that, at least *in vitro*, RNase E and GST-FinO compete for binding to FinP and this determines whether FinP is degraded or protected, respectively.

### 4.3 Discussion

The FinO protein enhances the chemical and functional stability of FinP antisense RNA. Preliminary evidence by Lee *et al.* (1992) suggested that this was due to the inhibition of degradation of FinP by the host endonuclease, RNase E. In Chapter 3, inactivation of the *rne* gene encoding RNase E was shown to have a stabilizing effect on FinP antisense RNA decay, whereas mutations in the genes encoding the major 3' exonucleases, RNase II and PNPase, had no effect. Further evidence that RNase E is the enzyme responsible for the degradation of FinP was obtained in the present study. *In*

*in vitro*, two major sites of RNase E cleavage were mapped on synthetic FinP-G<sub>4</sub>AUC. The first, producing intermediate I1, was an artifact due to transcription of vector-derived sequences downstream of the natural *finP* termination site. The second and relevant site (I2), is within the single-stranded spacer (in the sequence context **GACA**) between stem-loops I and II of FinP (Figure 4.1). Ehretsmann *et al.* (1992a) have proposed a single-stranded RNase E consensus recognition sequence of **RAUUW** (R = G or A; W = U or A) at the cleavage site. However more recent studies suggest that there is no simple relationship between the order of nucleotides and the phosphodiester bond cleaved (Lin-Chao *et al.*, 1994; McDowall *et al.*, 1994). Mackie (1992) suggests that RNase E prefers to cleave single-stranded RNA 5' to AU dinucleotides in an A/U-rich context. The major RNase E cleavage site in FinP does occur in a single-stranded region, matches 2 of the consensus bases (shown above in bold), but is 3' to an A/U-rich region.

Minor cleavage events within the stem I domain of FinP followed cleavage in the spacer *in vitro*, which could be due to RNase E or exonuclease activity. Kaberdin *et al.* (1996) have shown that regions of secondary and tertiary structure are destabilized by complex formation between the RNase E RNA binding domain and RNA I. Similarly, SLI may become destabilized following RNase E cleavage within the spacer, making this region more accessible to RNase E. Alternatively, RNase E may cleave FinP in stem-loop I in its native structured conformation, as seen for antisense RNA I of pAYCY184 (McDowall *et al.*, 1994) and pBR322 (Kaberdin *et al.*, 1996) and within 16S rRNA (Bessarab *et al.*, 1998). Since the structure of RNA is dynamic, it is unlikely that all RNA molecules in a given sample will assume a single conformation (Uhlenbeck, 1995).

Therefore a third possibility is that FinP exists as a mixture of conformations, with stem-loop I occasionally being single-stranded and exposing bases to RNase E.

Because the FinP molecule is relatively short and because of the inherent stability of stem-loop II, the positions of RNase E cleavage could not be mapped *in vivo* or *in vitro* using conventional methods. Nonetheless, two lines of evidence suggest that the major RNase E cleavage site mapped *in vitro*, within the single-stranded spacer, is relevant to FinP decay *in vivo*. First, mutation of the spacer sequence from GACA to GCCC increased the chemical half-life of FinP *in vivo*, indicating that the sequence of this region is important for FinP degradation, almost certainly by RNase E. Other degradative endonucleases, such as RNase I\* and RNase M, have been characterized, but should not be affected by these changes in the spacer sequence. RNase I\* generally degrades short oligomers in a sequence-independent manner (Cannistraro & Kennell, 1991) and RNase M cleaves pyrimidine-adenosine bonds (Cannistraro *et al.*, 1986). Second, the GST-FinO fusion protein protected FinP from RNase E cleavage at this site *in vitro*. Since FinO also prevents FinP decay *in vivo* (Chapter 3; Lee *et al.*, 1992), the most likely explanation for these results is that in the absence of FinO, the spacer sequence targets FinP for degradation by RNase E. Whether or not the minor RNase E cleavages observed within SLI of FinP *in vitro* have any relevance to FinP degradation *in vivo* cannot be resolved from the present study.

van Biesen & Frost (1994) have shown that GST-FinO binds to SLII of FinP *in vitro* and data presented in Chapter 6 indicate that the spacer and 3' tail enhance GST-FinO binding to SLII. Thus specific binding of FinO to SLII might sterically block RNase E cleavage of FinP within the spacer. The *in vitro* results obtained in this

communication reveal that GST-FinO inhibits both the binding and degradation of FinP by RNase E *in vitro*. GST-FinO reduced RNase E cleavage not only within the FinP spacer, but also within the 3' extended tail. GST-FinO was required in approximately 2-fold molar excess of RNase E to both inhibit RNase E binding and reduce (>80%) cleavage of FinP. These observations suggest that FinO does indeed inhibit RNase E cleavage by virtue of its binding to FinP. It remains possible that RNase E and FinO bind to FinP simultaneously and that FinO inhibits RNase E by blocking its access to the site of cleavage, without interfering with its binding.

## Chapter 5

### Characterization of the *finP305* mutation in FinP antisense RNA

\*A version of this chapter has been accepted for publication in the *Journal of Molecular Biology*. Jerome, L.J., van Biesen, T. & Frost, L.S.

## 5.1 Introduction

Antisense RNAs are generally short (usually <100 bases), constitutively transcribed molecules that exhibit a high degree of secondary structure and act as post-transcriptional repressors of gene expression (Wagner & Simons, 1994). In each system, the antisense RNA must accommodate changes in fluctuating target levels by adjusting its own concentration. Antisense RNA I which inhibits ColE1 primer formation, is transcribed from a strong promoter (Lin-Chao & Bremer, 1987), but exhibits a very short half-life (~2 min; Tomcsanyi & Apirion, 1985; Lin-Chao & Cohen, 1991). Such high level expression with rapid turnover enables RNA I to respond readily to decreases in ColE1 plasmid copy number, which might otherwise result in loss of the plasmid from the host during cell division. In contrast, antisense RNA-OUT which limits *IS10* transposition, is an exceptionally stable RNA (half-life ~60 min; Case *et al.*, 1989) that is expressed from a modest promoter (Simons *et al.*, 1983). Appropriately, the concentration of RNA-OUT changes slowly in concert with the gradual increase in *IS10* transposition.

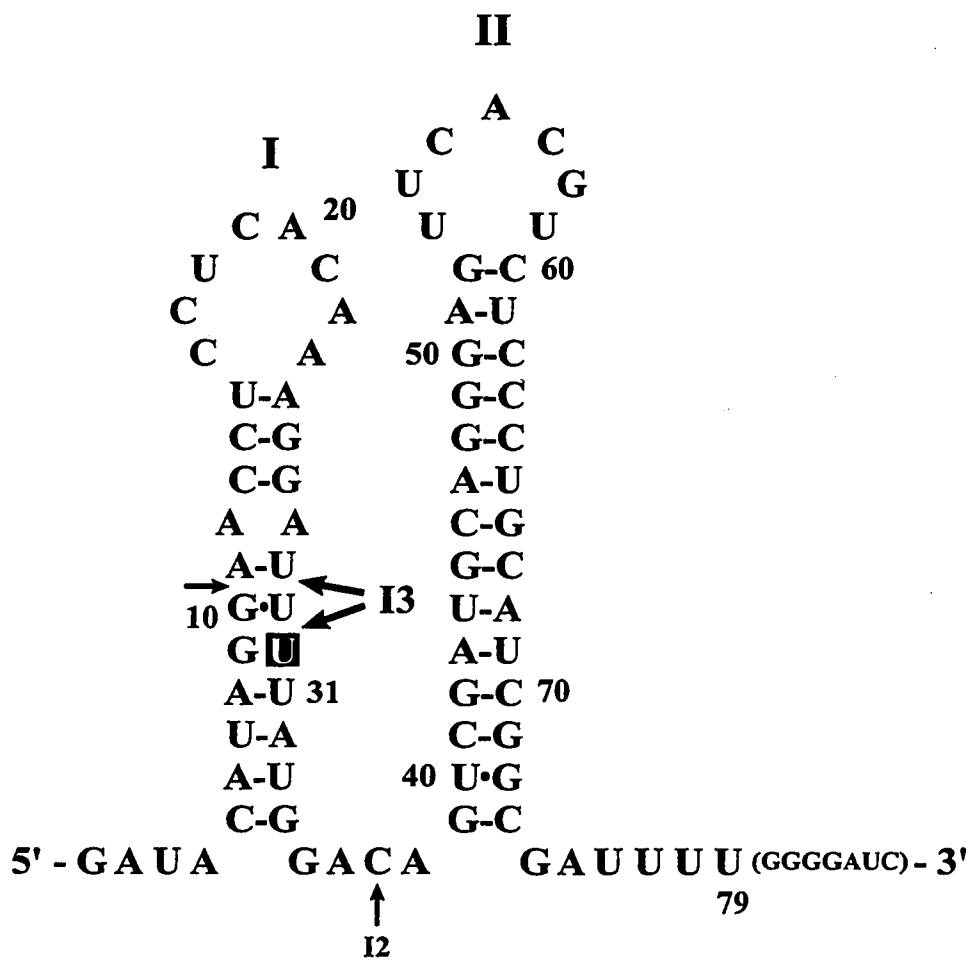
FinP antisense RNA, which represses transfer of F-like plasmids, is expressed from a weak promoter (Mullineaux & Willetts, 1985; Chapter 3) and is moderately stable (half-life ~14 min; Chapter 3). Unlike RNA I and RNA-OUT, FinP is absolutely dependent on a protein cofactor, FinO, to extend its chemical and functional half-life, thereby increasing its effective concentration and inhibitory effect (Frost *et al.*, 1989; Lee *et al.*, 1992). Previous studies have shown that mutations in either *finP* or *finO* lead to derepression of the transfer operon and maximal levels of transfer. Finnegan & Willetts (1971, 1973) described two classes of *finP* mutations, only one of which was fully



complementable *in trans*. The second class of mutants, which were poorly complemented, were thought to affect the *FinP* site of action with *FinO* and were thus designated *fisO*. For reasons of clarity (see below), these have been renamed as *finP* mutants. The *finP305* (formerly *fisO305*) mutation, which maps within stem-loop I of *FinP* (Figure 5.1) involves a C to U transition at position 30 (Frost *et al.*, 1989). Early attempts to characterize the defect associated with this mutation showed that steady-state levels of *finP305* antisense RNA do not increase in response to the presence of *FinO*, as compared to wild-type *FinP* (Frost *et al.*, 1989). From this result, the authors postulated that the mutation altered the *FinO* binding site, disengaging *FinO* from its role in preventing *FinP* cleavage. However, later studies (van Biesen, 1994) revealed that the *finP305* mutation does not affect the site of *FinO* action, since *FinO* binds to *finP305* RNA with the same relative affinity as the wild-type *FinP* RNA.

van Biesen *et al.* (1993) previously demonstrated that the *FinOP* complex causes a 50-fold reduction in the intracellular concentration of *traJ* mRNA *in vivo*. This is thought to be due to a decrease in *traJ* mRNA stability as a result of duplex formation with *FinP* and subsequent degradation by RNase III (Dempsey, 1994a; Chapter 3). Although *finP305* RNA is not impaired in its ability to duplex with *traJ* mRNA *in vitro*, its expression has a reduced effect on the steady-state level of *traJ* mRNA, as compared to wild-type *FinP* (van Biesen, 1994). The low level of *finP305* RNA observed in the presence of *FinO* could therefore indicate that the mutation affects the ability of bound *FinO* to protect *finP305* RNA from degradation, which would lead to an increase in the levels of *traJ* mRNA and conjugation (Lee *et al.*, 1992).

**Figure 5.1** The *finP305* mutation of FinP antisense RNA. The secondary structure of FinP is shown (van Biesen *et al.*, 1993) with the U substitution (C30:U) in stem I. The vector-derived sequence at the 3' end of *finP305* RNA synthesized *in vitro* is shown in brackets. The large arrows (I3) represent strong RNase E cleavages (*in vitro*) in SLI of *finP305* RNA. Small arrows indicate minor cleavage sites (I2 and at ~10 bases).



In this chapter, the effect of the *finP305* mutation on *finP305* RNA decay, in the presence and absence of FinO, is examined *in vivo* and *in vitro*.

## 5.2 Results

### 5.2.1 *finP305* RNA has a shorter half-life than FinP and accumulates in an RNase E-deficient strain

Previous studies demonstrated that in the presence of FinO, EDFL68 (the F plasmid with the *finP305* mutation) transfers constitutively (Frost *et al.*, 1989). The failure of *finP305* RNA to repress conjugation was thought to be due to lowered antisense RNA levels *in vivo*. Supplying *finP305* RNA *in trans* from a high copy-number plasmid does not alter the level of conjugation, indicating that increased expression of mutant *finP305* RNA does not affect the constitutive transfer phenotype (Frost *et al.*, 1989). Lee *et al.* (1992) suggested that the *finP305* mutation affects the stability of a FinP-like RNA expressed from the *tac* promoter and that FinO is unable to prevent its degradation. To test this hypothesis, authentic *finP305* RNA was expressed from its own promoter from the moderate copy-number plasmid (pLT185; Table 2.2) and its decay was examined by Northern analysis (as described in previous chapters) in the presence and absence of FinO (Figure 5.2). RNA was detected with Primer A (Figure 3.1) and bands were quantified by phosphorimager analysis. A graph of *finP305* RNA decay is shown in Figure 5.3.

In the absence of FinO, *finP305* RNA had a chemical half-life of 1.25 min at 44°C in the wild-type strain (MG1693). This is an 11-fold reduction in stability as compared to wild-type FinP, which has been shown to have a half-life of 14 min (section 3.2.1). The shorter half-life of *finP305* RNA might be due to increased susceptibility to RNase E,

**Figure 5.2** Northern analysis of *finP305* decay from a wild-type strain in the absence of FinO (RNase E<sup>+</sup> FinO<sup>-</sup>) and in the presence of FinO (RNase E<sup>+</sup> FinO<sup>+</sup>), and from a strain carrying a temperature-sensitive mutation in the gene encoding RNase E (RNase E<sup>-</sup> FinO<sup>-</sup>). Total cellular RNA samples were withdrawn at the times indicated (min) after the addition of rifampicin at 44°C, as described in Materials and Methods (section 2.6). Blots were hybridized with Primer A (Figure 3.1), which is complementary to nucleotides 2 to 16 of FinP.

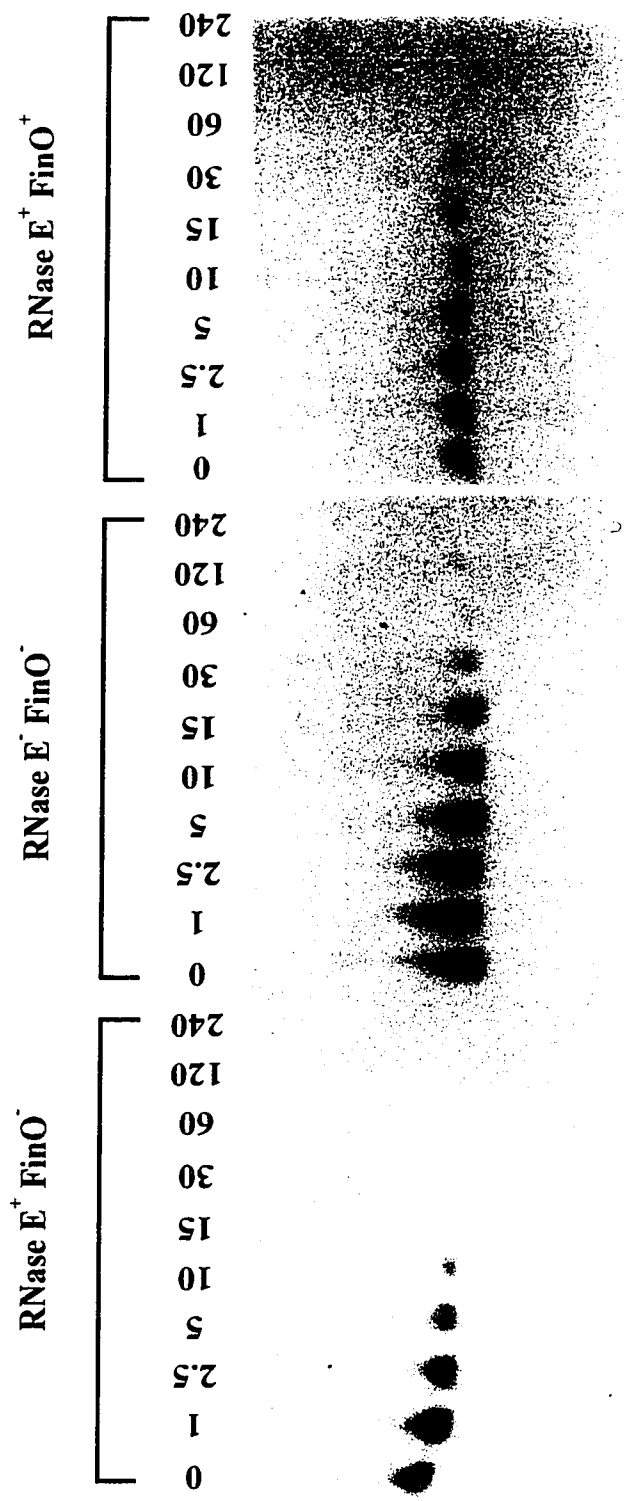
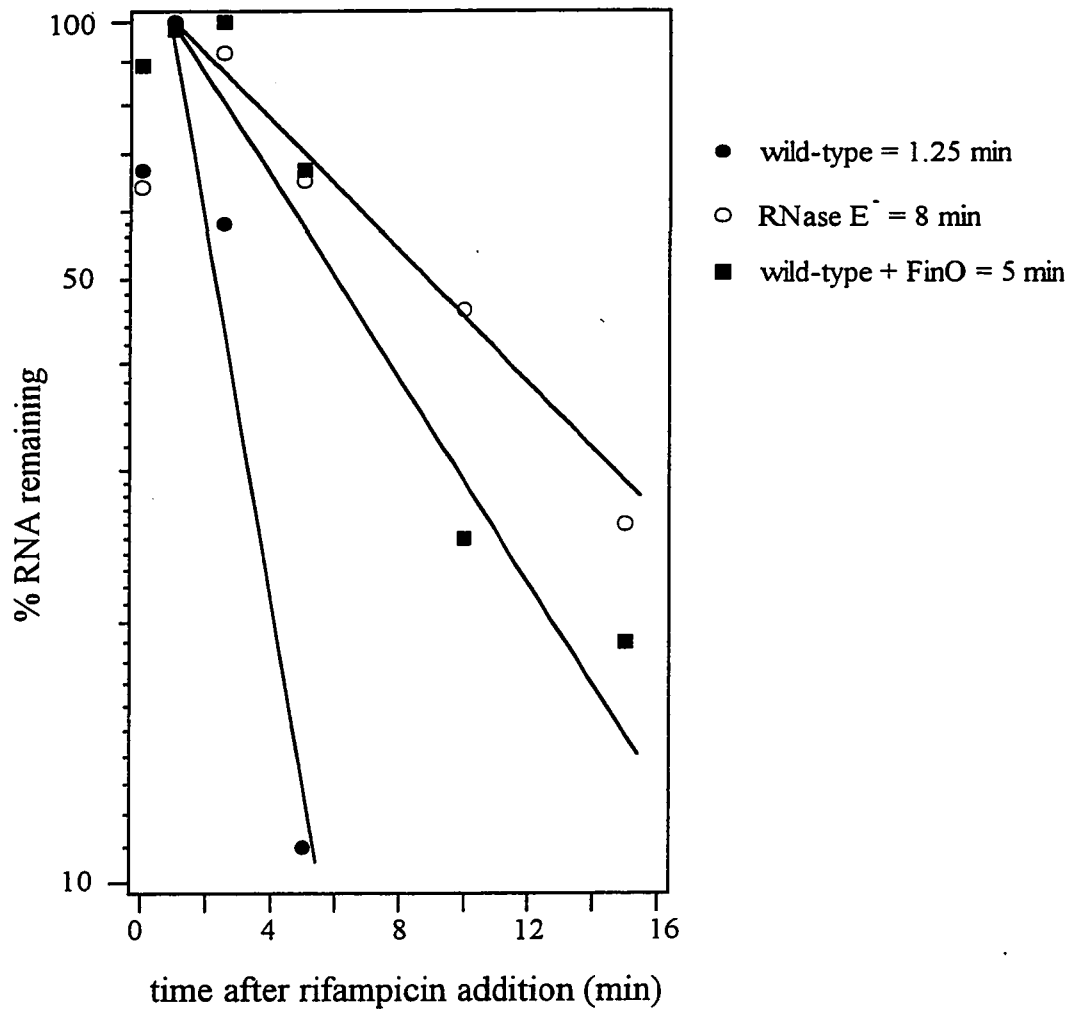


**Figure 5.3** Graphic representation of *finP305* RNA decay as a function of time. The relative amount of *finP305* RNA at each time point was expressed as a percentage of the highest value obtained for each independent strain. Thus, 100% indicates the maximum *finP305* RNA present, which differs for each strain. Only the first 15 min of the time courses are plotted, as most of the *finP305* RNA had decayed by this time. The half-life of *finP305* in each strain represents the average of two experiments.





since the *finP305* mutation (C30:U) makes this region of the RNA more AU-rich, a feature which is reportedly important for RNase E cleavage (Lin-Chao *et al.*, 1994; McDowall *et al.*, 1994; Mackie, 1992). To examine this possibility, *finP305* RNA decay was followed at the nonpermissive temperature (44°C), from a strain carrying a temperature-sensitive mutation in the gene encoding RNase E (SK5665; *rne-1*). Thermal inactivation of RNase E stabilized *finP305* RNA 6-fold, increasing its half-life to approximately 8 min (Figures 5.2 and 5.3). Expression of *finP305* RNA in the presence of FinO (pSnO104) in the wild-type strain resulted in an intermediate level of stabilization, increasing its half-life to 5 min. These results indicate that *finP305* RNA is less stable than FinP, perhaps as a result of increased susceptibility to RNase E and reduced FinO protection at the site of the mutation.

### 5.2.2 *In vitro* cleavage of *finP305* RNA by RNase E

The effect of the *finP305* mutation on the specificity of RNase E degradation was examined by mapping the sites of RNase E cleavage on *in vitro*-synthesized *finP305* RNA. pLJ305 DNA, linearized with *Bam*HI, was used as the template for T7 RNA polymerase-mediated transcription of an 86 base product (termed *finP305*-G<sub>4</sub>AUC), composed of *finP305* RNA (79 bases) with a 7 base 3' tail derived from the *Bam*HI site. A time course experiment of *finP305*-G<sub>4</sub>AUC cleavage using a purified extract of RNase E (generously provided by Dr. George Mackie, UBC), is shown in Figure 5.4. For comparison, intermediates obtained from a 30 min incubation of *finP305*-G<sub>4</sub>AUC and wild-type FinP-G<sub>4</sub>AUC with the RNase E extract is also shown. The amount of RNase E necessary for cleavage of >90% of the full-length transcript in 30 min was experimentally

**Figure 5.4** RNase E cleavage of *in vitro* synthesized *finP305-G<sub>4</sub>AUC* RNA. 5'-end-labelled *finP305-G<sub>4</sub>AUC* (1.8 pmol) was incubated with RNase E (1.6 pmol) at 30°C. Samples were withdrawn at the indicated times and electrophoresed on an 8 M urea 12% polyacrylamide gel. Lane L is an RNA ladder obtained by alkaline hydrolysis (20 sec) of 5'-labelled *finP305-G<sub>4</sub>AUC* (see Materials and Methods). As a negative control, labelled *finP305-G<sub>4</sub>AUC* was incubated without RNase E for 0, 30 and 90 min. The right panel shows a comparison of the products obtained from a 30 min incubation of *finP305-G<sub>4</sub>AUC* and *FinP-G<sub>4</sub>AUC* with the RNase E extract. The locations of RNase E intermediates I2 and I3 are indicated.



determined (data not shown). A 1:1 molar ratio of RNase E:*finP305*-G<sub>4</sub>AUC resulted in complete degradation of the full-length transcript in 30 min, whereas cleavage of FinP-G<sub>4</sub>AUC required an 8-fold molar excess of RNase E, suggesting that the *finP305*-G<sub>4</sub>AUC RNA was a better substrate.

The *finP305* mutation caused a much more complex cleavage pattern than seen with FinP (Figure 4.2 and Figure 5.4, lane FinP). In wild-type FinP-G<sub>4</sub>AUC the major degradation products were I2 (36 bases) and a series of small products under 10 bases in length. A small amount of I3 (28/29 bases) was also obtained. With *finP305* RNA, there was no detectable intermediate resembling I1 (~81 bases product from RNase E cleavage within the 3' vector sequence of FinP-G<sub>4</sub>AUC seen in Figure 4.2). There was a very small amount of I2, which resulted from RNase E cleavage within the spacer between stem-loops I and II. In contrast, I3 was a major cleavage product for *finP305*-G<sub>4</sub>AUC which accumulated with time and could represent an alternate site for RNase E cleavage. At 1 minute, a series of faint bands at positions 23-36 bases were observed which appear to represent alternate cleavage sites within stem-loop I as well as decay products caused by exonucleolytic trimming at the 3' end. With time, these bands were converted to a pool of small oligomers under 10 bases in length. Cleavage at ~9/10 bases was also observed at 2.5 min which was qualitatively comparable to wild-type FinP-G<sub>4</sub>AUC, but more intense (Figure 4.2). This intermediate also underwent exonucleolytic trimming by an undefined nuclease present in the extract. As mentioned in section 4.2.1, since the assay buffer did not contain phosphate, the exonuclease activity could not be due to PNPase, but could instead be due to either contaminating RNase II or RNase E itself, which has been shown to degrade RNA 3' tails (Huang *et al.*, 1998). These

results suggest that the *finP305* mutation facilitates RNase E cleavage within stem-loop I, especially at bases 28/29, which may contribute to the shorter half-life of *finP305* RNA *in vivo*.

### 5.2.3 GST-FinO does not protect *finP305* RNA from RNase E cleavage

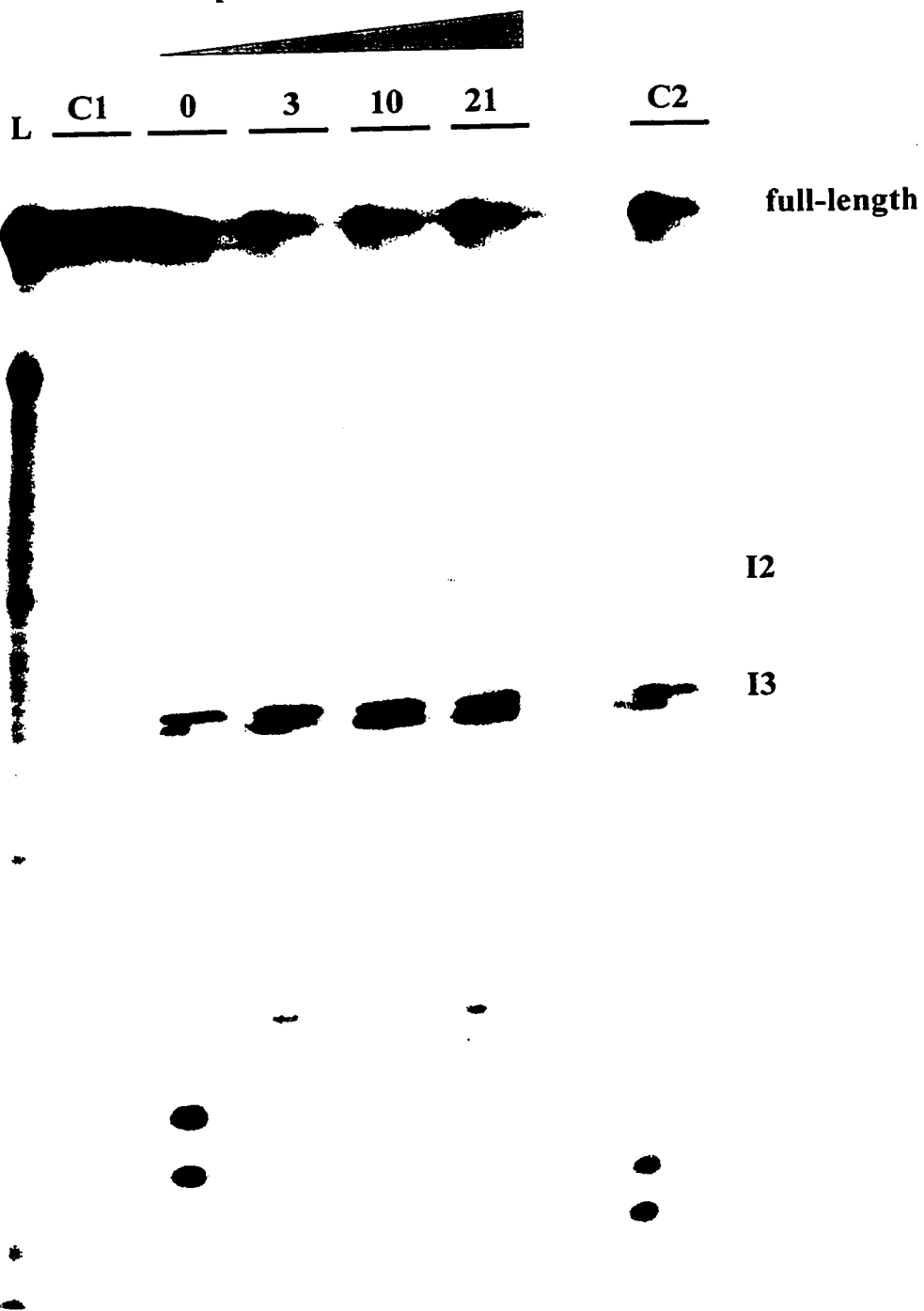
In Chapter 4, the GST-FinO fusion protein was shown to retard RNase E cleavage in the spacer of FinP synthesized *in vitro*. In order to determine whether GST-FinO could protect *finP305* RNA from RNase E, increasing amounts of GST-FinO (0, 3, 10 and 21 pmol) were premixed with 1.3 pmol of RNase E extract and then incubated with 5'-labelled *finP305*-G<sub>4</sub>AUC RNA (~0.5 pmol). Aliquots from each incubation were withdrawn 1, 5 and 30 minutes later, denatured and electrophoresed on a 12% denaturing polyacrylamide gel (Figure 5.5a). This autoradiogram was under-exposed to show the bands at 28 and 29 bases (I3) more clearly. Thus, the series of minor bands between 23 and 36 bases seen in Figure 5.4 are not visible here. A bar graph showing the relative amounts of full-length *finP305*-G<sub>4</sub>AUC, I3 and oligomers produced at 30 min is shown in Figure 5.5b.

A very small amount of I2 was present at all GST-FinO concentrations at 1 min which appeared to be converted to ~16 bases at 5 min and disappeared by 30 min. This could represent the fraction of *finP305*-G<sub>4</sub>AUC RNA not bound by GST-FinO, allowing RNase E cleavage within the spacer. The amount of I3 at 28/29 bases increased with time suggesting that GST-FinO did not prevent RNase E-mediated cleavage of *finP305*-G<sub>4</sub>AUC at this site, but did block further degradation of these intermediates. Interestingly, 29 base cleavage products accumulated more rapidly than those 28 bases in

**Figure 5.5a** RNase E cleavage of *in vitro* synthesized, 5' end-labelled *finP305-G<sub>4</sub>AUC* in the presence of GST-FinO. One point three picomoles of RNase E extract was premixed with the indicated amounts (pmol) of GST-FinO. This mixture was added to *finP305-G<sub>4</sub>AUC* (0.5 pmol) and samples were taken 1, 5 and 30 minutes later. C1, RNA incubated with 21 pmol GST-FinO in the absence of RNase E. C2, RNA incubated with 21 pmol GST in the presence of 1.3 pmol RNase E. The locations of RNase E intermediates I2 and I3 are indicated.

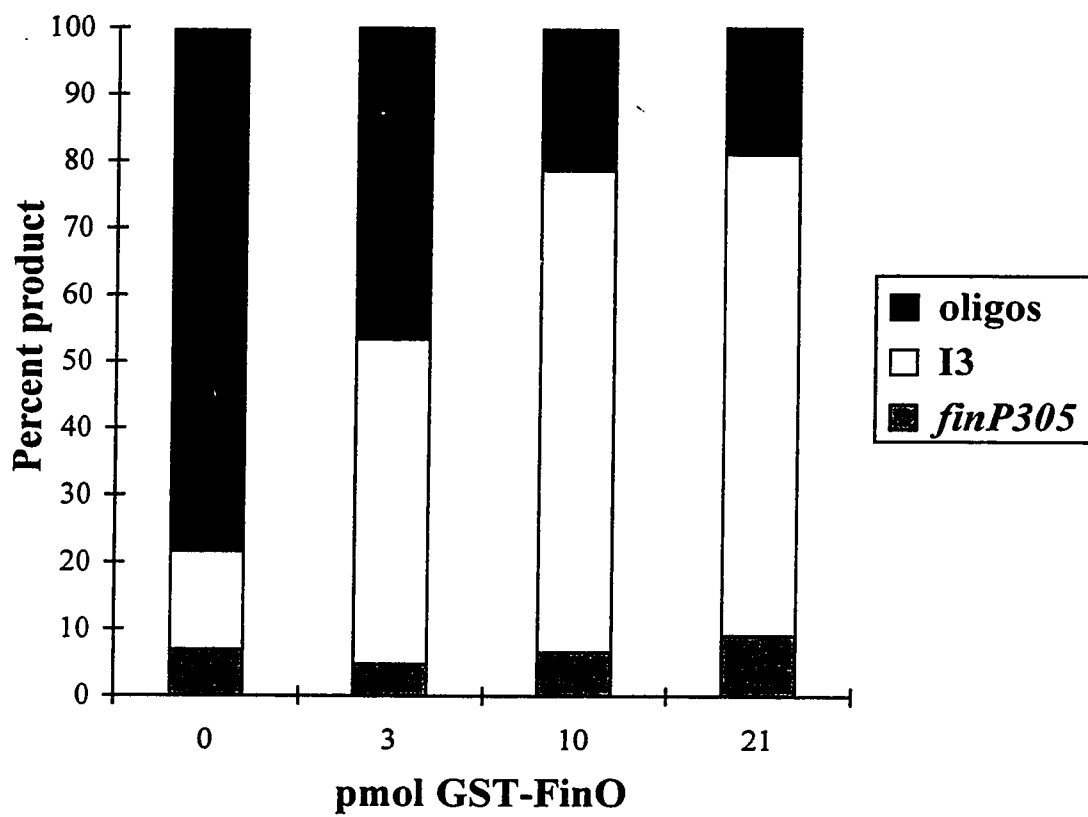
**a**

pmol GST-FinO



**Figure 5.5b** Graphic representation of the percent full-length *finP305-G<sub>4</sub>AUC*, I3 (28 plus 29 nt bands) and oligomers (from Figure 5.5a) present after a 30 min incubation with RNase E (1.3 pmol) and the indicated amounts of GST-FinO. Increasing amounts of GST-FinO led to an increase in I3, with a concomitant decrease in oligomers (see text for details).



**b**

length. Since the production of oligomers less than 10 bases was significantly reduced in the presence of GST-FinO, GST-FinO appeared to interfere with cleavage at a secondary site near bases 9/10 as well as exonucleolytic trimming of the smaller intermediates. This could result from steric interference of exonuclease activity by GST-FinO bound to the RNA. The presence of 21 pmol of GST had no effect on either RNase E or exonuclease activity (lanes C2, Figure 5.5a).

### 5.3 Discussion

The *finP305* mutation was identified 25 years ago and was thought to be a key to understanding the mechanism of FinOP action during repression of F transfer. Results presented here suggest that this mutation leads to a dramatic decrease in the RNA half-life, which is due, at least in part, to increased RNase E cleavage within stem-loop I of FinP and is outside of the region protected by FinO. This mutation reveals the portion of FinP that is exposed to RNases in a FinO/FinP complex and the critical dependence of FinP RNA levels on the FinO protein.

The *finP305* mutation imparted an RNA I-like half-life on FinP. *In vivo*, the chemical half-life of *finP305* RNA increased 6.5-fold, from 1.25 to 8 min upon inactivation of RNase E, but the half-life exhibited by wild-type FinP (104 min) under the same conditions was never achieved (section 3.2.1). This suggests that in the absence of RNase E, an alternate decay pathway might ensue which degrades *finP305* RNA more efficiently than FinP. *In vitro*, RNase E appeared to cleave *finP305*-G<sub>4</sub>AUC predominantly within stem-loop I (I3) and at ~9/10 bases, and to a lesser extent at 36 bases (I2), a site which predominates in wild-type FinP-G<sub>4</sub>AUC. It is conceivable that

RNase E cleavage of *finP305-G<sub>4</sub>AUC* at I3 followed an initial cut at I2, which would lead to reduced I2 accumulation. The experimental design, which only followed the decay of products containing the 5' label, does not allow for discrimination between these possibilities. A series of minor cleavage events within stem-loop I, whose products were degraded into smaller oligomers by 60 min, suggested that a certain portion of *finP305-G<sub>4</sub>AUC* molecules are in a conformation that allows extensive cleavage at several positions within stem-loop I. Whether these alternate conformations are important *in vivo* is unknown although the increased cleavage potential would be in agreement with the observation that *finP305* RNA has a shorter half-life within the cell. The very weak cleavage by RNase E within stem-loop I of wild-type FinP (I3) occurs within the sequence context UUCUA, as compared to UUUUA for strong cleavage of *finP305* RNA. These results are in agreement with the proposal by Mackie (1992) and McDowall *et al.* (1994), that RNase E prefers to cut within an AU-rich region and suggest that the *finP305* mutation optimizes RNase E recognition at this site. Whether or not cleavage occurs within the 3' vector-derived sequence of *finP305-G<sub>4</sub>AUC* as occurs for wild-type FinP-G<sub>4</sub>AUC is not apparent. It is possible that *finP305-G<sub>4</sub>AUC* is cut by RNase E at this position, but that the product is rapidly removed by the multitude of cleavages that occur within stem I and escapes detection. Evidence for this proposal awaits further study.

Mutational analysis of *IS10* antisense RNA revealed that base changes which decrease the predicted thermodynamic stability of the RNA-OUT stem, increase its susceptibility to exonucleases, reducing antisense inhibition of *IS10* transposition (Pepe *et al.*, 1994). Other single-base mutations that increased RNase III cleavage of RNA-

OUT also reduced inhibition, emphasizing the importance of the RNA secondary structure and stability to antisense RNA function. The single base change of C30:U is predicted to decrease the free energy of FinP stem-loop I from -6.7 kcal/mol to -4.7 kcal/mol (Zuker, 1989). This decrease in free energy could potentially destabilize stem-loop I, accounting for the increased RNase E cleavage within this region. However, mutations in neighbouring bases that equally decrease the free energy of stem-loop I (G9:A; Frost *et al.*, 1989), do not affect FinP function. Mutations that restore the free energy of stem-loop I of *finP305* RNA to nearly wild-type levels (U29:C) also have no effect on the half-life or function of *finP305* RNA. This suggests that it is not the structure, but the sequence of stem-loop I, particularly at position 30, that is important for cleavage by RNase E. RNase E cleavage events within structured regions have also been reported for antisense RNA I of pAYCY184 (McDowall *et al.*, 1994) and pBR322 (Kaberdin *et al.*, 1996), antisense RNA CopA of plasmid R1 (Söderbom & Wagner, 1998) and within 16S rRNA (Bessarab *et al.*, 1998), suggesting that the cleavage potential of RNase E may be less specific than previously believed.

The inactivation of RNase E has been shown to fully stabilize FinP RNA *in vivo*, while a GST-FinO fusion protein prevents RNase E cleavage within the single-stranded spacer of FinP *in vitro* (section 4.2.3). It is proposed that FinO protects FinP from degradation by sterically blocking access to RNase E within the spacer, through its binding to stem-loop II. Even though GST-FinO binds to *finP305* RNA with the same affinity as wild-type FinP (van Biesen, 1994), it does not prevent RNase E cleavage of *finP305* RNA on the 3' side of stem-loop I *in vitro*. Therefore cleavage of *finP305* RNA within stem-loop I is in a region not protected by FinO, accounting for its instability *in*

*vivo*. Interestingly, GST-FinO did prevent the production of oligomers <10 bases, likely by way of steric interference through its RNA-binding activity. Although FinO did have a very minimal stabilizing effect on *finP305* RNA degradation *in vivo*, the steady-state antisense RNA concentration was markedly reduced as compared to wild-type FinP. These combined results support the notion that the observed stabilization of FinP by FinO is an important part of FinO function and that the concentration of FinP antisense RNA must reach a critical level for effective repression of F plasmid transfer to occur. In conclusion, the results of the present and previous studies (Frost *et al.*, 1989; Lee *et al.*, 1992; van Biesen, 1994) indicate that the *finP305* mutation affects FinP stability, rather than FinP function, a finding that was not possible to consider when the mutation was first described twenty-five years ago (Finnegan & Willetts, 1971, 1973).

## **Chapter 6**

### **Characterization of the RNA features recognized by the FinO protein *in vitro*\***

\*A version of this chapter has been provisionally accepted for publication to the *Journal of Biological Chemistry*. Jerome, L.J. & Frost, L.S.

## 6.1 Introduction

RNA-protein interactions are important in the post-transcriptional regulation of RNA metabolism and expression. Characterization of the RNA targets and features contacted and used by a protein to discriminate against other potential binding sites often provides valuable insights with respect to how the protein promotes RNA function (Draper, 1995). The geometry of the A-form RNA helix, with its deep, narrow major groove and wide, shallow minor groove, determines its accessibility and potential for recognition by RNA-binding proteins (Weeks & Crothers, 1993). The introduction of loops or distortions into the RNA helix by noncanonical base pairs presents a rich diversity of hydrogen bonding contacts to proteins that are not available in fully duplexed RNA or in standard B-form DNA (Draper, 1995). For example, the HIV-1 Rev protein makes specific contacts with bases in the major groove of its high affinity binding site (Stem IIB) on either side of a bubble caused by a bulged-out uridine (Kjems *et al.*, 1992). In other cases, intra- or intermolecular RNA interactions may create a unique three-dimensional structure that is recognized by the protein. This is best illustrated by the Rom dimer which recognizes a bent A-form helix that forms between the interacting loops of antisense RNA I and its target, RNA II (Eguchi & Tomizawa, 1990, 1991).

To define the protein structures recognizing RNA, RNA-binding proteins have been classified into families based on amino acid sequence motif homologies. However, many RNA-binding protein sequences do not fall into any motif category and a single motif (such as the ARM that is present in HIV-1 Rev and Tat proteins) can adopt different conformations and recognize dissimilar RNA structures (Mattaj, 1993). These

results emphasize the need for detailed structural information of more RNA-protein complexes.

The focus of this study is the specificity of the RNA-protein interaction between FinP antisense RNA and the FinO protein. The FinP secondary structure (van Biesen *et al.*, 1993) consists of 2 stem-loop domains, separated by a 4 base spacer and terminated by a 6 base tail (Figure 6.1). Eight alleles of FinP have been described for F-like conjugative plasmids (Figure 6.2a), with sequence identity residing in the stem, spacer and tail regions and variability in the two loops (Frost *et al.*, 1994; Finlay *et al.*, 1986). FinO is a 21.2 kDa basic protein (van Biesen & Frost, 1992) which has been shown to bind to FinP SLII and the *traJ* mRNA leader (which forms the mirror image of FinP; Figure 6.1) *in vitro*, increasing the rate of duplex formation (van Biesen *et al.*, 1993) and preventing RNase E-mediated degradation of FinP (Lee *et al.*, 1992; Chapter 4). Two alleles of FinO exist (Figure 6.2b; Frost *et al.*, 1994), which show very little sequence variation, but are classified on the basis of their levels of repression of F-like plasmids, which is tied to their own levels of expression (van Biesen & Frost, 1992). FinO is not plasmid-specific, which suggests that the FinP loops are unimportant for RNA-protein recognition. Although the FinO protein does not share homology with any of the protein sequence motifs found in other RNA-binding proteins (Mattaj, 1993; Burd & Dreyfuss, 1994; Draper, 1995), a recent study by Sandercock & Frost (1998) indicates that the basic, N-terminal domain (amino acids 1-73) is required for RNA binding activity.

A preliminary characterization of the RNA targets recognized by FinO is presented in this chapter. Using RNA mobility shift analysis, the binding affinity of the



**Figure 6.1** Secondary structures of FinP antisense RNA and the *traJ* mRNA 5' UTR (van Biesen *et al.*, 1993). Nucleotides 1-34 (shaded in black) and 35-79 (white and gray) constitute synthetic SLI and SLII of FinP, respectively. The complementary sequences in *traJ* mRNA are shaded according to FinP and the *traJ* RBS and start codon are indicated. *traJ* mRNA variants are named according to the number of nucleotides extending from their 5' ends.



**Figure 6.2a** Comparison of the FinP RNA sequences from the F-like conjugative plasmids (modified from Frost *et al.*, 1994). The 5' terminus of FinP has been mapped for F, R1 and R100, whereas the others are arbitrarily chosen. The inverted repeats forming stem-loops I and II are underlined. The alignments gave rise to gaps (marked by dashes). Identical bases are marked with an asterisk, positions with two possibilities are marked with a colon and three possibilities are marked with a period.

**Figure 6.2b** Comparison between FinO Type I (F and ColB2) and Type II (R6-5 and R100) alleles, illustrating the near sequence identity (modified from Frost *et al.*, 1994). The sequences are arranged in order of their similarity to F FinO and the notation is the same as above. Regions predicted to fold as  $\beta$  sheets are shown in grey and predicted  $\alpha$  helical domains are enclosed by black boxes (Sandercock & Frost, 1998). The RNA-binding domain at the N-terminus (amino acids 1-73; Sandercock & Frost, 1998) is indicated by the bar above the sequence.



GST-FinO fusion protein for a series of synthetic FinP and *traJ* mRNA variants is examined.

## 6.2 Results

### 6.2.1 Mutations in stem II have minor effects on GST-FinO binding

The binding constants of FinP variants were determined by performing gel-shift assays in which radiolabelled RNA was combined with increasing amounts of purified GST-FinO protein (from R6-5). All uniformly-labelled RNA was synthesized by *in vitro* run-off transcription using PCR-generated templates, except for stem II mutants which were transcribed from cloned fragments and contained 7 additional bases (GGGGAUC) at their 3' ends derived from the *Bam*HI site in the vector used to linearize the plasmids (see Materials & Methods). The equilibrium association constant ( $K_a$ ) for GST-FinO binding to each RNA variant was calculated from the protein concentration which caused 50% of the RNA to shift in the gel (see Materials and Methods). Except where noted,  $K_a$  values were calculated from 3 independent determinations. The percent binding relative to FinP was calculated as  $100 \times (K_{a\text{variant}}/K_{a\text{FinP}})$ .

A comparison of GST-FinO binding to FinP, SLI (nucleotides 1-34, Figure 6.1) and SLII (nucleotides 35-79), which were transcribed from PCR-generated templates (without the 3' extended tail), is shown in Figure 6.3. The  $K_a$  for GST-FinO binding to FinP was  $2.0 \times 10^7 \text{ M}^{-1}$ , 50-fold higher than that for SLI and ~2-fold higher than SLII (summarized in Table 6.1). These values are higher than previously reported (van Biesen

**Figure 6.3** Comparison of GST-FinO binding to FinP, SLI and SLII. Seven and a half femtomoles of uniformly-labelled RNA was incubated with increasing amounts of GST-FinO (0, 0.1, 0.5 (SLI only), 1.1, 2.1, 5.3, 10.6 and 31.9 pmol) in a total volume of 30  $\mu$ l for 30 min at room temperature. Samples were resolved on a nondenaturing 8% polyacrylamide gel. The equilibrium association constants ( $K_a$ ) were calculated as described in the text and Materials and Methods (section 2.12). <sup>b</sup> % binding relative to FinP [=100 $\times$ ( $K_a$ variant/ $K_a$ FinP)].

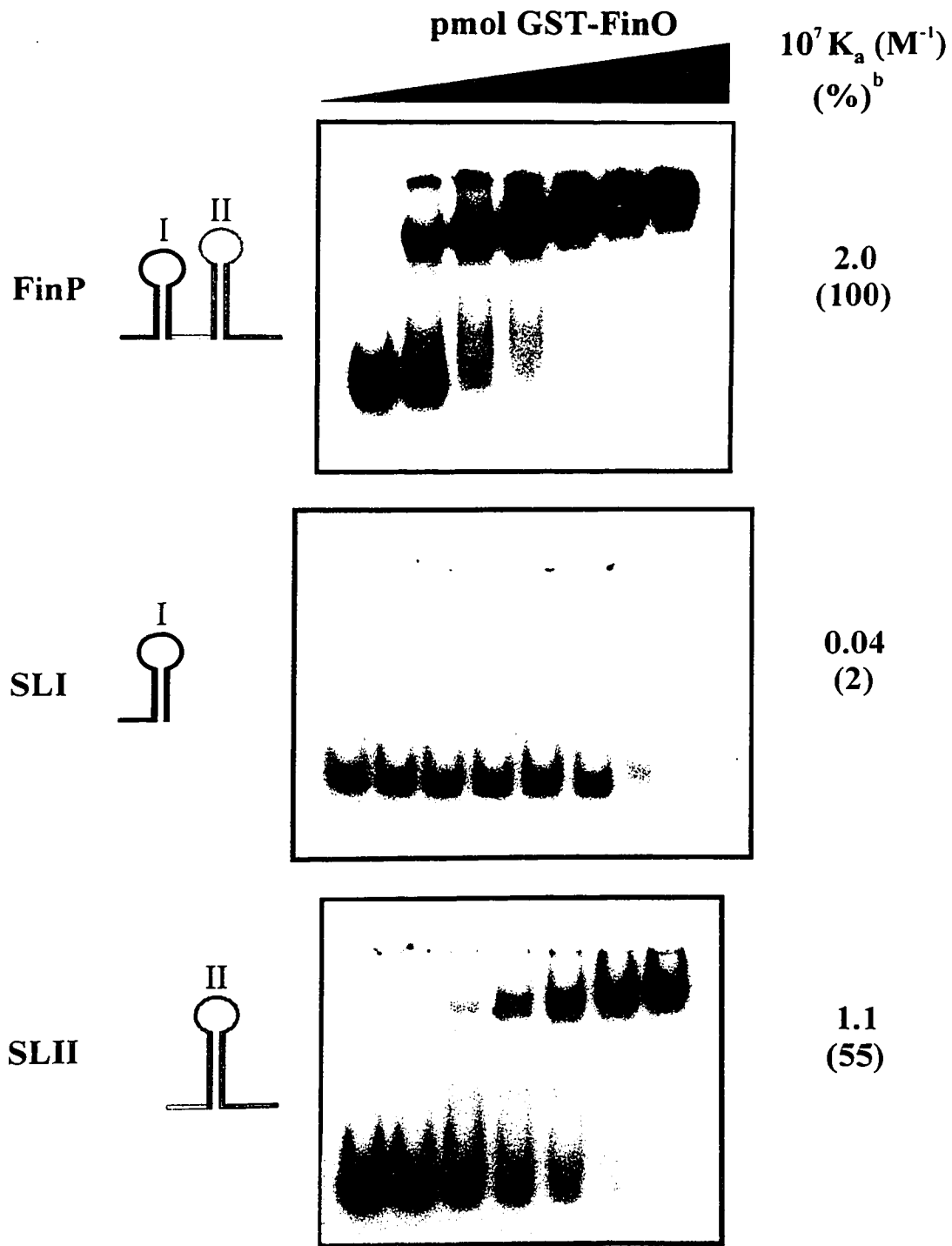


**Table 6.1** GST-FinO binding to FinP RNA variants. All stem II mutants contain the 3' extended tail unless otherwise noted. Measurement of GST-FinO binding was determined by gel-shift analysis using 7.5 fmol of uniformly-labelled RNA in the presence of increasing amounts of GST-FinO.

FinP variant <sup>a</sup>	$10^7 K_a$ (M <sup>-1</sup> ) <sup>b</sup>	Binding <sup>c</sup>
FinP	2.00 (2.00) <sup>d</sup>	100
SLII	1.10	55
SLI	0.04	2
SLI A12:U	0.04	2
<b>Stem II mutants</b>		
G42:A	1.39	70
G45:A	1.54	77
C46:U	1.57	79
A47:G	1.39	70
G48:A	1.14	57
G49:A	1.82	91
A51:G	1.13	57
C41:U/C46:U	1.36	68
G66:U/G71:U	1.30	65
C46:U/G66:U/G71:U	1.50	75
C41:U/C46:U/G66:U/G71:U	1.80 (1.70) <sup>d</sup>	90(85)
C70:A/G71:U/G72:U/C73:A	1.40	68
C62:A/C63:A/C64:A	1.70	85
<b>Other</b>		
ColB2	1.95	98
R100	2.34	117
RNA I (ColE1)	1.40	70

<sup>a</sup> variants are F unless otherwise stated

<sup>b</sup>  $K_a$  values are an average of two or more independent gel shifts

<sup>c</sup> % binding relative to F FinP [=100× ( $K_a$  variant/ $K_a$  F FinP)]

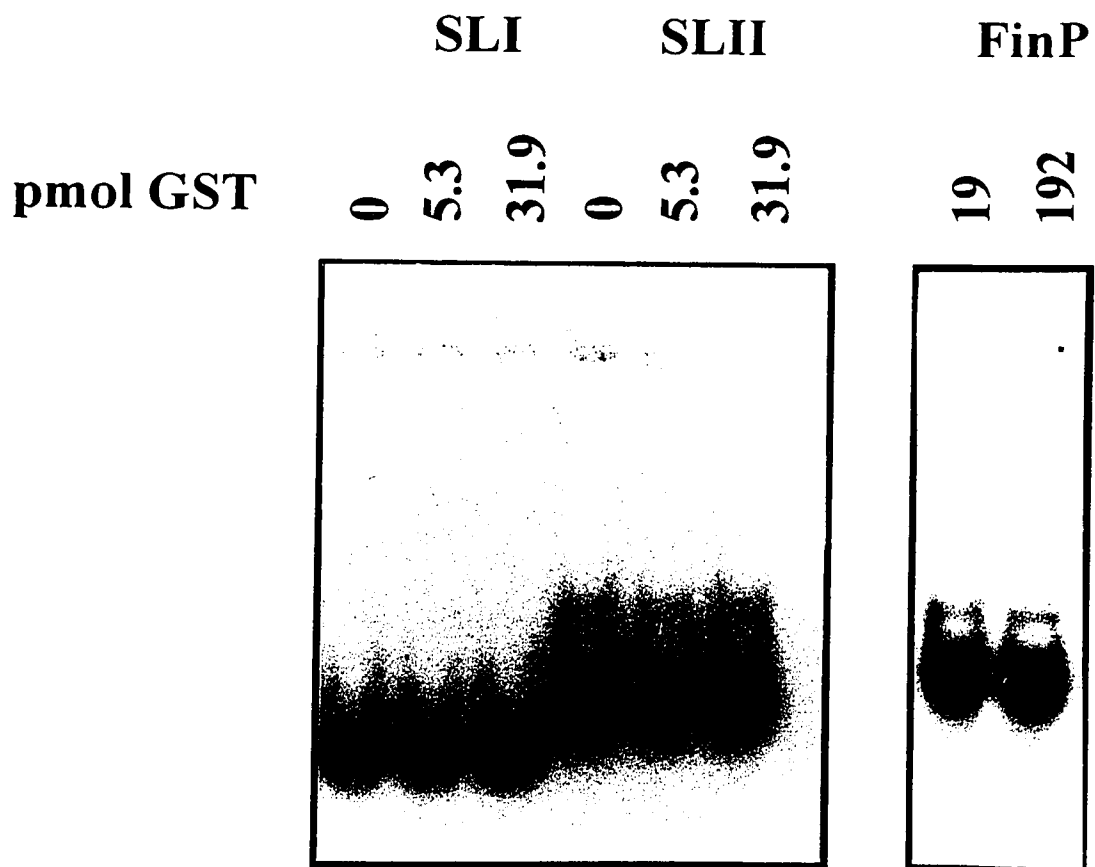
<sup>d</sup>  $K_a$  value of variant without 3' extended tail



& Frost, 1994) and likely reflect an increase in the fraction of active GST-FinO in the preparations using the French press method for cell lysis, rather than sonication. Since the fraction of GST-FinO that is active was not determined, these values may be underestimated. As a negative control, either FinP, SLI or SLII was incubated with GST alone (Figure 6.4). No shifted species were present in the gel, indicating that the complexes formed in the presence of the fusion protein were the result of RNA interaction with FinO.

In agreement with van Biesen & Frost (1994), these results suggest that the major determinants for FinO binding reside in SLII, which prompted us to look for differences between SLI and SLII. The most notable structural difference between SLI and SLII is an A-A mismatch within stem I (Figure 6.1). SLI A12:U, which creates an A-U base pair at this site, results in a fully duplexed SLI. Its ability to bind GST-FinO was tested and when compared to SLI with the natural A-A mismatch, was not improved (Table 6.1). Thus this 11 bp helix was not sufficient for recognition. A second obvious difference between stem-loops I and II is the sequence of the loops. To determine if the loops contributed to the specificity of GST-FinO binding, FinP RNAs from ColB2, R100-1 and ColE1 antisense RNA I were synthesized. ColB2 loop I is identical to F, but differs at 6 of the 7 bases comprising loop II (Figure 6.2). R100-1 differs from F at 1 base in loop I and 2 bases in loop II, which is also 1 base smaller than F loop II. The 3 loops of RNA I (Figure 1.8a) contain 7 bases each, but their sequences are considerably different from those of FinP. The  $K_a$  for GST-FinO binding to ColB2 was almost identical to F and was slightly increased for R100-1 (Table 6.1). Intriguingly, GST-FinO bound RNA I 70% as

**Figure 6.4** GST does not bind to FinP, SLI or SLII. Seven and a half femtomoles of uniformly-labelled RNA was incubated with the indicated amounts of the GST protein in a total volume of 30  $\mu$ l for 30 min at room temperature as described in Materials and Methods (section 2.12). Samples were resolved on a nondenaturing 8% polyacrylamide gel.



well as FinP, which suggests that not only are the sequences of the loops unimportant for FinO binding, but possibly also the stems (see below).

The sequences of FinP stems I and II, although highly conserved among the *finP* alleles (Figure 6.2), differ significantly from each other and could account for the preference by GST-FinO for SLII. The effect of mutations in stem II of full-length FinP on GST-FinO binding were examined and the binding data are summarized in Table 6.1. These mutants have 3' extensions due to transcription from linearized plasmid DNA. To ensure that the 7 bases from the vector did not alter the binding constants, FinP RNA and the quadruple mutant, FinP C41:U/C46:U/G66:U/G71:U, with or without the additional 3' bases, were synthesized and tested for GST-FinO binding. The presence of the 7 extra bases at the 3' end had no effect on GST-FinO binding (Table 6.1), therefore all other stem II mutants were synthesized with the extension, due to the ease of template preparation by this method. Single base mutations on the 5' side of stem II (G42:A, G45:A, C46:U) reduced the corresponding affinity constants by no more than 30% when compared to wild-type. In the 5' upper half of stem II, A47:G (naturally present in R100) and G49:A did not significantly reduce GST-FinO binding, whereas G48:A and A51:G, reduced binding by about 50%. Each of these mutations is expected to disrupt Watson-Crick base pairing, reducing the helical length of stem II. The C41:U/C46:U double mutant could lead to formation of two non-Watson-Crick G-U base pairs, maintaining the helicity of SLII and showed a 30% reduction in binding constant. To disrupt these potential interactions, FinP variants G66:U/G71:U, C46:U/G66:U/C71:U and C41:U/C46:U/G66:U/G71:U were created (Table 6.1). None of these mutations significantly altered GST-FinO binding, suggesting that a continuous duplex is not

important for efficient binding. In agreement with this, mutation of 4 consecutive base pairs at the base of stem II (C70:A/G71:U/G72:U/C73:A) and 3 base pairs in the 3' upper half of stem II (C62:A/C63:A/C64:A) had only minimal effects on GST-FinO binding.

The results obtained so far suggest that GST-FinO recognizes FinP in a sequence-independent manner and may be largely dependent on ionic contacts with the phosphate backbone. The effect of increasing ionic strength, which stabilizes RNA secondary structure (Draper, 1994; Pan *et al.*, 1993), but destabilizes electrostatic RNA-protein interactions (Witherell & Uhlenbeck, 1989; Bevilacqua & Cech, 1996), on GST-FinO binding to wild-type FinP was tested. Cations can interact electrostatically with the phosphate backbone of RNA, neutralizing electrostatic repulsions and thereby stabilizing double helical regions, optimizing the target structure recognized by the protein. However, for RNA-protein interactions that are dependent on ionic contacts, cations compete with positively charged protein side chains (eg. arginine and lysine) for phosphate binding sites on the RNA, reducing the binding constant (Record *et al.*, 1976). A limited range of mono- and divalent cation concentrations was tested to determine if either of these effects was important for GST-FinO/FinP binding and the results are shown in Table 6.2. The highest binding constant,  $2.5 \times 10^7 \text{ M}^{-1}$ , was achieved with 0.1 mM  $\text{MgCl}_2$ . This modest increase in binding affinity (25%) suggests that the FinP RNA secondary structure recognized by GST-FinO is not significantly enhanced by the presence of divalent cations. Conversely, the GST-FinO/FinP interaction was not significantly inhibited ( $\leq 2$ -fold) at the range of  $\text{MgCl}_2$  or  $\text{NaCl}$  concentrations tested. These preliminary results suggest that electrostatic contacts may not play a major role in the formation of the FinOP complex; however, a more thorough study, employing

**Table 6.2** Effect of ionic strength on GST-FinO binding to wild-type FinP. Buffer containing 10.0 mM NaCl was used for all prior and subsequent gel shift experiments.

Cation	Concentration (mM)	$10^7 K_a$ ( $M^{-1}$ ) <sup>a</sup>	Binding <sup>b</sup>
NaCl	10.0	2.0	100
NaCl	83.5	1.0	50
MgCl <sub>2</sub>	0.1	2.5	125
MgCl <sub>2</sub>	0.5	1.8	90
MgCl <sub>2</sub>	1.0	2.2	110
MgCl <sub>2</sub>	2.0	1.8	90
MgCl <sub>2</sub>	5.0	2.1	105
MgCl <sub>2</sub>	10.0	1.3	65

<sup>a</sup>  $K_a$  values are an average of two gel shifts

<sup>b</sup> % binding relative to 10 mM NaCl, which was arbitrarily set at 100%

different cations and a wider range of concentrations, is necessary to confirm this hypothesis. The results do indicate that the buffer used in previous experiments (containing 10 mM NaCl; no MgCl<sub>2</sub>) is essentially optimized for GST-FinO/FinP binding and was therefore used for all subsequent studies.

### **6.2.2 GST-FinO binding is enhanced by single-stranded regions on either side of SLII**

Since the stem II point mutants examined did not significantly alter the binding affinity of GST-FinO, the focus was changed to the conserved single-stranded regions of FinP: the 5' leader, spacer and 3' tail. Removal of 3 bases from the 5' leader following the initiating G required for T7 RNA polymerase transcription (FinP  $\Delta$ A2, U3, A4) had little effect on binding affinity (75%; Table 6.3), however the spacer and tail regions proved to be important, as shown in Figure 6.5 and summarized in Table 6.3. Deletion of either the spacer or 3' tail from SLII had minor to moderate effects on GST-FinO binding, reducing the  $K_{as}$  by 1.3-fold and 5.5-fold compared to spacer-SLII-tail, respectively. Deletion of both the spacer and 3' tail from SLII had a profound effect, reducing the binding constant 14-fold to 4%.

Previous work (van Biesen & Frost, 1994; Sandercock & Frost, 1998) indicates that GST-FinO binding is moderately specific, with a 17-fold preference for FinP over tRNA. In order to determine whether FinO had a non-specific affinity for single-stranded RNA, the ability of polyuridylic acid (poly(U)) to compete with FinP for GST-FinO binding was tested. Weight-equivalents of tRNA or poly(U) were combined with a fixed

**Table 6.3** The tail length, but not sequence, is critical for FinP recognition. Binding of GST-FinO to FinP variants was assessed as described in Table 6.1.

<b>F FinP variant</b>	<b><math>10^7 K_a</math> (M<sup>-1</sup>)<sup>a</sup></b>	<b>Binding<sup>b</sup></b>
FinP	2.00 ± 0.20	100
FinP ΔA2, U3, A4	1.50*	75
FinP G74:C/A75:C	1.40*	68
<b>SLII</b>		
spacer-SLII-tail	1.10 ± 0.02	55
spacer-SLII (no tail)	0.20 ± 0.04	10
SLII-tail (no spacer)	0.82 ± 0.05	41
SLII (no spacer, no tail)	0.08 ± 0.01	4
spacer-SLII-GAUU	0.38 ± 0.05	19
spacer-SLII-GA	0.06 ± 0.01	3
SLII-GAAAAA	0.69*	35
spacer-SLII-GACA	0.36*	18
<b>SLI</b>		
leader-SLI	0.04 ± 0.01	2
leader-SLI-spacer	0.13 ± 0.03	6
leader-SLI-tail	0.43 ± 0.05	21

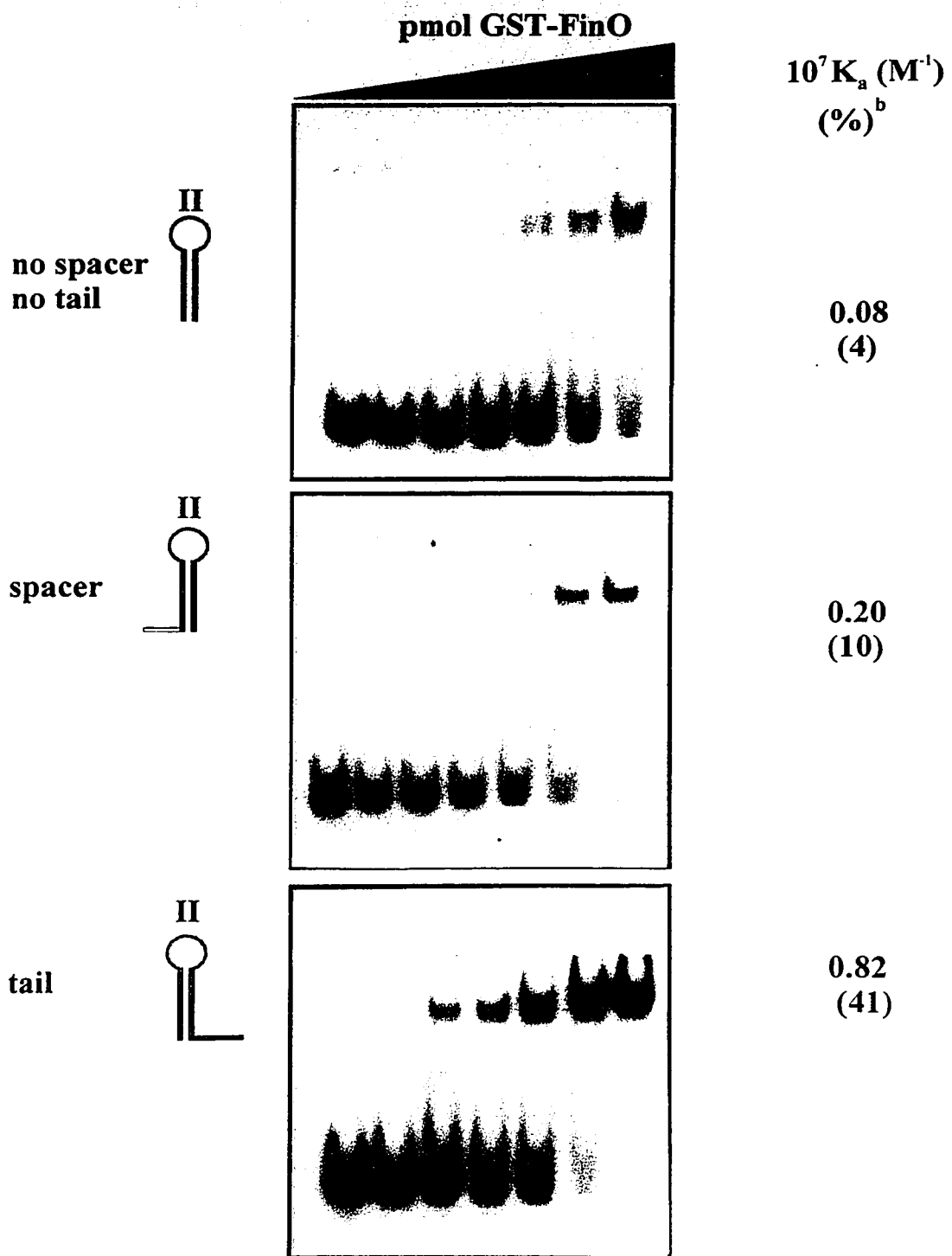
<sup>a</sup> Unless otherwise stated,  $K_a$  values are averages ± standard deviation of at least three independent gel shifts

<sup>b</sup> % binding relative to FinP [=100×(  $K_a$ variant/ $K_a$ FinP)]

\*  $K_a$  values are averages of two independent gel shifts



**Figure 6.5** The spacer and 3' tail contribute to high affinity SLII binding by GST-FinO. Labelled RNA (7.5 fmol) was incubated with increasing amounts (0, 0.1, 1.1, 2.1, 5.3, 10.6 and 31.9 pmol) of GST-FinO in a total volume of 30  $\mu$ l as described in Materials and Methods (section 2.12). Samples were resolved on a nondenaturing 8% polyacrylamide gel. <sup>b</sup> % binding relative to FinP [=100 $\times$ (K<sub>a</sub> variant/K<sub>a</sub>FinP)].



amount of labelled FinP (15 fmol) and incubated with excess GST-FinO (10.6 pmol; Figure 6.6). The amount of competitor necessary to free 50% of the label from the GST-FinO/FinP complex was determined from a plot of the percent complex remaining at each competitor concentration. The results indicate that 0.01  $\mu\text{g}$  of tRNA (a 19:1 molar ratio of tRNA:FinP) was required to compete 50% of the FinP from the complex. A four-fold increase in poly(U) (0.04  $\mu\text{g}$ ) was necessary for an equivalent level of competition, indicating that single-stranded RNA (poly(U)) is an ineffective competitor of FinP. These results suggest that the single-stranded spacer and 3' tail regions of FinP are part of a higher order structure that is recognized by FinO.

The nucleotide sequences of synthetic stem-loops I and II were arbitrarily chosen (van Biesen & Frost, 1994) such that SLI includes the 5' leader and stem-loop I, whereas SLII includes the spacer, stem-loop II and 3' tail (Figure 6.1). Since GST-FinO binding to SLII was strongly dependent on the presence of both single-stranded flanking sequences, the observed low affinity of GST-FinO for SLI might be due to the absence of a 3' single-stranded region. To test this hypothesis, SLI variants were constructed that had either the spacer or tail sequence added to their 3' ends. When assayed for GST-FinO binding, the  $K_a$  values for SLI-spacer and SLI-tail were increased 3-fold and 10-fold, respectively (Figure 6.7; Table 6.3). These results clearly demonstrate the importance of the 3' flanking sequence to the structure recognized by GST-FinO.

**Figure 6.6** Competition of GST-FinO binding to FinP with tRNA and poly(U). Indicated amounts ( $\mu\text{g}$ ) of tRNA and poly(U) were mixed with 15 fmol of uniformly-labelled FinP RNA and incubated with excess GST-FinO (10.6 pmol) in a total volume of 30  $\mu\text{l}$  for 30 min at room temperature as described in Materials and Methods (section 2.12). Samples were electrophoresed on a nondenaturing 8% polyacrylamide gel.

polyU

tRNA

30  
3.0  
0.3  
0.03  
0.003  
0

30  
3.0  
0.3  
0.03  
0.003  
0

μg competitor

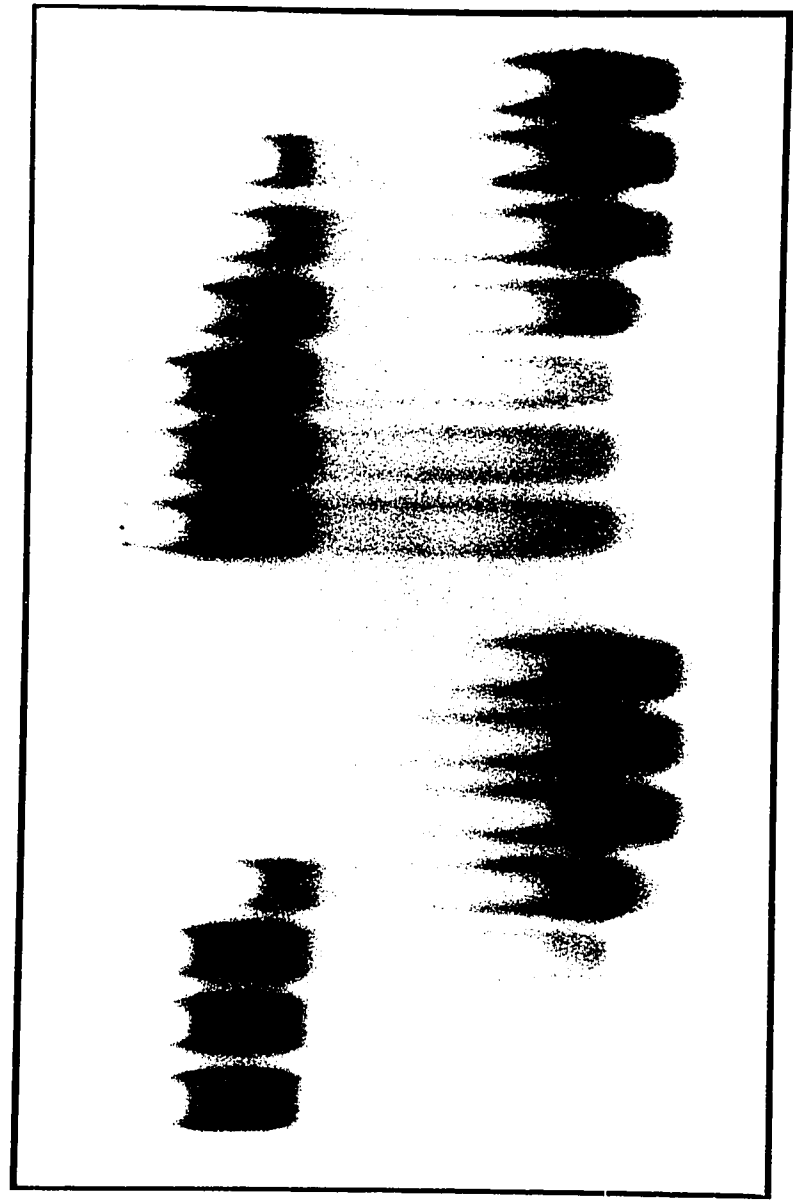
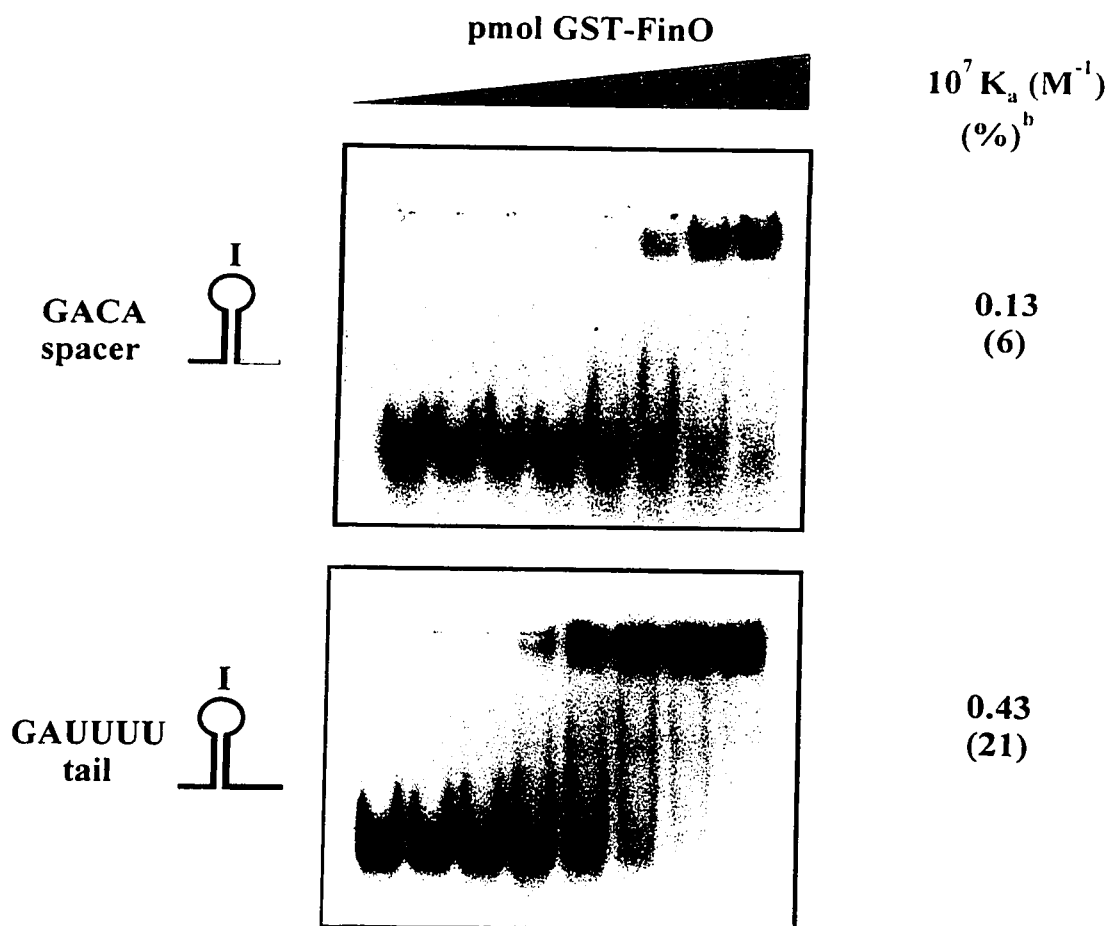


**Figure 6.7** The spacer and 3' tail improve SLI binding by GST-FinO. The binding affinity of GST-FinO for SLI with the attached spacer or tail sequence was determined using the gel shift conditions described in the legend to Figure 6.5, with the following amounts of GST-FinO in a total volume of 30  $\mu$ l: 0, 0.1, 0.5, 1.1, 2.1, 5.3, 10.6, 31.9 pmol. <sup>b</sup> % binding relative to FinP [=100 $\times$ ( $K_a$  variant/ $K_a$  FinP)].



### 6.2.3 The length, but not sequence, of the FinP 3' tail is important for GST-FinO binding

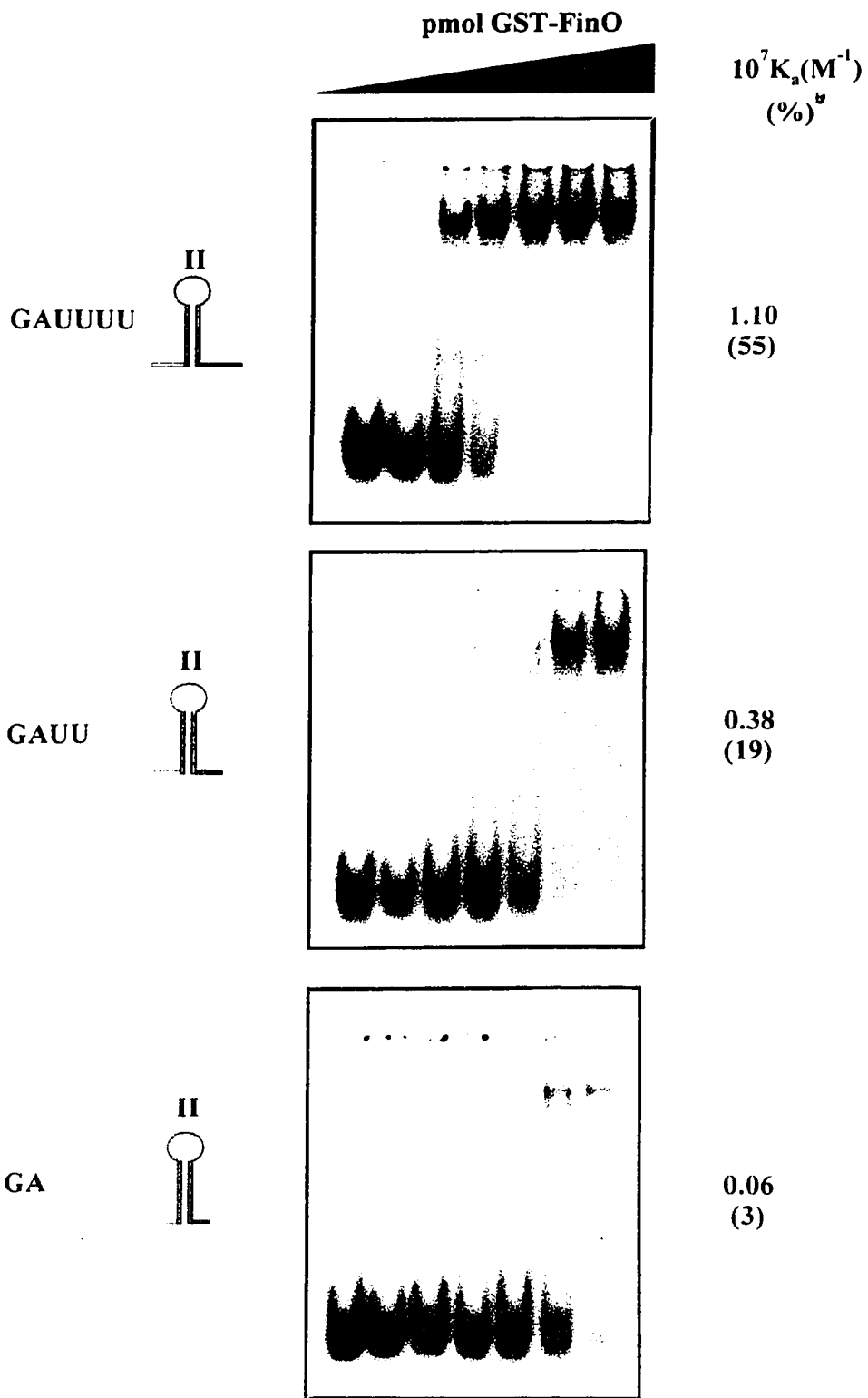
The effect of decreasing the length of the 3' tail following SLII on GST-FinO binding was examined, since addition of a 7 base extension had no effect (see above). Shortening of the SLII 3' tail from 6 bases (GAUUUU) to 4 bases (GAUU) decreased the  $K_a$  3-fold to  $0.38 \times 10^7 M^{-1}$  (Figure 6.8; Table 6.3). A further reduction in tail length to 2 bases (GA) decreased the  $K_a$  another 6-fold to  $0.06 \times 10^7 M^{-1}$ . These results suggest that a minimum 6 base 3' tail is necessary for efficient binding by GST-FinO. To determine whether the presence of the 3' tail reflected a sequence-specific or general requirement for additional bases flanking SLII, variants SLII-GAAAAA, spacer-SLII-GACA and FinP G74:C/A75:C were constructed (Table 6.3). The sequence of each variant was chosen to avoid introducing any other obvious secondary structural features. Comparison of the variant pairs (SLII-GAAAAA with SLII-tail; spacer-SLII-GACA with spacer-SLII-GAUU and FinP G74:C/A75:C with wild-type FinP) in Table 6.3 shows that these base transversions in the 3' tail had minor effects on GST-FinO binding. These results indicate that the length, but not sequence, of the FinP 3' tail is important for high affinity binding by GST-FinO.

### 6.2.4 GST-FinO recognizes the same structural features in *traJ* mRNA

The results of an earlier study (van Biesen & Frost, 1994) showed that GST-FinO binds to a truncated 184 base version of the sense mRNA, *traJ*, with a  $K_a$  similar to that for FinP. The sequence and secondary structure of the first 117 bases of F *traJ* mRNA



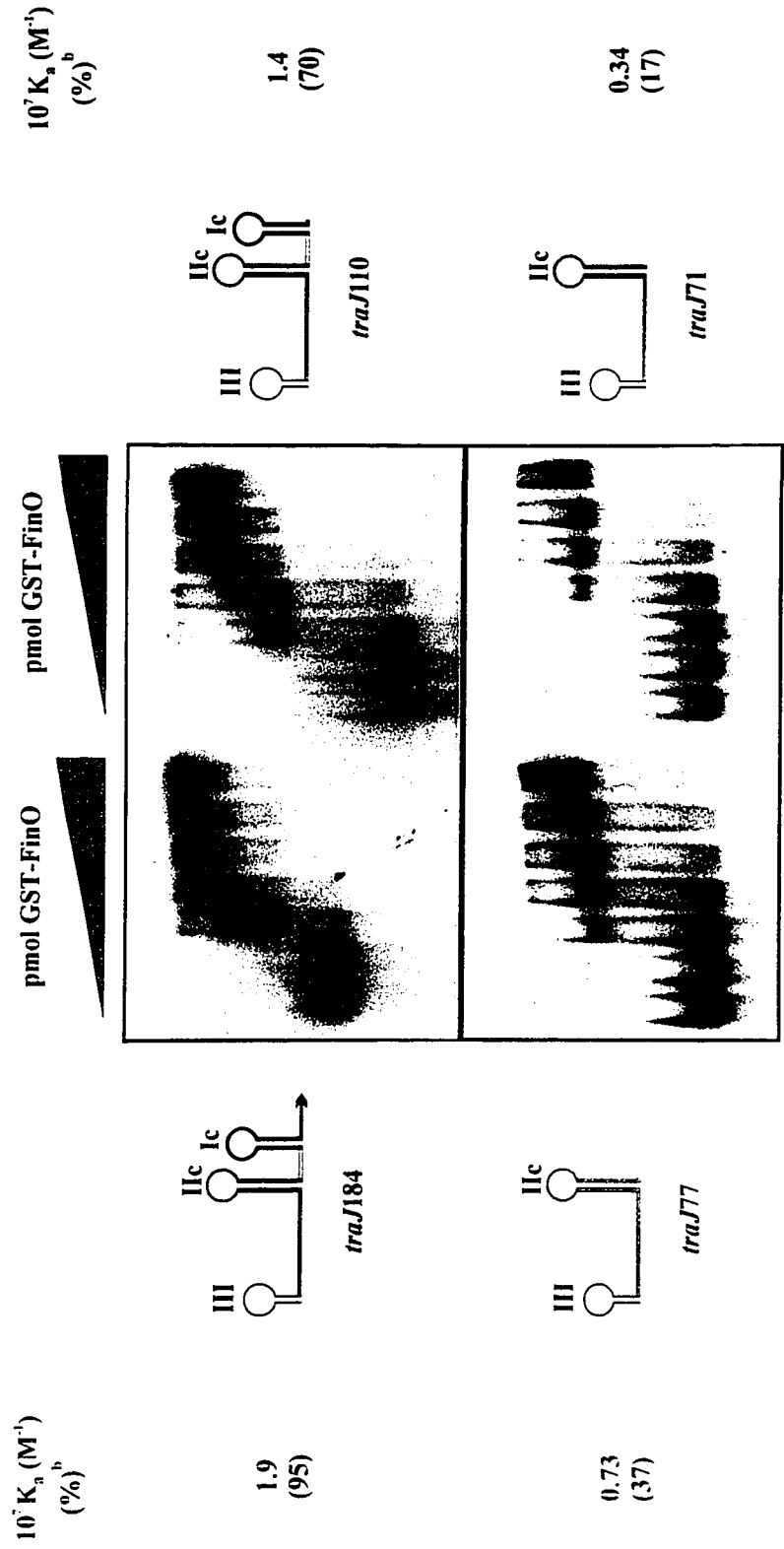
**Figure 6.8** The length of the SLII 3' tail is important for RNA recognition. The effect of 3' tail-length on GST-FinO binding to SLII was examined by gel shift analysis as detailed in Figure 6.5. Seven and a half femtomoles of RNA was incubated with 0, 0.1, 1.1, 2.1, 5.3, 10.6, 31.9 pmol GST-FinO in a total volume of 30  $\mu$ l. <sup>b</sup> % binding relative to FinP [=100 $\times$ (K<sub>a</sub>variant/K<sub>a</sub>FinP)].



are shown in Figure 6.1. The secondary structure of *traJ* mRNA between nucleotides 33 and 111 is almost identical to FinP, with the following exceptions: SLIc of *traJ* mRNA has an additional mismatch (A-C) which is paired in FinP SLI; SLIc of *traJ* is 2 bases shorter than SLII of FinP, resulting in a 6 base *traJ* spacer, as compared to 4 bases for FinP.

To further characterize the interaction between GST-FinO and F plasmid-encoded *traJ*184 (previously called TraJ211; van Biesen & Frost, 1994), a series of 3' truncated *traJ* variants (Figure 6.1) were created and their binding to GST-FinO was compared with that of FinP. As seen in Figure 6.9, addition of increasing amounts of GST-FinO led to the conversion of low molecular weight bands to one or more higher molecular weight bands (see the Discussion for further comments). For RNA variants that gave more than one band shift,  $K_a$ s were calculated by considering all bound RNA as a single species. GST-FinO bound *traJ*184 almost as well as FinP (95%), with a  $K_a$  of  $1.9 \times 10^7 \text{ M}^{-1}$ . Deletion of 74 bases from the 3' end of *traJ*184, creating *traJ*110 (see Figure 6.1), yielded a modest 25% reduction in GST-FinO binding to  $1.4 \times 10^7 \text{ M}^{-1}$ . Removal of SLIc from *traJ*110, which results in a transcribed product of 77 bases (*traJ*77; similar to SLII of FinP, Figure 6.1) reduced GST-FinO binding by 48% to  $0.73 \times 10^7 \text{ M}^{-1}$ . This is similar to the 45% reduction in the binding constant observed for the removal of SLI from FinP (see Figure 6.3; Table 6.1). Further mutation of *traJ*77 to eliminate the spacer residues 3' to SLIc (A72 to C77), creating *traJ*71, decreased the  $K_a$  for GST-FinO binding another 53% to  $0.34 \times 10^7 \text{ M}^{-1}$ . As with FinP, this result suggests that SLIc and its 3' flanking sequence are important determinants for high affinity GST-FinO binding.

**Figure 6.9** GST-FinO recognizes the same structural features in *traJ* mRNA as it does in FinP. Four *traJ* variants of different length, indicated by their names, were synthesized and subjected to gel shift analysis using the conditions described in Figure 6.5, except that the samples were resolved on a nondenaturing 6% polyacrylamide gel. Seven and a half femtomoles of RNA was incubated for 30 min at room temperature with 0, 0.1, 1.1, 2.1, 5.3, 10.6, 31.9 pmol GST-FinO in a total volume of 30  $\mu$ l as described in Materials and Methods (section 2.12). <sup>b</sup> % binding relative to FinP [=100 $\times$ ( $K_a$ *traJ* variant/ $K_a$ FinP)].



### 6.3 Discussion

This communication describes the RNA structural features recognized by the FinO protein. RNA-binding proteins have generally been shown to target single-stranded regions caused by loops, bulges and mismatches or those which occur between helical stems, rather than the duplexed regions themselves (Mattaj, 1993; Steitz, 1993; Varani & Pardi, 1994). Duplexed regions are necessary, however, for spacing and presentation of single-stranded nucleotides in the correct orientation (Steitz, 1993). The hairpin loops represent an obvious single-stranded region of FinP available for protein binding. Three lines of evidence suggest that FinO does not make sequence-specific contacts with bases in the FinP loops. First, although the loop sequences vary between *finP* alleles (Finlay *et al.*, 1986), FinO is exchangeable among F-like plasmids (Willetts & Maule, 1986; van Biesen & Frost, 1992). Second, the *traJ* mRNA loops are complementary in sequence to FinP, and yet GST-FinO bound *traJ* and FinP with nearly equal affinity. Third, GST-FinO bound F, ColB2 and R100 FinPs with the same relative affinity, even though the sequences of the loops vary considerably, especially within loop II.

The results reported by van Biesen & Frost (1994) and in this study indicate that the sequence between nucleotides 35 and 79 (SLII) of FinP is sufficient and necessary for high affinity GST-FinO binding. Stem II is fully duplexed in FinP and presents a relatively poor sequence-specific target for FinO. Attempts to disrupt the helical nature of SLII by introduction of internal loops and base-substitutions were freely tolerated, indicating that a continuous duplex is not necessary for FinO binding. In agreement with this, single mutations at three of the sites tested (C41, C46, G49) and at G50, have no effect on FinP repressor activity from the related conjugative plasmid R1, as measured by

conjugation frequency (Koraimann *et al.*, 1991). Thus, the mutant FinP RNAs are also fully stabilized *in vivo* by FinO (Koraimann *et al.*, 1996). These results indirectly demonstrate that FinO binding is not affected by these base substitutions *in vivo*, in accord with the results obtained in this study, *in vitro*.

Earlier studies (van Biesen & Frost, 1994) showed that GST-FinO could bind to a FinP/*traJ*184 duplex or a duplex formed between SLI and the complementary sequence of *traJ* mRNA. However, the present results indicate that a 14 bp duplex, SLII alone, was not sufficient for high affinity GST-FinO binding. These apparently conflicting results can be reconciled by the finding that single-stranded regions adjacent to the duplexed RNA were necessary for binding by GST-FinO. Collectively, these results suggest that FinO may have a nonspecific affinity for double-stranded RNA of indeterminate length (>14 bp), but that specific binding to FinP requires additional sequences flanking the stems. In this respect, FinO resembles the stem-loop binding protein (SLBP) which binds to the 3' end of histone mRNA in mammalian cells (Williams & Marzluff, 1995). Efficient binding by SLBP requires at least three nucleotides each 3' and 5' of a stem-loop. FinO requires at least 6 nucleotides 3' to SLII and as many as 4 nucleotides 5' to SLII, although the length of the 5' spacer was not examined in this study. Like FinO, SLBP does not have a strict loop size requirement, suggesting that specific contacts do not involve the loop. However, unlike the interaction between FinO and FinP, the sequence of the stem and flanking regions is important for SLBP binding.

Since no evidence was obtained for sequence-specific contacts between GST-FinO and FinP, these present data suggest that FinO recognizes the overall shape of the RNA conferred by a stem-loop structure, flanked on either side by single-stranded

regions. Congruent with this, GST-FinO recognizes the same structural features in *traJ* mRNA. The requirement for a six nucleotide flanking region 3' to SLIIc is fulfilled by the *traJ* spacer, which is two bases longer than the FinP spacer (Figure 6.1). In addition the *traJ* spacer, which differs from the FinP 3' tail at 4 of the 6 bases, can serve as a functional 3' flanking region, indicating that sequence is unimportant for binding by FinO. Addition of the FinP tail sequence (GAUUUU) to the 3' side of SLI conferred moderate GST-FinO binding, although the binding constant was 2-fold lower than that for SLII with the equivalent 3' tail. These results suggest that the RNA conformation recognized by GST-FinO can be adopted quite efficiently by three different sequences: *traJ* mRNA with its 6 base single-stranded spacer, SLI with the FinP 3' tail and SLII with the 3' tail.

The functionally related RNA-binding protein, Rom, has also been shown to recognize RNA in a structure-dependent, rather than sequence-dependent fashion. Rom binds to an unstable complex formed between the complementary hairpin loops of RNA I and RNA II of ColE1 plasmids (Tomizawa & Som, 1984). The results of three independent studies indicate that Rom is capable of binding and stabilizing any complex formed by pairs containing fully complementary loop sequences (Eguchi & Tomizawa, 1991, Predki *et al.*, 1995; Gregorian & Crothers, 1995). Unexpectedly, GST-FinO bound pBR322 antisense RNA I with an affinity constant 70% of that for FinP. The secondary structure of pBR322 RNA I consists of a 9 base leader followed by three stem-loop domains, with a 2 base spacer between stem-loops I and II (Helmer-Citterich *et al.*, 1988; Tamm & Polisky, 1983). Although it has not been proven experimentally, RNA I is often represented as a tRNA-like cloverleaf structure (Figure 1.8a). As such, if stems I and III



are co-axial, then it is conceivable that FinO recognizes these stems as a continuous duplex, similar to the FinP/*traJ* mRNA duplex. Since the specificity of these two interactions (GST-FinO/RNA I and GST-FinO/FinP-*traJ* mRNA duplex) has not been determined, it is possible that they reflect a nonspecific affinity of FinO for double-stranded RNA. Further experiments are needed to define the FinO binding site within RNA I and establish the specificity of the interaction.

Interestingly, binding of GST-FinO to *traJ*184 gave rise to four shifted bands of different mobility, with the largest complex being retained in the well (Figure 6.9). The fastest migrating complex was converted to the more slowly-migrating complexes with increasing GST-FinO concentration. GST-FinO interaction with *traJ*110 resulted in 3 distinct complexes, whereas 2 complexes were formed with either *traJ*77 or *traJ*71. Whether GST-FinO binds to RNA as a monomer or multimer has not been established, but preliminary results using size-exclusion chromatography suggest that the fusion protein exists as a monomer in solution (van Biesen & Frost, 1994). One possible explanation for the formation of multiple complexes may therefore be step-wise binding of GST-FinO monomers to multiple sites on its RNA target. The bands retained in the well likely represent complexes formed due to GST-FinO aggregation. Cooperative binding has been reported for the HIV Rev-RRE interaction (Heaphy *et al.*, 1990; Kjems *et al.*, 1991; Malim & Cullen, 1991; Iwai *et al.*, 1992) and between p24 (a 220 amino acid truncated polypeptide of the protein kinase, PKR) and HIV dsTAR RNA (Bevilacqua & Cech, 1996). A closer look at GST-FinO binding to its antisense RNA targets (Figure 6.3) shows that only one complex was formed between GST-FinO and either SLI or SLII, whereas 2 complexes were formed with full-length FinP (more readily distinguished by

under-exposure of this gel; data not shown). Although the strongest GST-FinO binding was achieved with SLII, low-affinity binding was observed between GST-FinO and SLI with its attached 4 base spacer. Thus, binding of GST-FinO to its primary binding site, SLII, may promote binding to the low-affinity site, SLI, resulting in the more slowly migrating complex observed at high GST-FinO concentrations. Similarly, the higher molecular weight complexes observed with the *traJ* mRNA variants may represent successive GST-FinO binding to stem-loops IIc, Ic and III. Alternatively, since the second and third shifts appear only after all of the substrate is bound, these bands may simply represent nonspecific binding of the excess protein to low-affinity sites. Further experiments are needed to determine the specificity of FinO binding to these potential low-affinity sites. In addition, since the physiological FinO concentration is not presently known but is thought to be low based on mRNA levels (van Biesen & Frost, 1992), the relevance of the higher molecular weight complexes, which are formed at high FinO concentrations, remains to be established.

## **Chapter 7**

### **Discussion & Conclusions**

## 7.1 Degradation of FinP antisense RNA in the absence of FinO

The results described in this thesis confirm many of the hypotheses set forth by previous workers in the field and refine our understanding of the mechanism by which the FinO protein optimizes transfer repression of F-like plasmids by FinP. Prior to this work, FinO had been assigned two roles in fertility inhibition: 1) stabilization of FinP antisense RNA by an unknown mechanism *in vivo* and 2) promotion of duplex formation between FinP and *traJ* mRNA *in vitro*. The primary objective of this thesis was to determine how the FinO protein stabilizes FinP antisense RNA. To answer this question, it was first necessary to characterize FinP degradation in the absence of FinO. FinP was expressed in the absence and presence of *traJ* and its decay was followed in wild-type and RNase-deficient strains. The first part of this discussion deals with FinP decay in the absence of *traJ*.

The chemical half-life obtained for FinP in the absence of *traJ* was 14 minutes in a wild-type background. The dramatic stabilization of FinP in RNase E mutants (*rne-1* = 104 min; *rne-3071* = 64 min) indicates that its degradation is triggered by RNase E. Experiments using purified RNase E identified one major cleavage site within the single-stranded spacer between stem-loops I and II of FinP synthesized *in vitro*, and one within the 3' extended tail derived from the vector sequence. Mutation of the spacer sequence stabilized FinP *in vivo*, confirming that this region of the RNA is required for initiation of FinP degradation. Secondary RNase E cleavages were observed within structured regions of FinP SLI (at positions ~29/30 and ~9/10) *in vitro*; however, their significance was not examined *in vivo*. RNase E cleaves the much larger *rspO* mRNA (encoding ribosomal protein S15) and *rpsT* mRNA (encoding ribosomal protein S20) at 11 (Braun *et al.*, 1996)

and 12 (Mackie, 1991) sites (respectively) *in vitro*, but only 2 of these can be detected for each transcript *in vivo*. These results suggest that other factors present in the cell (ie. components of the degradosome and/or translating ribosomes) may restrict RNase E cleavage site selection *in vivo*.

RNase E cleavage within the 5' leader sequence of antisense RNA I is necessary to initiate its rapid exonucleolytic degradation, but on its own, this cleavage is insufficient to inactivate RNA I because the remainder of the RNA (RNA L<sub>5</sub>) can inhibit primer maturation (He *et al.*, 1993). Although it was not tested, RNase E cleavage within the FinP spacer might suffice to functionally inactivate FinP, since it separates stem-loops I and II. If FinP must remain intact for duplex formation or if the single-stranded spacer region is necessary for initiation of duplex formation, further degradation of FinP beyond cleavage of the spacer may not be required for its inactivation. It is not presently known whether SLI can repress *traJ* mRNA translation on its own or if it would remain intact following its separation from SLII. The integrity of SLI is certainly necessary for fertility inhibition, as demonstrated by the detrimental effect of the *finP305* mutation (C30:U) on FinP repressor activity (Finnegan & Willetts, 1971, 1973; Frost *et al.*, 1989). In the present study, this SLI mutation was shown to dramatically reduce the FinP half-life, but it could be partially rescued in an RNase E mutant. Purified RNase E cleaved the *finP305* RNA predominantly at the site of the mutation (positions 28/29 and 29/30) *in vitro*, but several secondary cleavages within stem I, its attached loop and the spacer were observed. Because the *finP305* mutation makes SLI more A/U rich, this could account for the increased RNase E cleavage seen *in vitro* and partly explains its reduced half-life *in vivo* (see below).

Since inactivation of RNase E resulted in stabilization of full-length FinP *in vivo*, this indicates that SLII (which consists of a 14 bp uninterrupted helix followed by a 6 base single-stranded tail;  $\Delta G = -24.3$  kcal/mol) must impede exonuclease activity for at least this long. In fact, the metabolic stability of FinP was not increased by mutations in RNase II or PNPase, individually or in combination, indicating that RNase E is responsible for initiating the degradation of FinP and does so, independent of these enzymes. These results are in agreement with the notion that the exonucleases, especially RNase II, are sensitive to secondary structure (Klee & Singer, 1968; Nossal & Singer, 1968; Mott *et al.*, 1985; McLaren *et al.*, 1991) and bind inefficiently to transcripts with fewer than 6-10 unpaired 3' bases (Coburn & Mackie, 1996a). The exceptionally long half-life of IS10 antisense RNA-OUT (~60 min) is determined entirely by exonuclease activity, since it is devoid of RNase E and RNase III endonuclease cleavage sites (Case *et al.*, 1989; Pepe *et al.*, 1994). The RNA-OUT secondary structure consists of a single stem-loop domain terminated by 5 unpaired bases (Figure 1.8b; Kittle *et al.*, 1989), with a predicted thermodynamic stability ( $\Delta G = -22.1$  kcal/mol; Case *et al.*, 1989) similar to FinP SLII. Thus, in the absence of endonucleolytic cleavage, FinP might be expected to display a comparable half-life to RNA-OUT. Indeed this is the case, since mutation of the FinP spacer sequence (at the site of RNase E cleavage) increased its half-life to 48 minutes.

The apparent strength of SLII is exemplified by its inefficient hybridization to oligonucleotide probes under denaturing conditions (Northern hybridization and primer extension analysis). For this reason, the fate of the 3' intermediate of RNase E cleavage (SLII) could not be followed by Northern analysis. The 5' intermediate (SLI) escaped

detection using Primer A, which hybridizes efficiently to the 5' side of SLI within full-length FinP, in wild-type and RNase II PNPase<sup>-</sup> strains, indicating that it is rapidly degraded. A similar result was obtained with the 5' intermediate resulting from RNase E cleavage of plasmid R1 CopA antisense RNA, which remained undetectable in all RNase mutants (Söderbom & Wagner, 1998). These results do not rule out the possibility that the 5' intermediates are degraded by RNase II or PNPase, but instead suggest that they can be effectively removed by alternative pathways in their absence (see below). Several full-length transcripts including plasmid R1 Sok antisense RNA (Mikkelsen & Gerdes, 1997), *trxA*, *lpp* and *ompA* mRNAs (O'Hara *et al.*, 1995) are destabilized by the addition of a poly(A) tail to their 3' ends catalyzed by PAP I. Similar destabilization is observed for RNase E degradative intermediates of antisense RNAs CopA (Söderbom *et al.*, 1997) and RNA I (He *et al.*, 1993; Xu *et al.*, 1993), *rpsT* mRNA (Coburn & Mackie, 1996b, 1998), and for full-length *rpsO* mRNA in an RNase E-deficient strain (Hajnsdorf *et al.*, 1995). Polyadenylation is thought to facilitate mRNA decay, particularly if stable stem-loop structures are present, by providing a single-stranded platform for the exonucleases (Coburn & Mackie, 1996a). Inactivation of PAP I had no effect on the stability of full-length FinP and the 5' RNase E intermediate remained undetectable. Therefore polyadenylation, at least that catalyzed by PAP I, is not required for the rapid degradation of this intermediate or full-length FinP. Although PAP I accounts for >90% of the polyadenylation activity in *E. coli* (O'Hara *et al.*, 1995), it remains possible that PAP II is involved in FinP decay.

The chemical stability of FinP was lower in a triple *rne-1 rnb pnp* mutant than in a single *rne-1* mutant. Thus, although the degradation pathway involving RNase E

determines the FinP half-life, other RNases can degrade FinP, albeit much less efficiently. Similar results were obtained with *rpsO* (Hajnsdorf *et al.*, 1994; Hajnsdorf *et al.*, 1996), *ompA*, *lpp*, and *trxA* mRNAs (O'Hara *et al.*, 1995) and CopA antisense RNA (Söderbom & Wagner, 1998). The enzymes responsible for degradation in the absence of these major RNases are unknown, but could include the broad specificity RNases (RNase I\*, RNase M and oligoribonuclease) or other uncharacterized RNases. It should be noted that a pathway involving RNase I\* and RNase M would be less energetically favourable since these enzymes cleave RNA to yield products with 3' phosphates, which presumably require dephosphorylation prior to recycling (Nierlich & Murakawa, 1996). Appropriately, these enzymes appear to serve as a back-up system when more efficient pathways (including RNase E, RNase III, RNase II, PNPase and PAP I) are compromised.

Prior to this work, van Biesen *et al.* (1993) had shown that F FinP could form a duplex with the *traJ* mRNA *in vitro*; however, direct evidence for duplex formation in F had not been obtained *in vivo*. In the current study, the analysis of FinP decay in the presence of *traJ* revealed two F FinP transcripts (with different 3' ends) that formed duplexes with the *traJ* mRNA in an RNase III mutant. Neither duplex was detected in the wild-type strain, indicating that they were rapidly degraded by RNase III. Only the shorter FinP transcript (79 bases) was detected in the absence of *traJ* transcription and it was not a substrate for RNase III. It is believed that the longer FinP transcript forms if part or all of the stem-loop II sequence pairs with the *traJ* mRNA before it has a chance to fold back on itself and form a rho-independent terminator structure, allowing transcription to terminate further downstream. This could explain why the longer transcript was not seen when FinP was expressed without *traJ*. The related *finO* plasmid



R100-1 also produces two detectable FinP/*traJ* mRNA duplexes (~74 and 135 bp) in an RNase III mutant (Dempsey, 1994a), whose sizes are determined by FinP. The experiments performed in these studies (this thesis and Dempsey, 1994a) did not address the contribution of RNase III to fertility inhibition and therefore it is not known if degradation of the duplexes is necessary to prevent *traJ* translation. It is possible that, like the IS10 RNA-IN/RNA-OUT duplex, occlusion of the RBS is sufficient for repression (Case *et al.*, 1990).

## 7.2 The role of FinO in stabilizing FinP

Prior to this work, the results of several studies indicated that FinO increases the steady-state concentration of FinP (Dempsey, 1987; Frost *et al.*, 1989; Koraimann *et al.*, 1991, 1996; van Biesen & Frost, 1994) by an unknown mechanism that does not involve an increase in *finP* promoter activity (Mullineaux & Willetts, 1985). This increase in FinP concentration (imparted by FinO) correlates with decreased levels of *traJ* mRNA (van Biesen *et al.*, 1993), due to RNase III-mediated cleavage of FinP/*traJ* mRNA duplexes (Dempsey, 1994a; this study). Although duplex formation is enhanced by FinO *in vitro*, FinP and *traJ* mRNA have the innate ability to duplex on their own as demonstrated *in vitro* (van Biesen *et al.*, 1993) and *in vivo* (Dempsey, 1994a; section 3.2.2). This suggests that the most important function of FinO is to maintain sufficiently high FinP concentrations to sequester and inactivate *traJ* mRNA. Early investigations directed at determining how FinO increases the concentration of FinP showed that the half-life of a FinP-like intermediate, obtained from a *lacZ-finP* fusion, increased in the presence of FinO (Lee *et al.*, 1992). In agreement, the results of the present study showed

that FinO increases the half-life of authentic FinP (transcribed from its own promoter), indicating that FinO prevents FinP antisense RNA decay. However, FinO was unable to stabilize *finP305* RNA. Since RNase E was shown to be the primary enzyme responsible for FinP degradation in the absence of FinO (see above), the effect of the GST-FinO fusion protein on RNase E degradation of FinP was examined *in vitro*. The data showed that GST-FinO reduced cleavage at the major RNase E site within the FinP spacer, at the secondary site on the 5' side of SLI and at a site within the vector-derived 3' extension. A similar experiment performed with *finP305* RNA indicated that GST-FinO could not repress RNase E cleavage events on the 3' side of SLI (at the site of the mutation), which explains why FinO does not prevent *finP305* RNA decay *in vivo*.

Two lines of evidence indicate that GST-FinO prevents RNase E cleavage by steric interference due to its RNA-binding activity. (1) Previous studies (van Biesen & Frost, 1994; van Biesen, 1994) showed that GST-FinO binds to FinP and *finP305* RNA with similar affinity; however, the present data indicate that *finP305* RNA remains susceptible to RNase E. This argues that, as suggested by Lee *et al.* (1992), FinO does not prevent cleavage by inactivating RNase E. (2) There is a direct relationship between GST-FinO binding and GST-FinO inhibition of RNase E activity. Since *finP305* RNA was cut at positions 28/29 and 29/30 in the presence of GST-FinO, this indicates that GST-FinO does not cover the 3' side of SLI. A recent study by Sandercock (1997) indicates that although the N-terminus (amino acids 1-73) is required for FinP binding, the C-terminal region of FinO (amino acids 142-186) is necessary for protection of FinP degradation *in vivo*. Thus, either the C-terminus itself sterically interferes with RNase E cleavage within the spacer or the C-terminus is necessary for appropriate folding of FinO,

allowing another region of the protein to protect the spacer. Further RNA-binding studies (see below) indicate that the single-stranded region on the 3' side of SLII is necessary for GST-FinO binding to FinP and likely explains the protection observed in this region (ie. within the 3' extended tail). Protection on the 5' side of SLI might be conferred by the C-terminus of FinO or by a second monomer bound to SLI (see below). Deletion analysis of RNase E indicates that RNA binding is necessary for RNase E endonucleolytic activity (Taraseviciene *et al.*, 1995). Whether FinO and RNase E binding to FinP is mutually exclusive or whether both proteins bind simultaneously and FinO simply masks the cleavage sites, could not be resolved from the present study.

FinO is not unique in its ability to block RNase activity. Several proteins, including the poly(A)-binding protein (PABP) and the iron regulatory protein (IRP) in eukaryotes (reviewed in Ross, 1995) and GroEL (Georgellis *et al.*, 1995), ribosomes (Braun *et al.*, 1998) and the exonuclease impeding factor (EIF; Causton *et al.*, 1994) in prokaryotes, have been shown to possess this property. However, in only a few cases, has the RNase been identified whose activity is inhibited. Braun *et al.* (1998) have shown that the RNase E cleavage event that initiates the exonucleolytic decay of the *rspO* mRNA is sensitive to the presence of ribosomes. An increase in the distance between the *rspO* UAA termination codon and the downstream RNase E cleavage site decreases the mRNA's stability, whereas a decrease in this distance has the opposite effect. Since ribosomes cover ~15 bases downstream of the codon in their P sites, the authors propose that steric hindrance prevents access of RNase E to its cleavage site 10 bases downstream. Unlike the interaction between FinO and FinP, the stabilizing effect of ribosomes must be transient since it could occur only when translating ribosomes arrive at the termination

site and would not operate on untranslated antisense RNAs. In another example, the EIF was identified from an *E. coli* extract as a component of a stem-loop binding activity that specifically impeded PNPase activity *in vitro* (Causton *et al.*, 1994). A second component of the binding activity was identified as PNPase itself. Unlike FinO, EIF was not capable of binding to the RNA on its own and had therefore copurified with PNPase by virtue of its RNA-binding activity. This suggests that EIF impedes PNPase via direct association, rather than by masking the substrate RNA, as seen for FinO.

### 7.3 Recognition of RNA by FinO

Earlier work on the specificity of the FinOP interaction suggested that FinO recognizes extended regions of double-stranded RNA (van Biesen & Frost, 1994). This proposal was based on the finding that the GST-FinO protein bound RNA duplexes formed between FinP and *traJ* mRNA and that GST-FinO showed a preference for SLII, which is fully duplexed, over SLI. This interaction is predicted to be sequence-independent since the accessible minor groove of a fully paired A-form helix presents an indistinguishable array of hydrogen bond donors and acceptors and the bases in the major groove are largely inaccessible (Steitz, 1993). Sequence-dependent recognition of bases within helices can occur, but requires disruption of the helix to open up the major groove, as seen in the Rev-RRE interaction (Bartel *et al.*, 1991; Heaphy *et al.*, 1991; Iwai *et al.*, 1992). Attempts to disrupt the continuity of base pairing in SLII by introducing bulges and internal loops in the present study reduced GST-FinO affinity by no more than 50%, suggesting that a smooth duplex was in fact not necessary for binding. Mutations in 16 of the 28 bases in SLII did not significantly alter binding, reinforcing the suggestion that

sequence-specific contacts are not made with the RNA. Instead, GST-FinO binding was found to be critically dependent on the number of unpaired bases on the 3' side of the stem-loop structure and to a lesser extent, on the 5' side, which again proved to be sequence-independent.

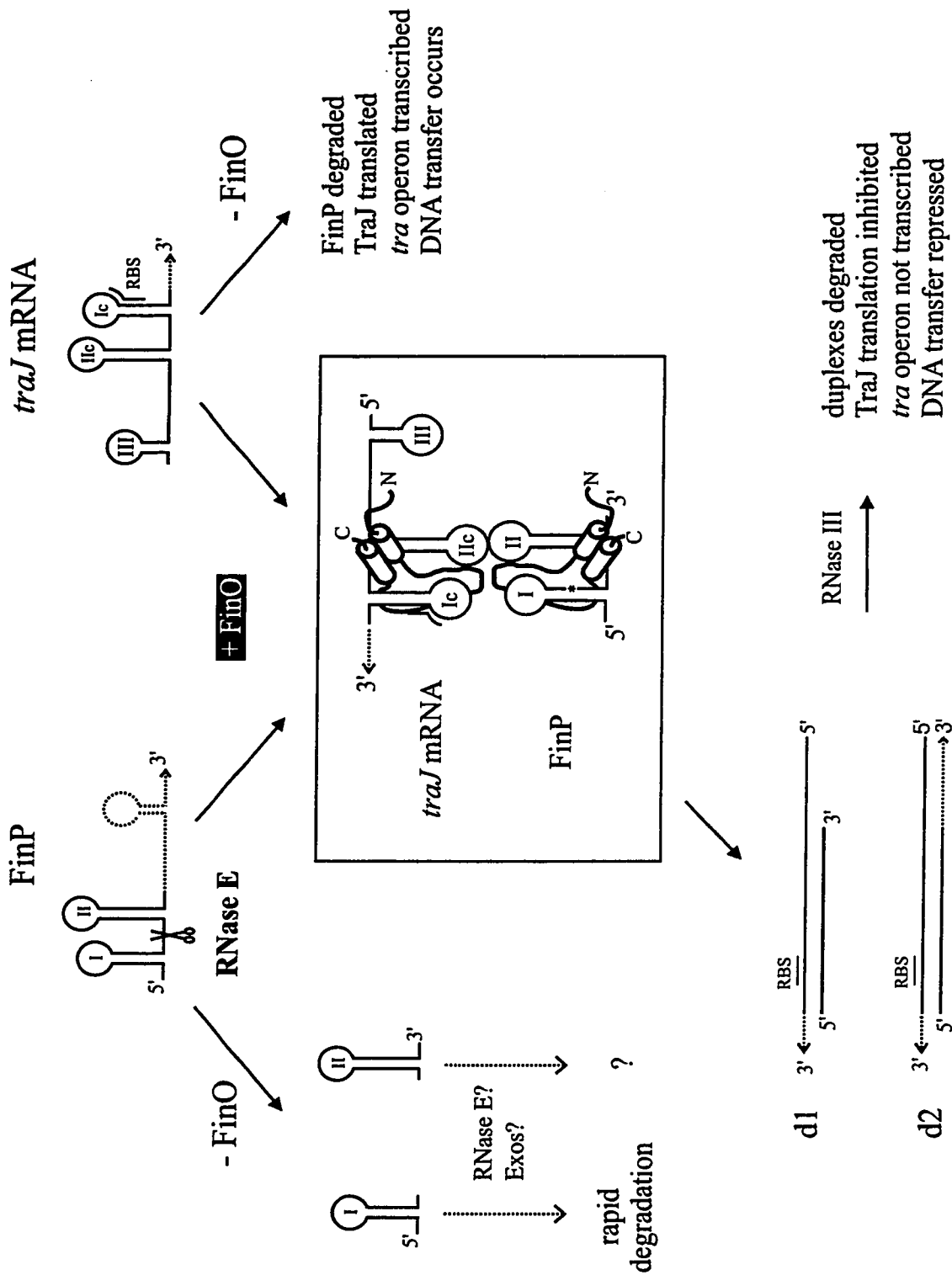
Collectively the data suggest that FinO may bind nonspecifically to double-stranded RNA (eg. *FinP/traJ* mRNA duplex, RNA I), but that specific interaction requires a distinct three-dimensional shape of the target RNA formed by a stem-loop structure flanked by unpaired bases. The stem need not be fully duplexed and the exact sequence of the flanking bases is unimportant. The SLBP also recognizes a stem-loop structure flanked by single-stranded bases, but does so in a sequence-dependent manner. Presumably, this level of sequence-specificity allows the SLBP to discriminate between the highly conserved SL at the 3' end of histone mRNA and other targets within the cell. However, like Rom, which binds any complex formed by pairs of fully complementary sequences, FinO might be expected to have many targets in the cell. The data obtained in this thesis does not explain how FinO would discriminate between target (*FinP* and *traJ* mRNA) and nontarget mRNA *in vivo*, given the number of transcripts that undoubtedly end with similar rho-independent terminators and given the low concentration of FinO. Studies with Rev indicate that a domain within the N-terminus (amino acids 1-66) determines its ability to distinguish between target RRE RNA and nontarget antisense RNA (Daly *et al.*, 1995). It is possible that a segment of the FinO protein or perhaps its interaction with an unidentified protein cofactor, determines whether a potential substrate is bound. A more exhaustive mutational analysis of SLII might reveal sequence-specific protein contacts with one or more of the 12 bases that were not tested in the present study.

#### 7.4 A refined model for Fertility Inhibition

The results obtained in this thesis have been used to generate an updated model of fertility inhibition (Figure 7.1). Immediately following transfer and replication of F-like plasmids, FinP and *traJ* mRNA are transcribed from their own promoters at the 5' end of the *tra* region. A limited amount of FinP is expressed from a weak promoter and terminates either at the rho-independent terminator (SLII) or occasionally, if it pairs with the *traJ* mRNA as it is being synthesized, at an unidentified site downstream. In the absence of FinO, the majority of FinP (79 bases) is cleaved by RNase E between stem-loops I and II. The 5' and 3' fragments are then degraded by an unknown mechanism, which may involve subsequent cuts by RNase E and/or exonuclease activity. In contrast, the *traJ* mRNA is transcribed from a much stronger promoter and accumulates in excess of FinP. This allows for translation of the TraJ protein which activates the *tra* operon, the transfer proteins are synthesized and DNA transfer proceeds. A few rounds of this derepressed state allows the plasmid to establish itself in a new population.

At the same time, the FinO protein (which is weakly expressed from an unknown promoter) begins to accumulate and bind to FinP (79 bases) and *traJ* mRNA. A FinO monomer is shown in the diagram. Its interaction with the RNA is based on a previous model by Sandercock (1997) in combination with the data obtained in this thesis and a very crude approximation of its binding is shown. Specifically, the N-terminal RNA-binding domain is shown to interact with the 3' end of FinP, which would prevent cleavage in the 3' extension of FinP synthesized *in vitro*, whereas the C-terminal  $\alpha$  helix is shown protecting the spacer. The intervening region is shown to weave around SLI, protecting FinP from RNase E cleavage on the 5' side of stem I, but leaving the site of the

**Figure 7.1** Refined model for FinOP fertility inhibition of F-like plasmids (updated from van Biesen, 1994). The majority of FinP terminates at SLII (79 bases). A limited amount of FinP pairs with the *traJ* mRNA before its transcription is complete and terminates at a site further downstream. This longer FinP is indicated with the dotted 3' extension. Based on a model of its functional domains (Sandercock, 1997) and a study of its interactions with RNA (Chapter 6), FinO is shown bound to FinP and *traJ* mRNA as a monomer. Additional monomers (not shown) may interact with FinP SLI and *traJ* mRNA SLIc. The model is described in detail in the text and the drawing is not to scale.





*finP305* mutation on the 3' side exposed. Prevention of FinP degradation and its constitutive expression from a weak promoter, gradually increases its steady-state concentration, favouring its association with the *traJ* mRNA. FinO monomers bound to FinP and *traJ* mRNA enhance formation of duplex d1 by an unknown mechanism. Alternatively, a second monomer of FinO could be bound to FinP SLI and *traJ* mRNA SLIc, as suggested by gel-shift analysis. The longer duplex (d2) would form prior to FinO binding, as FinP is being transcribed. Degradation of both duplexes by RNase III eliminates FinP and *traJ* mRNA from the cell. Consequently, TraJ translation is inhibited, the *tra* operon is no longer transcribed and DNA transfer becomes repressed.

This model is based on the supposition that FinO is transcribed from a promoter other than pY, otherwise repression of the *tra* operon due to sequestration of the *traJ* mRNA by FinP would also repress expression of *finO*. In the absence of FinO, the concentration of FinP would once again fall below that of the *traJ* mRNA and the operon would be reactivated. This would result in continuous cycling between repressed and derepressed states of conjugation, which contradicts the observed 20- to 1000-fold transfer repression conferred by the FinO protein. *finO* might possess its own promoter or could be transcribed from a secondary upstream promoter, such as that for *traD*.

The use of competing activities, RNase E degradation and FinO protection, allows for temporal regulation of FinP antisense RNA levels. This is important because it permits the plasmid to become established in a population, without compromising the survival of its host by the continuous threat of pilus-specific bacteriophage infection. The expression of FinP from a weak promoter and its intermediate half-life (determined by RNase E) is well-suited to respond to FinO. If FinP decayed very rapidly like RNA I,

FinO might not have sufficient time to find and stabilize FinP. However if FinP was expressed from a strong promoter, like RNA I, or if it decayed very slowly, like RNA-OUT, it might accumulate too quickly. In turn, TraJ might never be translated, repression would occur too early and the plasmid might be lost from the population. Instead, the weak expression of FinP and its degradation by RNase E initially keeps the antisense RNA concentration below that of its target, *traJ* mRNA, and permits transient derepression of mating. As the concentration of FinO rises, it competes with RNase E and gradually increases the concentration of FinP to a level that represses conjugation, but only after the plasmid is established in the population.

## 7.5 Future experiments

The present study showed that FinP decay is initiated by RNase E, but the enzymes involved in subsequent degradation of the intermediates were not identified. This was primarily due to the difficulty encountered in detection of the intermediates. Future experiments using alternative denaturants (eg. glyoxal, formaldehyde or methyl mercury) and higher specific activity probes (ie. internally labelled RNA) should facilitate the complete characterization of FinP degradation in a more comprehensive series of RNase-deficient strains. The degradation of *traJ* mRNA was not directly examined in this thesis and might provide additional information with respect to the relative steady-state levels of FinP and *traJ* mRNA. It is unknown whether the enhanced degradation of *traJ* mRNA in the presence of FinP by RNase III is required for prevention of its translation. This could be resolved by comparing FinOP fertility inhibition in wild-type and RNase III strains. If occlusion of the *traJ* mRNA RBS (duplex formation) is

sufficient for inhibition, removal of RNase III should not alter the mating efficiency. Direct evidence for translational inhibition by ribosomal occlusion could be obtained by determining the effect of FinP on the *traJ* mRNA ribosomal “toeprint” (Ma & Simons, 1990).

FinO is proposed to serve two functions in fertility inhibition, only one of which may be essential. Can FinO’s role in FinP stabilization be separated from its role in FinP/*traJ* mRNA duplex formation? The FinP mutation which prevented its decay, *finPcc*, should prove instrumental in answering this question, since it can be crossed into F and its effect on conjugation measured. If mating is repressed by *finPcc* in the absence of FinO, the latter’s role in duplex formation is not essential. On the other hand, if mating is not repressed, this could either indicate that FinO is necessary for efficient duplex formation *in vivo* or that mutation of the spacer sequence prevented duplex formation. A series of experiments could be performed, using the *finPcc* mutant and other variants constructed in this thesis, to define the regions of FinP required for duplex formation with *traJ* mRNA. It would also be of interest to determine whether SLI could repress *traJ* mRNA translation independent of SLII.

Despite years of research, we still do not know from which promoter FinO is transcribed or what its concentration is in the cell. Very simple genetic experiments should reveal the identity of the *finO* promoter and production of highly specific FinO antibodies will allow determination of the intracellular concentration of FinO. Our understanding of the physical interaction between FinO and FinP is clearly in its infancy. Future experiments should include SELEX (systematic evolution of ligands by exponential enrichment; Tuerk & Gold, 1990; Klug & Famulok 1994) to more

extensively characterize the potential RNA targets recognized by FinO. Lacking evidence for base-specific contacts, chemical modification studies to identify amino acid interactions with the ribose 2'-OH group (using partially substituted 2'-deoxy or 2'-methoxy oligomers; Bevilacqua & Cech, 1996) and phosphates (ethylation interference and methylphosphonate substitution) should be performed. A more thorough characterization of the ionic strength-dependence and contribution of electrostatic interactions to FinOP binding should be conducted. Finally, the FinO amino acids required for RNA binding, protection and duplex formation could be identified by alanine-scanning mutagenesis.

## **Chapter 8**

### **References**

- Achtman, M. & Skurray, R.A. (1977). A redefinition of the mating phenomenon in bacteria. In *Microbial interactions: receptors and recognition* (Reissig, J.L., ed), pp. 233-279, Chapman & Hall, Ltd., London.
- Arraiano, C.M., Yancey, S.D. & Kushner, S.R. (1988). Stabilization of discrete mRNA breakdown products in *ams pnp rnb* multiple mutants of *Escherichia coli* K-12. *J. Bacteriol.* **170**, 4625-4633.
- Austin, S. & Nordström, K. (1990). Partition-mediated incompatibility of bacterial plasmids. *Cell* **60**, 351-354.
- Babitzke, P. & Kushner, S.R. (1991). The Ams (altered mRNA stability) protein and ribonuclease E are encoded by the same structural gene of *Escherichia coli*. *Proc. Natl. Acad. Sci., USA* **88**, 1-5.
- Babitzke, P., Granger, L., Olszewski, J. & Kushner, S.R. (1993). Analysis of mRNA decay and rRNA processing in *Escherichia coli* multiple mutants carrying a deletion in RNase III. *J. Bacteriol.* **175**, 229-239.
- Banner, D.W., Kokkinidis, M. & Tsernoglou, D. (1987). Structure of the ColE1 Rop protein at 1.7 angstrom resolution. *J. Mol. Biol.* **196**, 657-675.
- Bartel, D.P., Zapp, M.L., Green, M.R. & Szostak, J.W. (1991). HIV-1 Rev regulation involves recognition of non-Watson-Crick base pairs in viral RNA. *Cell* **67**, 529-536.
- Battiste, J.L., Mao, H., Rao, N.S., Tan, R., Muhandiram, D.R., Kay, L.E., Frankel, A.D. & Williamson, J.R. (1996).  $\alpha$  helix-RNA major groove recognition in an HIV-1 Rev peptide-RRE RNA complex. *Science* **273**, 1547-1551.
- Belasco, J.G. & Higgins, C.F. (1988). Mechanisms of mRNA decay in bacteria: a perspective. *Gene* **72**, 15-23.
- Bessarab, D.A., Kaberdin, V.R., Wei, C-L., Liou, G-G. & Lin-Chao, S. (1998). RNA components of *Escherichia coli* degradosome: Evidence for rRNA decay. *Proc. Natl. Acad. Sci., USA* **95**, 3157-3161.
- Bevilacqua, P.C. & Cech, T.R. (1996). Minor-groove recognition of double-stranded RNA by the double-stranded RNA-binding domain from the RNA-activated protein kinase PKR. *Biochemistry* **35**, 9983-9994.
- Blum, E., Py, B., Carpousis, A.J. & Higgins, C.F. (1997). Polyphosphate kinase is a component of the *Escherichia coli* RNA degradosome. *Mol. Microbiol.* **26**, 387-398.

- Braun, F., Hajnsdorf, E. & Régnier, P. (1996). Polynucleotide phosphorylase is required for the rapid degradation of the RNase E-processed *rpsO* mRNA of *Escherichia coli* devoid of its 3' hairpin. *Mol. Microbiol.* **19**, 997-1005.
- Braun, F., Le Derout, J. & Régnier, P. (1998). Ribosomes inhibit an RNase E cleavage which induces the decay of the *rpsO* mRNA of *Escherichia coli*. *EMBO J.* **17**, 4790-4797.
- Brinton, C.C., Gemski, P. & Carnahan, J. (1964). A new type of bacterial pilus genetically controlled by the fertility factor of *Escherichia coli* K 12 and its role in chromosome transfer. *Proc. Natl. Acad. Sci., USA* **52**, 776-783.
- Broda, P. (1975). Transience of the donor state in an *Escherichia coli* K 12 strain carrying a repressed R factor. *Mol. Gen. Genet.* **138**, 65-69.
- Burd, C.G. & Dreyfuss, G. (1994). Conserved structures and diversity of functions of RNA-binding proteins. *Science* **265**, 615-621.
- Cannistraro, V.J., Subbarao, M.N. & Kennell, D. (1986). Specific endonucleolytic cleavage sites for decay of *Escherichia coli* mRNA. *J. Mol. Biol.* **192**, 257-274.
- Cannistraro, V.J. & Kennell, D. (1991). RNase I\*, a form of RNase I, and mRNA degradation in *Escherichia coli*. *J. Bacteriol.* **173**, 4653-4659.
- Cannistraro, V.J. & Kennell, D. (1993). The 5' ends of RNA oligonucleotides in *Escherichia coli* and mRNA degradation. *Eur. J. Biochem.* **213**, 285-293.
- Cao, G-J. & Sarkar, N. (1992). Identification of the gene for an *Escherichia coli* poly(A)polymerase. *Proc. Natl. Acad. Sci., USA* **89**, 10380-10384.
- Cao, G-J., Kalapos, M.P. & Sarkar, N. (1997). Polyadenylated mRNA in *Escherichia coli*: modulation of poly(A) RNA levels by polynucleotide phosphorylase and ribonuclease II. *Biochimie* **79**, 211-220.
- Carpousis, A.J., Van Houwe, G., Ehretsmann, C. & Krisch, H.M. (1994). Copurification of *E. coli* RNase E and PNPase: evidence for a specific association between two enzymes important in RNA processing and degradation. *Cell* **76**, 889-900.
- Case, C.C., Simons, E.L., & Simons, R.W. (1990). The IS10 transposase mRNA is destabilized during antisense RNA control. *EMBO J.* **9**, 1259-1266.
- Case, C.C., Roels, S.M., Jensen, P.D., Lee, J., Kleckner, N. & Simons, R.W. (1989). The unusual stability of the IS10 antisense RNA is critical for its function and is determined by the structure of its stem-domain. *EMBO J.* **8**, 4297-4305.

- Causton, H., Py, B., McLaren, R.S. & Higgins, C.F. (1994). mRNA degradation in *Escherichia coli*: a novel factor which impedes the exoribonucleolytic activity of PNPase at stem-loop structures. *Mol. Microbiol.* **14**, 731-741.
- Cesareni, G., Cornelissen, M., Lacatena, R. & Castagnoli, L. (1984). Control of pMB1 replication: inhibition of primer formation by Rop requires RNA I. *EMBO J.* **3**, 1365-1369.
- Cesareni, G., Muesing, M.A. & Polisky, B. (1982). Control of ColE1 DNA replication: the Rop gene product negatively affects transcription from the replication primer promoter. *Proc. Natl. Acad. Sci., USA* **79**, 6313-6317.
- Chandler, M., & Galas, D. (1983). Cointegrate formation mediated by Tn9. II. Activity of IS1 is modulated by external DNA sequences. *J. Mol. Biol.* **170**, 61-91.
- Chang, A.C.Y. & Cohen, S.N. (1978). Construction and characterization of amplifiable multicopy DNA cloning vehicles derived from the p15A cryptic miniplasmid. *J. Bacteriol.* **134**, 1141-1156.
- Chang, K-Y. & Tinoco, I. Jr. (1997). The structure of an RNA "kissing" hairpin complex of the HIV TAR hairpin loop and its complement. *J. Mol. Biol.* **269**, 52-66.
- Cheah, K-C., Ray, A. & Skurray, R. (1984). Cloning and molecular analysis of the *finO* region from the antibiotic resistance plasmid R6-5. *Plasmid* **12**, 222-226.
- Cheah, K-C. & Skurray, R. (1986). The F plasmid contains an IS3 insertion within *finO*. *J. Gen. Microbiol.* **132**, 3269-3275.
- Coburn, G.A. & Mackie, G.A. (1996a). Overexpression, purification, and properties of *Escherichia coli* Ribonuclease II. *J. Biol. Chem.* **271**, 1048-1053.
- Coburn, G.A. & Mackie, G.A. (1996b). Differential sensitivities of portions of the mRNA for ribosomal protein S20 to 3'-exonucleases dependent on oligoadenylation and RNA secondary structure. *J. Biol. Chem.* **271**, 15776-15781.
- Coburn, G.A. & Mackie, G.A. (1998). Reconstitution of the degradation of the mRNA for ribosomal protein S20 with purified enzymes. *J. Mol. Biol.* **279**, 1061-1074.
- Cohen, S.N. (1995). Surprises at the 3' end of prokaryotic RNA. *Cell* **80**, 829-832.
- Cormack, R.S., Genereaux, J.L. & Mackie, G.A. (1993). RNase E activity is conferred by a single polypeptide: Overexpression, purification, and properties of the *ams/rne/hmp1* gene product. *Proc. Natl. Acad. Sci., USA* **90**, 9006-9010.



- Court, D. (1993). RNA processing and degradation by RNase III. In *Control of mRNA stability* (Belasco, J.G. & Brawerman, G., eds), pp. 71-116, Academic Press, Orlando, FL.
- Cullen, B.R. (1992). Mechanism of action of regulatory proteins encoded by complex retroviruses. *Microbiol. Rev.* **56**, 375-394
- Daly, T.J., Rusche, J.R., Maione, T.E. & Frankel, A.D. (1990). Circular dichroism studies of the HIV-1 Rev protein and its specific RNA binding site. *Biochemistry* **29**, 9791-9795.
- Daly, T.J., Doten, R.C., Rusche, J.R. & Auer, M. (1995). The amino terminal domain of HIV-1 Rev is required for discrimination of the RRE from nonspecific RNA. *J. Mol. Biol.* **253**, 243-258.
- Danese, P.N. & Silhavy, T.J. (1998). CpxP, a stress-combative member of the Cpx regulon. *J. Bacteriol.* **180**, 831-839.
- Danese, P.N., Snyder, W.B., Cosma, C.L., Davis, L.J.B. & Silhavy, T.J. (1995). The Cpx two-component signal transduction pathway of *Escherichia coli* regulates transcription of the gene specifying the stress-inducible periplasmic protease, DegP. *Genes Dev.* **9**, 387-398.
- Datta, N. (1975). Epidemiology and classification of plasmids. In *Microbiology-1974* (Schlessinger, D., ed), pp. 9-15, American Society for Microbiology, Washington, D.C.
- Davis, B.D. (1950). Nonfiltrability of the agents of genetic recombination in *Escherichia coli*. *J. Bacteriol.* **60**, 507-508.
- Dempsey, W.B. (1987). Transcript analysis of the plasmid R100 *traJ* and *finP* genes. *Mol. Gen. Genet.* **209**, 533-544.
- Dempsey, W.B. (1989). Sense and antisense transcripts of *traM*, a conjugal transfer gene of the antibiotic resistance plasmid R100. *Mol. Microbiol.* **3**, 561-570.
- Dempsey, W.B. (1994a). *traJ* sense RNA initiates at two different promoters in R100-1 and forms two stable hybrids with antisense *finP* RNA. *Mol. Microbiol.* **13**, 313-326.
- Dempsey, W.B. (1994b). Regulation of R100 conjugation requires *traM* in cis to *traJ*. *Mol. Microbiol.* **13**, 987-1000.
- Deutscher, M.P. (1993). Ribonuclease multiplicity, diversity, and complexity. *J. Biol. Chem.* **268**, 13011-13014.

- Deutscher, M.P. & Reuven, N.B. (1991). Enzymatic basis for hydrolytic versus phosphorylytic mRNA degradation in *Escherichia coli* and *Bacillus subtilis*. *Proc. Natl. Acad. Sci., USA* **88**, 3277-3280.
- Di Laurenzio, L., Finlay, B.B., Frost, L.S. & Paranchych, W. (1991). Characterization of the *oriT* region of the IncFV plasmid pED208. *Mol. Microbiol.* **5**, 1779-1790
- Di Laurenzio, L., Frost, L.S. & Paranchych, W. (1992). The TraM protein of the conjugative plasmid F binds to the origin of transfer of the F and ColE1 plasmids. *Mol. Microbiol.* **6**, 2951-2959.
- Donovan, W.P. & Kushner, S.R. (1986). Polynucleotide phosphorylase and ribonuclease II are required for cell viability and mRNA turnover in *Escherichia coli* K-12. *Proc. Natl. Acad. Sci., USA* **83**, 120-124.
- Draper, D.E. (1994). RNA-protein interactions in ribosomes. In *RNA-Protein Interactions* (Nagai, K. & Mattaj, I.W., eds), pp. 82-102, Oxford University Press, Oxford.
- Draper, D.E. (1995). Protein-RNA recognition. *Annu. Rev. Biochem.* **64**, 593-620.
- Eguchi, Y. & Tomizawa, J-I. (1990). Complex formed by complementary RNA stem-loops and its stabilization by a protein: function of ColE1 Rom protein. *Cell* **60**, 199-209.
- Eguchi, Y., Itoh, T. & Tomizawa, J-I. (1991). Antisense RNA. *Annu. Rev. Biochem.* **60**, 631-652.
- Eguchi, Y. & Tomizawa, J-I. (1991). Complexes formed by complementary RNA stem-loops. Their formations, structures and interaction with ColE1 Rom protein. *J. Mol. Biol.* **220**, 831-842.
- Ehretsmann, C.P., Carpousis, A.J. and Krisch, H.M. (1992a). Specificity of *Escherichia coli* endoribonuclease RNase E: *in vivo* and *in vitro* analysis of mutants in a bacteriophage T4 mRNA processing site. *Genes & Dev.* **6**, 149-159.
- Ehretsmann, C.P., Carpousis, A.J. and Krisch, H.M. (1992b). mRNA degradation in prokaryotes. *FASEB J.* **6**, 3186-3192.
- Finnegan, D.J. & Willetts, N.S. (1971). Two classes of *Flac* mutants insensitive to transfer inhibition by an F-like R factor. *Mol. Gen. Genet.* **111**, 256-264.
- Finnegan, D.J. & Willetts, N.S. (1973). The site of action of the F transfer inhibitor. *Mol. Gen. Genet.* **127**, 307-316.

- Finlay, B.B., Frost, L.S., Paranchych, W. & Willetts, N.S. (1986). Nucleotide sequences of five IncF plasmid *finP* alleles. *J. Bacteriol.* **167**, 754-757.
- Firth, N., Ippen-Ihler, K. & Skurray, R.A. (1996). Structure and function of the F factor and mechanism of conjugation. In *Escherichia coli and Salmonella*, 2<sup>nd</sup> edition (Neidhardt, F.C., ed), pp. 2377-2401, American Society for Microbiology, Washington, D.C.
- Frost, L.S., Ippen-Ihler, K. & Skurray, R.A. (1994). Analysis of the sequence and gene products of the transfer region of the F sex factor. *Microbiol. Rev.* **58**, 162-210.
- Frost, L.S., Lee, S., Yanchar, N., & Paranchych, W. (1989). *finP* and *fisO* mutations in FinP antisense RNA suggest a model for FinOP action in the repression of bacterial conjugation by the *Flac* plasmid JCFLO. *Mol. Gen. Genet.* **218**, 152-160.
- Gaffney, D., Skurray, R. & Willetts, N.S. (1983). Regulation of the F conjugation genes studied by hybridization and *tra-lacZ* fusion. *J. Mol. Biol.* **168**, 103-122.
- Gaudin, H.M. & Silverman, P.M. (1993). Contributions of promoter context and structure to regulated expression of the F plasmid *traY* promoter in *Escherichia coli* K-12. *Mol. Microbiol.* **8**, 335-342.
- Gegenheimer, P., Watson, N. & Apirion, D. (1977). Multiple pathways for primary processing of ribosomal RNA in *Escherichia coli*. *J. Biol. Chem.* **252**, 3064-3073.
- Georgellis, D., Sohlberg, B., Hartl, F.U. & von Gabain, A. (1995). Identification of GroEL as a constituent of an mRNA-protection complex in *Escherichia coli*. *Mol. Microbiol.* **16**, 1259-1268.
- Ghora, B.K. & Apirion, D. (1978). Structural analysis and *in vitro* processing of p5 rRNA of a 9S RNA molecule isolated from an *rne* mutant of *E. coli*. *Cell* **15**, 1055-1066.
- Goldblum, K. & Apirion, D. (1981). Inactivation of the ribonucleic acid-processing enzyme ribonuclease E blocks cell division. *J. Bacteriol.* **146**, 128-132.
- Graus-Goldner, A., Graus, H., Schlacher, T. & Hogenauer, G. (1990). The sequences of genes bordering *oriT* in the enterotoxin plasmid P307: comparison with the sequences of plasmids F and R1. *Plasmid* **24**, 119-131.
- Gregorian, R.S. & Crothers, D.M. (1995). Determinants of RNA hairpin loop-loop complex stability. *J. Mol. Biol.* **248**, 968-984.

- Griffith, F. (1928). The significance of pneumococcol types. *J. Hygiene* **27**, 113-159.
- Hajnsdorf, E., Steier, O., Coscoy, L., Teyssset, L. & Régnier, P. (1994). Roles of RNase E, RNase II and PNPase in the degradation of the *rpsO* transcripts of *Escherichia coli*: stabilizing function of RNase II and evidence for efficient degradation in an *ams pnp rnb* mutant. *EMBO J.* **13**, 3368-3377.
- Hajnsdorf, E., Braun, F., Haugel-Nielsen, J. & Régnier, P. (1995). Polyadenylation destabilizes the *rpsO* mRNA of *Escherichia coli*. *Proc. Natl. Acad. Sci., USA* **92**, 3973-3977.
- Hajnsdorf, E., Braun, F., Haugel-Nielsen, J., Le Derout, J. & Régnier, P. (1996). Multiple degradation pathways of the *rpsO* mRNA of *Escherichia coli*. RNase E interacts with the 5' and 3' extremities of the primary transcript. *Biochimie* **78**, 416-424.
- Hanahan, D. (1983). Studies on the transformation of *Escherichia coli* with plasmids. *J. Mol. Biol.* **166**, 557-580.
- Hanson, R.J., Sun, J-H., Willis, D.G. & Marzluff, W.F. (1996). Efficient extraction and partial purification of the polyribosome-associated stem-loop binding protein bound to the 3' end of histone mRNA. *Biochemistry* **35**, 2146-2156.
- Harwood, C.R. & Meynell, E. (1975). Cyclic AMP and the production of sex pili by *E. coli* K-12 carrying derepressed sex factors. *Nature* **254**, 628-630.
- Haugel-Nielsen, J., Hajnsdorf, E. & Régnier, P. (1996). The *rpsO* mRNA of *Escherichia coli* is polyadenylated at multiple sites resulting from endonucleolytic processing and exonucleolytic degradation. *EMBO J.* **15**, 3144-3152.
- Hayes, W. (1952). Recombination in *Bact. coli* K12: Unidirectional transfer of genetic material. *Nature* **169**, 118-119.
- Hayes, W. (1953). Observations on a transmissible agent determining sexual differentiation in *Bacterium coli*. *J. Gen. Microbiol.* **8**, 72-88.
- He, L., Söderbom, F., Wagner, E.G.H., Binnie, U., Binns, N. & Masters, M. (1993). PcnB is required for the rapid degradation of RNA I, the antisense RNA that controls the copy number of ColE1-related plasmids. *Mol. Microbiol.* **9**, 1131-1142.
- Heaphy, S., Dingwall, C., Ernberg, I., Gait, M.J., Green, S.M., Karn, J., Lowe, A.D., Singh, M. & Skinner, M.A. (1990). HIV-1 regulator of virion expression (Rev) protein binds to an RNA stem-loop structure located within the Rev response element region. *Cell* **60**, 685-693.

- Heaphy, S., Finch, J.T., Gait, M.J., Karn, J. & Singh, M. (1991). Human immunodeficiency virus type I regulator of virion expression, *rev*, forms nucleoprotein filaments after binding to a purine-rich "bubble" located within the *rev*-responsive region of viral RNA. *Proc. Natl. Acad. Sci., USA* **88**, 7366-7370.
- Hedges, R.W., Datta, N., Coetzee, J.N. & Dennison, S. (1973). R factors from *Proteus morganii*. *J. Gen. Microbiol.* **77**, 249-259.
- Heinemann, J.A. & Ankenbauer, R.G. (1993a). Retrotransfer in *Escherichia coli* conjugation: bidirectional exchange or de novo mating? *J. Bacteriol.* **175**, 583-588.
- Heinemann, J.A. & Ankenbauer, R.G. (1993b). Retrotransfer of IncP plasmid R751 from *Escherichia coli* maxicells: evidence for the genetic sufficiency of self-transferable plasmids for bacterial conjugation. *Mol. Microbiol.* **10**, 57-62.
- Heinemann, J.A., Scott, H.E. & Williams, M. (1996). Doing the conjugative two-step: Evidence of recipient autonomy in retrotransfer. *Genetics* **143**, 1425-1435.
- Helmer-Citterich, M., Anceschi, M.M., Banner, D.W. & Cesareni, G. (1988). Control of ColE1 replication: low affinity specific binding of Rop (Rom) to RNAI and RNAII. *EMBO J.* **7**, 557-566.
- Hjalt, T.A. & Wagner, E.G.H. (1992). The effect of loop size in antisense and target RNAs on the efficiency of antisense RNA control. *Nucl. Acids. Res.* **20**, 6723-6732.
- Hjalt, T.A. & Wagner, E.G.H. (1995). Bulged-out nucleotides protect an antisense RNA from RNase III cleavage. *Nucl. Acids Res.* **23**, 571-579.
- Huang, H., Liao, J. & Cohen, S.N. (1998). Poly(A)- and poly(U)-specific RNA 3' tail shortening by *E. coli* ribonuclease E. *Nature.* **391**, 99-102.
- Ippen-Ihler, K. & Skurray, R.A. (1993). Genetic organization of transfer-related determinants on the sex factor F and related plasmids. In *Bacterial Conjugation* (Clewell, D., ed), pp. 23-52, Plenum Press, New York.
- Itoh, T. & Tomizawa, J-I. (1980). Formation of an RNA primer for initiation of replication of ColE1 DNA by ribonuclease H. *Proc. Natl. Acad. Sci., USA* **77**, 2450-2454.
- Iwai, S., Pritchard, C., Mann, D.A., Karn, J. & Gait, M.J. (1992). Recognition of the high affinity binding site in *rev*-response element RNA by the Human Immunodeficiency Virus type-1 *rev* protein. *Nucl. Acids Res.* **20**, 6465-6472.

- Jacob, F. & Wollman, E.L. (1955). Étapes de la recombinaison génétiques chez *Escherichia coli* K 12. *Comptes rendus Académie des Sciences* **240**, 2566-2568.
- Jain, C. (1995). IS10 antisense control *in vivo* is affected by mutations throughout the region of complementarity between the interacting RNAs. *J. Mol. Biol.* **246**, 585-594.
- Kaberdin, V.R., Chao, Y-H, and Lin-Chao, S. (1996). RNase E cleaves at multiple sites in bubble regions of RNA I stem loops yielding products that dissociate differentially from the enzyme. *J. Biol. Chem.* **271**, 13103-13109.
- Kalapos, M.P., Cao, G-J., Kushner, S.R. & Sarkar, N. (1994). Identification of a second poly(A)polymerase in *Escherichia coli*. *Biochem. Biophys. Res. Com.* **198**, 459-465.
- Kittle, J.D., Simons, R.W., Lee, J. & Kleckner, N. (1989). Insertion sequence IS10 antisense pairing initiates by an interaction between the 5' end of the target RNA and a loop in the antisense RNA. *J. Mol. Biol.* **210**, 561-572.
- Kjems, J., Brown, M., Chang, D.D. & Sharp, P.A. (1991). Structural analysis of the interaction between the human immunodeficiency virus Rev protein and the Rev response element. *Proc. Natl. Acad. Sci., USA* **88**, 683-687.
- Kjems, J., Calnan, B., Frankel, A.D. & Sharp, P.A. (1992). Specific binding of a basic peptide from HIV-1 Rev. *EMBO J.* **11**, 1119-1129.
- Klee, C.B. & Singer, M.F. (1968). The processive degradation of individual polyribonucleotide chains. II. *Micrococcus lysodeikticus* polynucleotide phosphorylase. *J. Biol. Chem.* **243**, 923-927.
- Klug, S.J. & Famulok, M. (1994). All you wanted to know about SELEX. *Mol. Biol. Rep.* **20**, 97-107.
- Knee, R. & Murphy, P.R. (1997). Regulation of gene expression by natural antisense RNA transcripts. *Neurochem. Int.* **31**, 379-392.
- Koraimann, G., Koraimann, C., Koronakis, V., Schlager, S & Högenauer, G. (1991). Repression and derepression of conjugation of plasmid R1 by wild-type and mutated *finP* antisense RNA. *Mol. Microbiol.* **5**, 77-87.
- Koraimann, G., Teferle, K., Markolin, G., Woger, W. & Högenauer, G. (1996). The FinOP repressor system of plasmid R1: analysis of the antisense RNA control of *traJ* expression and conjugative DNA transfer. *Mol. Microbiol.* **21**, 811-821.

- Kraft, R., Tardiff, J., Krauter, K.S. & Leinwand, L.A. (1988). Using mini-prep plasmid DNA for sequencing double-stranded templates with Sequenase. *Biotechniques* **6**, 544-547.
- Krinke, L. & Wulff, D.L. (1990). The cleavage specificity of RNase III. *Nucl. Acids. Res.* **18**, 4809-4815.
- Lacatena, R.M., Banner, D.W., Castagnoli, L. & Cesareni, G. (1984). Control of initiation of pMB1 replication: purified Rop protein and RNA I affect primer formation *in vitro*. *Cell* **37**, 1009-1014.
- Lacatena, R.M. & Cesareni, G. (1981). Base-pairing of RNA I with its complementary sequence in the primer precursor inhibits ColE1 replication. *Nature* **294**, 623-626.
- Lawn, A.M., Meynell, G.G., Meynell, E. & Datta, N. (1967). Sex pili and the classification of sex factors in the *Enterobacteriaceae*. *Nature* **216**, 343-346.
- Lazinski, D., Grzadzielska, E. & Das, A. (1989). Sequence-specific recognition of RNA hairpins by bacteriophage antiterminators requires a conserved arginine-rich motif. *Cell* **59**, 207-218.
- Lederberg, J., Cavalli, L.J. & Lederberg, E.M. (1952). Sex compatibility in *Escherichia coli*. *Genetics* **37**, 720-730.
- Lederberg, J. & Tatum, E.L. (1946). Gene recombination in *Escherichia coli*. *Nature* **158**, 558.
- Lee, S.H., Frost, L.S. & Paranchych, W. (1992). FinOP repression of the F plasmid involves extension of the half-life of FinP antisense RNA by FinO. *Mol. Gen. Genet.* **235**, 131-139.
- Lin-Chao, S. & Bremer, H. (1987). Activities of the RNA I and RNA II promoters of plasmid pBR322. *J. Bacteriol.* **169**, 1217-1222.
- Lin-Chao, S. & Cohen, S.N. (1991). The rate of processing and degradation of antisense RNA I regulates the replication of ColE1-type plasmids *in vivo*. *Cell* **65**, 1233-1242.
- Lin-Chao, S., Chen, W-T. & Wong, T-T. (1992). High copy number of the pUC plasmid results from a Rom/Rop-suppressible point mutation in RNA II. *Mol. Microbiol.* **6**, 3385-3393.

- Lin-Chao, S., Wong, T.T., McDowall, K.J. & Cohen, S.N. (1994). Effects of nucleotide sequence on the specificity of *rne*-dependent and RNase E-mediated cleavages of RNA I encoded by the pBR322 plasmid. *J. Biol. Chem.* **269**, 10797-10803.
- Littauer, U.Z. & Soreq, H. (1982). Polynucleotide phosphorylase. In *The Enzymes* (Boyer, D., ed), vol. XV, part B, pp. 518-553, Academic Press, New York.
- Lynch, A.S. & Lin, C.C. (1996). Transcriptional control mediated by the ArcA two-component response regulator protein of *Escherichia coli*: characterization of DNA binding at target promoters. *J. Bacteriol.* **178**, 6238-6249.
- Ma, C. & Simons, R.W. (1990). The IS10 antisense RNA blocks ribosome binding at the transposase translation initiation site. *EMBO J.* **9**, 1267-1274.
- Mackie, G.A. (1991). Specific endonucleolytic cleavage of the mRNA for ribosomal protein S20 of *Escherichia coli* requires the product of the *ams* gene *in vivo* and *in vitro*. *J. Bacteriol.* **173**, 2488-2497.
- Mackie, G.A. (1992). Secondary structure of the mRNA for ribosomal protein S20: implications for cleavage by ribonuclease E. *J. Biol. Chem.* **267**, 1054-1061.
- Mackie, G.A., Genereaux, J.L. & Masterman, S.K. (1997). Modulation of the activity of RNase E *in vitro* by RNA sequences and secondary structures 5' to cleavage sites. *J. Biol. Chem.* **272**, 609-616.
- Malim, M.H. & Cullen, B.R. (1991). HIV-1 structural gene expression requires the binding of multiple Rev monomers to the viral RRE: implications for HIV-1 latency. *Cell* **65**, 241-248.
- Mann, D.A., Mikaélian, I., Zimmel, R.W., Green, S.M., Lowe, A.D., Kimura, T., Singh, M., Butler, P.J.G., Gait, M.J. & Karn, J. (1994). A molecular rheostat: cooperative Rev binding to stem I of the Rev-response element modulates Human Immunodeficiency Virus Type-I late gene expression. *J. Mol. Biol.* **241**, 193-207.
- Marino, J.P., Gregorian, R.S. Jr., Csankovszki, G. & Crothers, D.M. (1995). Bent helix formation between RNA hairpins with complementary loops. *Science* **268**, 1448-1454.
- Marmur, J., Rownd, R., Falkow, S., Baron, L.S., Schildkraut, C. & Doty, P. (1961). The nature of intergeneric episomal infection. *Proc. Natl. Acad. Sci., USA* **47**, 972-979.
- Marzluff, W.F. (1992). Histone 3' ends: essential and regulatory functions. *Gene Exp.* **2**, 93-97.



- Masukata, H.W. & Tomizawa, J-I. (1986). Control of primer formation of ColE1 plasmid replication: conformational change of the primer transcript. *Cell* **44**, 125-136.
- Mattaj, I.W. (1993). RNA Recognition: A Family Matter? *Cell* **73**, 837-840
- Mazodier, P. & Davies, J. (1991). Gene transfer between distantly related bacteria. *Annu. Rev. Genet.* **25**, 147-171.
- McDowall, K.J., Hernandez, R.G., Lin-Chao, S. & Cohen, S.N. (1993). The *ams-1* and *mre-3071* temperature-sensitive mutations in the *ams* gene are in close proximity to each other and cause substitutions within a domain that resembles a product of the *Escherichia coli mre* locus. *J. Bacteriol.* **175**, 4245-4249.
- McDowall, K.J., Lin-Chao, S., & Cohen, S.N. (1994). A + U content rather than a particular nucleotide order determines the specificity of RNase E cleavage. *J. Biol. Chem.* **269**, 10790-10796.
- McDowall, K.J. & Cohen, S.N. (1996). The N-terminal domain of the *mre* gene product has RNase E activity and is non-overlapping with the arginine-rich RNA-binding site. *J. Mol. Biol.* **255**, 349-355.
- McIntire, S.A. & Dempsey, W.B. (1987). Fertility inhibition gene of plasmid R100. *Nucl. Acids Res.* **15**, 2029-2042.
- McLaren, R.S., Newbury, S.F., Dance, G.S.C., Causton, H.C. & Higgins, C.F. (1991). mRNA degradation by processive 3'-5' exoribonucleases *in vitro* and the implications for prokaryotic mRNA decay *in vivo*. *J. Mol. Biol.* **221**, 81-95.
- Miczak, A., Kaberdin, V.R., Wei, C-L & Lin-Chao, S. (1996). Proteins associated with RNase E in a multicomponent ribonucleolytic complex. *Proc. Natl. Acad. Sci., USA* **93**, 3865-3869.
- Mikkelsen, N.D. & Gerdes, K. (1997). Sok antisense RNA from plasmid R1 is functionally inactivated by RNase E and polyadenylated by poly(A) polymerase I. *Mol. Microbiol.* **26**, 311-320.
- Miller, J.H. (1992). *In A short course in bacterial genetics.* pp. 72-74, Cold Spring Harbor Press, Cold Spring Harbor, New York.
- Misra, T.K. & Apirion, D. (1979). RNase E an RNA processing enzyme from *Escherichia coli*. *J. Biol. Chem.* **254**, 11154-11159.
- Morisato, D., Way, J.C., Kim, H-J. & Kleckner, N. (1983). *Tn10* transposase acts preferentially on nearby ends *in vivo*. *Cell* **32**, 799-807.

- Mott, J.E., Galloway, J.C. & Platt, T. (1985). The mature 3' end of *E. coli* tryptophan operon mRNA appears to be generated by processing after rho-dependent termination. *EMBO J.* **4**, 1887-1891.
- Mudd, E.A., Krisch, H.M. & Higgins, C.F. (1990). RNase E, an endoribonuclease, has a general role in the chemical decay of *Escherichia coli* mRNA: evidence that *rne* and *ams* are the same genetic locus. *Mol. Microbiol.* **4**, 2127-2135.
- Mullineaux, P. & Willetts, N.S. (1985). Promoters in the transfer region of plasmid F. In *Plasmids in bacteria* (Helinski, D.R., Cohen, S.N., Clewell, D.B., Jackson, D.A. & Hollaender, A., eds), pp. 605-614, Plenum Publishing Corp., New York.
- Nakazato, H., Venkatesan, S. & Edmonds, M. (1975). Polyadenylic acid sequences in *E. coli* messenger RNA. *Nature* **256**, 144-146.
- Nelson, W.C., Morton, B.S., Lahue, E.E. & Matson, S.W. (1993). Characterization of the *Escherichia coli* F factor *traY* gene product and its binding sites. *J. Bacteriol.* **175**, 2221-2228.
- Nierlich, D.P. & Murakawa, G.J. (1996). The decay of bacterial messenger RNA. *Prog. Nucl. Acids Res.* **52**, 153-216.
- Niyogi, S.K. & Datta, A.K. (1975). A novel oligoribonuclease of *Escherichia coli*. I. Isolation and properties. *J. Biol. Chem.* **250**, 7307-7312.
- Nossal, N.G. & Singer, M.F. (1968). The processive degradation of individual polyribonucleotide chains. I. *Escherichia coli* ribonuclease II. *J. Biol. Chem.* **243**, 913-922.
- Novotny, C.P. & Fives-Taylor, P. (1974). Retraction of F pili. *J. Bacteriol.* **117**, 1306-1311.
- O'Hara, E.B., Chekanova, J.A., Ingle, C.A., Kushner, Z.R., Peters, E. & Kushner, S.R. (1995). Polyadenylation helps regulate mRNA decay in *Escherichia coli*. *Proc. Natl. Acad. Sci., USA* **92**, 1807-1811.
- Ono, M. & Kuwano, M. (1979). A conditional lethal mutation in an *Escherichia coli* strain with a longer chemical lifetime of mRNA. *J. Mol. Biol.* **129**, 343-357.
- Pan, T., Long, D.M. & Uhlenbeck, O.C. (1993). Divalent metal ions in RNA folding and catalysis. In *The RNA World* (Gesteland, R.F. & Atkins, J.F., eds), pp. 271-302, Cold Spring Harbor Laboratory Press, New York.

- Pandey, N.B. & Marzluff, W.F. (1987). The stem-loop structure at the 3' end of histone mRNA is necessary and sufficient for regulation of histone mRNA stability. *Mol. Cell. Biol.* **7**, 4557-4559.
- Pandey, N.B., Sun, J-H. & Marzluff, W.F. (1991). Different complexes are formed on the 3' end of histone mRNA in nuclear and polysomal extracts. *Nucl. Acids Res.* **19**, 5653-5659.
- Pandey, N.B., Williams, A.S., Sun, J-H., Brown, V.D., Bond, U. & Marzluff, W.F. (1994). Point mutations in the stem-loop at the 3' end of mouse histone mRNA reduce expression by reducing the efficiency of 3' end formation. *Mol. Cell. Biol.* **14**, 1709-1720.
- Paranchych, W., Finlay, B.B. & Frost, L.S. (1986). Studies on the regulation of IncF plasmid transfer operon expression. In *Antibiotic resistance genes: ecology, transfer and expression* (Levy, S.B. & Novick, R.P., eds), pp. 117-129, Cold Spring Harbor Laboratory, Cold Spring Harbor, New York.
- Penfold, S.S. (1995). PhD Thesis, University of Alberta. Edmonton, Alberta.
- Penfold, S.S., Simon, J. & Frost, L.S. (1996). Regulation of the expression of the *traM* gene of the F sex factor of *Escherichia coli*. *Mol. Microbiol.* **20**, 549-558.
- Pepe, C.M., Maslesa-Galic, S. & Simons, R.W. (1994). Decay of the *IS10* antisense RNA by 3' exoribonucleases: evidence that RNase II stabilizes RNA-OUT against PNPase attack. *Mol. Microbiol.* **13**, 1133-1142.
- Peterson, R.D. & Feigon, J. (1996). Structural change in Rev responsive element RNA of HIV-1 on binding Rev peptide. *J. Mol. Biol.* **264**, 863-877.
- Plumbridge, J.A., Dondon, J., Nakamura, Y. & Grunberg-Manago, M. (1985). Effect of NusA protein on expression of the *nusA*, *infB* operon in *E. coli*. *Nucl. Acids Res.* **13**, 3371-3388.
- Predki, P.F., Nayak, L.M., Gottlieb, M.B.C. & Regan, L. (1995). Dissecting RNA-protein interactions: RNA-RNA recognition by Rop. *Cell* **80**, 41-50.
- Py, B., Causton, H., Mudd, E.A. & Higgins, C.F. (1994). A protein complex mediating mRNA degradation in *Escherichia coli*. *Mol. Microbiol.* **14**, 717-729.
- Py, B., Higgins, C.F., Krisch, H.M. & Carpousis, A.J. (1996). A DEAD-box RNA helicase in the *Escherichia coli* RNA degradosome. *Nature* **381**, 169-172.
- Record, M.T., Lohman, T.M. & de Haseth, P. (1976). Ion effects on ligand-nucleic acid interactions. *J. Mol. Biol.* **107**, 145-158.

- Robertson, H.D., Webster, R.E. & Zinder, N.D. (1968). Purification and properties of ribonuclease III from *Escherichia coli*. *J. Biol. Chem.* **243**, 82-91.
- Ronald, S.L., Kropinski, A.M. & Farinha, M.A. (1990). Construction of broad-host-range vectors for the selection of divergent promoters. *Gene* **90**, 145-148.
- Ross, J. (1995). mRNA stability in mammalian cells. *Microbiol. Rev.* **59**, 423-450.
- Sachs, A.B. (1993). mRNA degradation in eukaryotes. *Cell* **74**, 413-421.
- Sandercock, J.R. (1997). MSc Thesis, University of Alberta. Edmonton, Alberta.
- Sandercock, J.R. & Frost, L.S. (1998). Analysis of the major domains of the F fertility inhibition protein, FinO. *Mol. Gen. Genet.* **259**, 622-629.
- Shen, V. & Schlessinger, D. (1982). RNases I, II, and IV of *Escherichia coli*. In *The enzymes* (Boyer, P.D., ed), vol. XV, part B, pp. 501-515, Academic Press, New York.
- Silver, L.L. & Bostian, K.A. (1993). Discovery and development of new antibiotics: the problem of antibiotic resistance. *Antimicrob. Agents Chemother.* **37**, 377-383.
- Silverman, P.M., Wickersham, E. & Harris, R. (1991). Regulation of the F plasmid *traY* promoter in *Escherichia coli* by host and plasmid factors. *J. Mol. Biol.* **218**, 119-128.
- Silverman, P.M., Tran, L., Harris, R. & Gaudin, H.M. (1993). Accumulation of the F plasmid TraJ protein in *cpx* mutants of *Escherichia coli*. *J. Bacteriol.* **175**, 921-925.
- Silverman, P.M. & Scholl, A. (1996). Effect of *traY* amber mutations on F-plasmid *traY* promoter activity *in vivo*. *J. Bacteriol.* **178**, 5787-5789.
- Simons, R.W. & Kleckner, N. (1983). Translational control of IS10 transposition. *Cell* **34**, 683-691.
- Simons, R.W., Hoopes, B., McClure, W. & Kleckner, N. (1983). Three promoters near the termini of IS10: pIN, pOUT, and pIII. *Cell* **34**, 673-682.
- Simonsen, L. (1990). Dynamics of plasmid transfer on surfaces. *J. Gen. Microbiol.* **136**, 1001-1007.
- Singer, M.F. & Tolbert, G. (1965). Purification and properties of a potassium-activated phosphodiesterase (RNase II) from *Escherichia coli*. *Biochemistry* **4**, 1319-1330.

- Skurray, R.A., Nagaishi, H. & Clark, A.J. (1978). Construction and *Bam*HI analysis of chimeric plasmids containing *Eco*RI DNA fragments of the F sex factor. *Plasmid* **1**, 174-186.
- Söderbom, F., Binnie, U., Masters, M. & Wagner, E.G.H. (1997). Regulation of plasmid R1 replication: PcnB and RNase E expedite the decay of the antisense RNA, CopA. *Mol. Microbiol.* **26**, 493-504.
- Söderbom, F. & Wagner, E.G.H. (1998). Degradation pathway of CopA, the antisense RNA that controls replication of plasmid R1. *Microbiol.* **144**, 1907-1917.
- Srinivasan, P.R., Ramanarayanan, M. & Rabbani, E. (1975). Presence of polyriboadenylate sequences in pulse-labelled RNA of *Escherichia coli*. *Proc. Natl. Acad. Sci., USA* **72**, 2910-2914.
- Srivastava, S.K., Cannistraro, V.J. & Kennell, D. (1992). Broad-specificity endoribonucleases and mRNA degradation in *Escherichia coli*. *J. Bacteriol.* **174**, 56-62.
- Stark, M.J.R. (1987). Multicopy expression vectors carrying the *lac* repressor gene for regulated high-level expression of genes in *Escherichia coli*. *Gene* **51**, 255-267.
- Steitz, T.A. (1993). Similarities and differences between RNA and DNA recognition by proteins. In *The RNA World* (Gesteland, R.F. & Atkins, J.F., eds), pp. 219-237, Cold Spring Harbor Laboratory Press, New York.
- Stockwell, D.T. & Dempsey, W.B. (1997). The *finM* promoter and the *traM* promoter are the principal promoters of the *traM* gene of the antibiotic resistance plasmid R100. *Mol. Microbiol.* **26**, 455-467.
- Strohmaier, H., Noiges, R., Kotschan, S., Sawers, G., Högenauer, G., Zechner, E.L. & Koraimann, G. (1998). Signal transduction and bacterial conjugation: characterization of the role of ArcA in regulating conjugative transfer of the resistance plasmid R1. *J. Mol. Biol.* **277**, 309-316.
- Tabor, S. & Richardson, C.C. (1985). A bacteriophage T7 RNA polymerase/promoter system for controlled exclusive expression of specific genes. *Proc. Natl Acad. Sci., USA* **82**, 1074-1078.
- Takeda, Y., Ohlendorf, D.H., Anderson, W.F. & Matthews, B.W. (1983). DNA-binding proteins. *Science* **221**, 1020-1026.
- Tamm, J. & Polisky, B. (1983). Structural analysis of RNA molecules involved in plasmid copy number control. *Nucl. Acids Res.* **11**, 6381-6397.

- Tan, R., Chen, L., Buettner, J.A., Hudson, D. & Frankel, A.D. (1993). RNA recognition by an isolated  $\alpha$  helix. *Cell* **73**, 1031-1040.
- Tan, R. & Frankel, A.D. (1994). Costabilization of peptide and RNA structure in an HIV Rev peptide-RRE complex. *Biochemistry* **33**, 14579-14585.
- Taraseviciene, L., Björk, G.R. & Uhlin, B.E. (1995). Evidence for an RNA binding region in the *Escherichia coli* processing endoribonuclease RNase E. *J. Biol. Chem.* **270**, 26391-26398.
- Tomcsanyi, T. & Apirion, D. (1985). Processing enzyme ribonuclease E specifically cleaves RNA I, an inhibitor of primer formation in plasmid DNA synthesis. *J. Mol. Biol.* **185**, 713-720.
- Tomizawa, J-I. (1984). Control of ColE1 plasmid replication: the process of binding of RNA I to the primer transcript. *Cell* **38**, 861-870.
- Tomizawa, J-I. (1985). Control of ColE1 plasmid replication: initial interaction of RNA I and the primer is reversible. *Cell* **40**, 527-535.
- Tomizawa, J-I. (1986). Control of ColE1 plasmid replication: binding of RNA I to RNA II and inhibition of primer formation. *Cell* **47**, 89-97.
- Tomizawa, J-I. (1990a). Control of ColE1 plasmid replication: intermediates in the binding of RNA I to RNA II. *J. Mol. Biol.* **212**, 683-694.
- Tomizawa, J-I. (1990b). Control of ColE1 plasmid replication: interaction of Rom protein with an unstable complex formed by RNA I and RNA II. *J. Mol. Biol.* **212**, 695-708.
- Tomizawa, J-I. & Itoh, T. (1981). Plasmid ColE1 incompatibility determined by interaction of RNA I with primer transcript. *Proc. Natl. Acad. Sci., USA* **78**, 6096-6100.
- Tomizawa, J-I., Itoh, T., Selzer, G. & Som, T. (1981). Inhibition of ColE1 RNA primer formation by a plasmid-specified small RNA. *Proc. Natl. Acad. Sci., USA* **78**, 1421-1425.
- Tomizawa, J-I. & Som, T. (1984). Control of ColE1 plasmid replication: enhancement of binding of RNA I to the primer transcript by the Rom protein. *Cell* **38**, 871-878.
- Tsai, M-M., Fu, Y-H.F. & Deonier, R.C. (1990). Intrinsic bends and integration host factor binding at F plasmid *oriT*. *J. Bacteriol.* **172**, 4603-4609.

- Twigg, A.J. & Sherratt, D. (1980). *Trans-complementable copy-number mutants of plasmid ColE1. Nature* **283**, 216-218.
- Tuerk, C. & Gold, L. (1990). Systematic evolution of ligands by exponential enrichment: RNA ligands to bacteriophage T4 DNA polymerase. *Science* **249**, 505-510.
- Uhlenbeck, O.C. (1995). Keeping RNA happy. *RNA* **1**, 4-6.
- van Biesen. (1994). PhD Thesis. University of Alberta. Edmonton, Alberta.
- van Biesen, T. & Frost, L.S. (1992). Differential levels of fertility inhibition among F-like plasmids are related to the cellular concentration of *finO* mRNA. *Mol. Microbiol.* **6**, 771-780.
- van Biesen, T. & Frost, L.S. (1994). The FinO protein of IncF plasmids binds FinP antisense RNA and its target, *traJ* mRNA, and promotes duplex formation. *Mol. Microbiol.* **14**, 427-436.
- van Biesen, T., Söderbom, F., Wagner, E.G.H. & Frost, L.S. (1993). Structural and functional analyses of the FinP antisense RNA regulatory system of the F conjugative plasmid. *Mol. Microbiol.* **10**, 35-43.
- Varani, G. & Pardi, A. (1994). Structure of RNA. In *RNA-Protein Interactions* (Nagai, K. & Mattaj, I.W., eds), pp. 1-24, Oxford University Press, Oxford.
- Vieira, J. & Messing, J. (1982). The pUC plasmids, an M13mp7-derived system for insertion mutagenesis and sequencing with synthetic universal primers. *Gene* **19**, 259-268.
- Wagner, E.G.H. & Simons, R.W. (1994). Antisense RNA control in bacteria, phages, and plasmids. *Annu. Rev. Microbiol.* **48**, 713-742.
- Wang, J-Y., Qui, L., Wu, E-D. & Drlica, K. (1996a). RNases involved in ribozyme degradation in *Escherichia coli*. *J. Bacteriol.* **178**, 1640-1645.
- Wang, Z-F., Whitfield, M.L., Ingledue, T.C., Dominski, Z. & Marzluff, W.F. (1996b). The protein that binds the 3' end of histone mRNA: a novel RNA-binding protein required for histone pre-mRNA processing. *Genes Dev.* **10**, 3028-3040.
- Watanabe, T. (1963). Infective heredity of multiple drug resistance in bacteria. *Bacteriol. Rev.* **27**, 87-115.
- Watanabe, T. (1966). Infectious drug resistance in enteric bacteria. *New England J. Med.* **275**, 888.

- Weeks, K.M. & Crothers, D.M. (1993). Major groove accessibility of RNA. *Science* **261**, 1574-1577.
- Willetts, N.S. (1974). The kinetics of inhibition of *Flac* transfer by R100 in *E. coli*. *Mol. Gen. Genet.* **129**, 123-130.
- Willetts, N.S. (1977). The transcriptional control of fertility in F-like plasmids. *J. Mol. Biol.* **112**, 141-148.
- Willetts, N.S. & Maule, J. (1986). Specificities of IncF plasmid conjugation genes. *Genet. Res.* **47**, 1-11.
- Williams, A.S., Ingledue, T.C., Kay, B.K. & Marzluff, W.F. (1994). Changes in the stem-loop at the 3' terminus of histone mRNA affects its nucleocytoplasmic transport and cytoplasmic regulation. *Nucl. Acids Res.* **22**, 4660-4666.
- Williams, A.S. & Marzluff, W.F. (1995). The sequence of the stem and flanking sequences at the 3' end of histone mRNA are critical determinants for the binding of the stem-loop binding protein. *Nucl. Acids Res.* **23**, 654-662.
- Witherell, G.W. & Uhlenbeck, O.C. (1989). Specific RNA binding by Q $\beta$  coat protein. *Biochemistry* **28**, 71-76.
- Wyngaarden, J., Cotter, F., Martin, R.R., Mehta, V., Sudhir, A., Eckstein, F., Levin, A., Black, L., Ryszard, C., Crooke, S., Kreig, A. & Diasio, R. (1997). Antisense '97: A roundtable on the state of the industry. *Nature Biotechnology* **15**, 519-528.
- Xu, F. & Cohen, S.N. (1995). RNA degradation in *Escherichia coli* regulated by 3' adenylation and 5' phosphorylation. *Nature* **374**, 180-183.
- Xu, F., Lin-Chao, S. & Cohen, S.N. (1993). The *Escherichia coli* *pcnB* gene promotes adenylation of antisense RNA I of ColE1-type plasmids *in vivo* and degradation of RNA I decay intermediates. *Proc. Natl. Acad. Sci., USA* **90**, 6756-6760.
- Yoshioka, Y., Ohtsubo, H., & Ohtsubo, E. (1987). Repressor gene *finO* in plasmid R100 and F: constitutive transfer of plasmid F is caused by insertion of IS3 in F *finO*. *J. Bacteriol.* **169**, 619-623.
- Yu, D. & Deutscher, M.P. (1995). Oligoribonuclease is distinct from the other known exoribonucleases of *Escherichia coli*. *J. Bacteriol.* **177**, 4137-4139.
- Zhang, X., Zhu, L & Deutscher, M.P. (1998). Oligoribonuclease is encoded by a highly conserved gene in the 3'-5' exonuclease superfamily. *J. Bacteriol.* **180**, 2779-2781.



Zuker, M. (1989). On finding all suboptimal foldings of an RNA molecule. *Science*, **244**, 48-52.